

INFORMATION TO USERS

This manuscript has been reproduced from the microfilm master. UMI films the text directly from the original or copy submitted. Thus, some thesis and dissertation copies are in typewriter face, while others may be from any type of computer printer.

The quality of this reproduction is dependent upon the quality of the copy submitted. Broken or indistinct print, colored or poor quality illustrations and photographs, print bleedthrough, substandard margins, and improper alignment can adversely affect reproduction.

In the unlikely event that the author did not send UMI a complete manuscript and there are missing pages, these will be noted. Also, if unauthorized copyright material had to be removed, a note will indicate the deletion.

Oversize materials (e.g., maps, drawings, charts) are reproduced by sectioning the original, beginning at the upper left-hand corner and continuing from left to right in equal sections with small overlaps. Each original is also photographed in one exposure and is included in reduced form at the back of the book.

Photographs included in the original manuscript have been reproduced xerographically in this copy. Higher quality 6" x 9" black and white photographic prints are available for any photographs or illustrations appearing in this copy for an additional charge. Contact UMI directly to order.

UMI

A Bell & Howell Information Company
300 North Zeeb Road, Ann Arbor MI 48106-1346 USA
313/761-4700 800/521-0600

University of Alberta

AN ANALYSIS OF PEROXISOME ASSEMBLY MUTANTS
OF THE YEAST *YARROWIA LIPOLYTICA*

By

GARY A. EITZEN, B.Sc.



A Thesis Submitted to the School of Graduate Studies and Research
in Partial Fulfilment of the Requirements
for the Degree
Doctor of Philosophy

Department of Cell Biology and Anatomy

Edmonton, Alberta

Fall, 1997



National Library
of Canada

Acquisitions and
Bibliographic Services

395 Wellington Street
Ottawa ON K1A 0N4
Canada

Bibliothèque nationale
du Canada

Acquisitions et
services bibliographiques

395, rue Wellington
Ottawa ON K1A 0N4
Canada

Your file Votre référence

Our file Notre référence

The author has granted a non-exclusive licence allowing the National Library of Canada to reproduce, loan, distribute or sell copies of this thesis in microform, paper or electronic formats.

The author retains ownership of the copyright in this thesis. Neither the thesis nor substantial extracts from it may be printed or otherwise reproduced without the author's permission.

L'auteur a accordé une licence non exclusive permettant à la Bibliothèque nationale du Canada de reproduire, prêter, distribuer ou vendre des copies de cette thèse sous la forme de microfiche/film, de reproduction sur papier ou sur format électronique.

L'auteur conserve la propriété du droit d'auteur qui protège cette thèse. Ni la thèse ni des extraits substantiels de celle-ci ne doivent être imprimés ou autrement reproduits sans son autorisation.

0-612-22978-5

University of Alberta

Library Release Form

Name of Author: GARY A. EITZEN

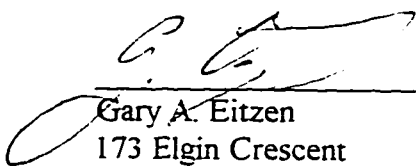
Title of Thesis: AN ANALYSIS OF PEROXISOME ASSEMBLY MUTANTS
OF THE YEAST *YARROWIA LIPOLYTICA*

Degree: Doctor of Philosophy

Year this Degree Granted: 1997

Permission is hereby granted to the University of Alberta Library to reproduce single copies of this thesis and to lend or sell such copies for private, scholarly, or scientific research purposes only.

The author reserves all other publication and other rights in association with the copyright in the thesis, and except as hereinbefore provided, neither the thesis nor any substantial portion thereof may be printed or otherwise reproduced in any material form whatever without the author's prior written permission.



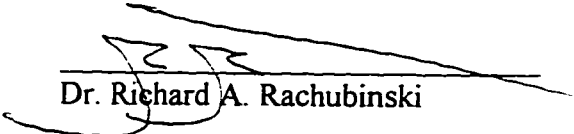
Gary A. Eitzen
173 Elgin Crescent
Waterloo, ON N2J 2S7

Date: May 7 1997


University of Alberta

Faculty of Graduate Studies and Research

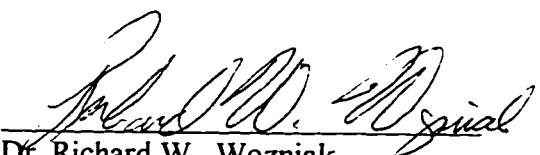
The undersigned certify that they have read, and recommend to the Faculty of Graduate Studies and Research for acceptance, a thesis entitled: An analysis of peroxisome assembly mutants of the yeast *Yarrowia lipolytica*, submitted by Gary A. Eitzen in partial fulfillment of the requirements for the degree of doctor of philosophy.



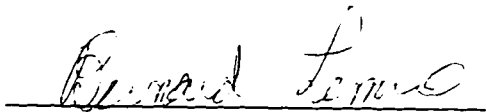
Dr. Richard A. Rachubinski



Dr. Tom C. Hobman



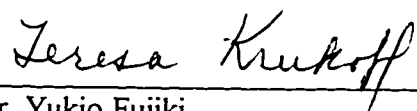
Dr. Richard W. Wozniak



Dr. Bernard D. Lemire



Dr. Colin D. Rasmussen



for Dr. Yukio Fujiki

Date: MAY 6, 1997

ABSTRACT

This thesis describes studies using the yeast *Yarrowia lipolytica* as a model organism for the investigation of peroxisome biogenesis. It is divided into three parts. Each part describes the biochemical and morphological characterization of an individual peroxisome assembly, or, *pex* mutant strain. For each *pex* strain, the corresponding *PEX* gene was cloned by functional complementation with a *Y. lipolytica* genomic DNA library. *PEX* genes encode peroxins, which are proteins required for peroxisome assembly. A functional role for each peroxin is proposed.

The *pex9* mutant cannot import the bulk of peroxisomal matrix proteins. Electron microscopic analysis of *pex9* cells showed clusters of non-functional peroxisomal “ghosts” similar to the vesicular structures found in fibroblasts of some patients with Zellweger syndrome, a human genetic disorder of peroxisome assembly. Peroxisome assembly is restored in *pex9* by functional complementation with the *YIPEX9* gene. *YIPEX9* encodes the peroxin, Pex9p (44,913 Da). Antibodies raised against Pex9p recognize a 42 kDa protein localized to carbonate-stripped peroxisomal membranes. Pex9p is essential for peroxisomal import but not for the initial steps of peroxisomal membrane proliferation.

The *pex2* strain lacks normal peroxisomes and instead accumulates irregular vesicular structures surrounded by multiple membranes. Subcellular fractionation showed that this strain contains multiple peroxisomal subpopulations. Each population is characterized by differences in density and protein distribution. The complementing gene, *YIPEX2*, encodes

Pex2p, a 380 amino acid peroxin of 41,720 Da. Pex2p is integral to the peroxisomal membrane. Pex2p can be targeted to mammalian peroxisomes, demonstrating the evolutionary conservation of the targeting mechanisms for peroxisomal membrane proteins. *YIPex2p* is a homologue of mammalian PAF-1 proteins, which are also essential for peroxisome assembly. PAF-1 mutations result in Zellweger syndrome. Our results indicate that defects in Pex2p block normal peroxisomal membrane assembly.

The *pex16* strain lacks normal peroxisomes; however, some peroxisomal matrix proteins are contained within two vesicular populations of different densities. The *YIPEX16* gene encodes a 391 amino acid peroxin, Pex16p, of 44,479 Da. Pex16p is localized to the matrix face of the peroxisome membrane. Overproduction of Pex16p results in cells with a few enlarged, functional peroxisomes. Pex16p is proposed to act to inhibit peroxisome fission.

ACKNOWLEDGEMENTS

I would first and foremost like to acknowledge my supervisor, Dr. Richard Rachubinski, for all of his hard work and encouragement throughout the course of this work. I would also like to thank the members of my supervisory committee Dr. Bernard Lemire and Dr. Colin Rasmussen for their input, and the Alberta Heritage Foundation for Medical Research for financial assistance.

I am indebted to the former members of the Rachubinski lab, John Aitichson, John Glover, Bill Nuttley, Tony Brade and Baowei Zhang, whose time and effort went into "educating" me, early in my scientific career. I also thank the present members of the Rachubinski biogenesis group for their scientific contributions and assistance: Melchior Evers, Eileen Reklow, Jennifer Smith, Rachel Szilard, Arjuna Thiagarajah and Vladimir Titorenko. I enjoyed the atmosphere and rivalry with the Rachubinski peroxisome proliferator group: Altaf Kassam, Pam Lagali, Sandra Marcus and Chris Windrow. Special thanks go to Rachel Szilard and Jennifer Smith for spending many hours of their time critically reviewing manuscripts, fellowships and this thesis. Also, a million thanks to Honey Chan for her time and effort spent teaching me the fine art of electron microscopy.

Of course none of my accomplishments would have amounted to anything without the encouragement, perseverance and technical assistance (while working in our lab) of my loving wife Kristine Decker-Eitzen; this thesis work is dedicated to you. Thanks to my parents, Annie and George Eitzen, for moral and financial support. Thanks to Ron and Kathy Eitzen for periodically taking me away from it all (usually in the dead of winter when it was forty below in Edmonton...but warm and sunny in Lake Louise).

TABLE OF CONTENTS

1. INTRODUCTION

1.1 Overview	1
1.2 Organelle biogenesis	2
1.3 The functions of peroxisomes	3
1.4 Protein import into peroxisomes	4
1.5 Human genetic disorders of peroxisome assembly	7
1.6 Peroxisome assembly using a genetic approach in yeast	8
1.7 Focus of this thesis	10

2. MATERIALS AND METHODS

2.1 Materials	12
2.1.1 Reagents and chemicals	12
2.1.2 Enzymes	13
2.1.3 Molecular size standards	13
2.1.4 Radiochemicals and detection kits	14
2.1.5 Plasmids	14
2.1.6 Antibodies	14
2.2 DNA manipulation	17
2.2.1 Cultivation of <i>Escherichia coli</i>	17
2.2.2 Isolation of nucleic acids	17
2.2.3 Restriction endonuclease digestion	18
2.2.4 Generation of blunt-ended DNA	18
2.2.5 Purification of DNA fragments	19
2.2.6 Ligation of DNA fragments	19
2.2.7 Labelling of DNA probes	20
2.2.8 Southern blot analysis	20
2.2.9 Northern blot analysis	21
2.2.10 DNA sequencing	22
2.2.11 Epitope-tagging of Pex16p	23
2.2.12 Overexpression of the <i>YIPEX16</i> gene	23

2.3	Yeast cultivation	25
2.3.1	Yeast strains and culture conditions	25
2.3.2	Mutagenesis and genetic screening	25
2.3.3	Mating and genetic analysis	27
2.3.4	Transformation of <i>Y. lipolytica</i>	28
2.3.5	Construction of yeast gene-deletion/conversion strains	29
2.3.5.1	Integrative disruption of the <i>YIPEX9</i> gene	29
2.3.5.2	Integrative disruption of the <i>YIPEX2</i> gene	30
2.3.5.3	Integrative disruption of the <i>YIPEX16</i> gene	31
2.3.5.4	Integrative disruption of the <i>Y. lipolytica</i> isocitrate lyase gene (<i>ICLI</i>)	31
2.3.5.5	Integration of the construct encoding Pex16p-HA	32
2.3.5.6	Integration of the <i>Y. lipolytica</i> <i>PEX16</i> overexpression construct	32
2.4	Preparation of subcellular fractions	34
2.4.1	Whole cell lysates	34
2.4.2	Organelle isolation	34
2.4.3	Membrane extraction	36
2.4.4	Protease protection	37
2.5	Analysis of Proteins	37
2.5.1	Electrophoresis and protein blotting	37
2.5.2	Immunoblot analysis	38
2.5.3	Protein determination	38
2.5.4	Enzymatic assays	39
2.6	Microscopy	41
2.6.1	Immunofluorescence microscopy	41
2.6.2	Electron microscopy	42
2.7	Antibody production	44
2.7.1	Anti-Pex9p antibodies	45
2.7.2	Anti-Pex2p antibodies	45
2.7.3	Anti-Pex16p antibodies	46
2.7.4	Anti-thiolase antibodies	46
2.7.5	Anti-isocitrate lyase antibodies	47
2.7.6	Anti-(<i>S. cerevisiae</i>)acyl-CoA oxidase antibodies	47

RESULTS AND DISCUSSION	49
3. The <i>Y. lipolytica</i> <i>PEX9</i> gene encodes a 42 kDa peroxisomal integral membrane peroxin essential for matrix protein import and peroxisome enlargement but not for peroxisome membrane proliferation	50
3.1 <i>pex9</i> cells can proliferate peroxisome-like structures but are deficient for peroxisome growth	50
3.2 <i>pex9</i> cells mislocalize PTS1- and PTS2-containing proteins to a subcellular fraction enriched for cytosol	50
3.3 Isolation of the <i>YIPEX9</i> gene	53
3.4 Nucleotide sequence of the <i>YIPEX9</i> gene and the deduced amino acid sequence of Pex9p	58
3.5 Analysis of the Pex9p amino acid sequence	58
3.6 Pex9p is a peroxisomal integral membrane protein	61
3.7 The levels of Pex9p mRNA and Pex9p are induced by growth on oleic acid	61
3.8 Summary and discussion	66
3.8.1 <i>pex9</i> mutant cells contain peroxisomal ghosts	66
3.8.2 Role of Pex9p in a common peroxisomal import machinery	66
4. Mutation of the <i>PEX2</i> gene encoding a <i>Y. lipolytica</i> homologue of mammalian peroxisome assembly factor-1 results in abnormal peroxisomal structures	68
4.1 The <i>pex2-1</i> mutant shows abnormal peroxisome morphology	68
4.2 Isolation and characterization of the <i>YIPEX2</i> gene	70
4.3 Pex2p is a <i>Y. lipolytica</i> homologue of mammalian PAF-1 proteins	74
4.4 Pex2p is a peroxisomal integral membrane protein	78
4.5 Peroxisomal proteins are mislocalize to the 20KgS enriched for cytosol to varying extents in <i>pex2</i> mutant cells	81
4.6 <i>pex2</i> mutant strains accumulate peroxisomal intermediates that are associated with endoplasmic reticulum and Golgi elements	83

4.7 Summary and discussion	87
4.7.1 <i>pex2</i> mutant cells accumulate intermediate peroxisomal vesicles that are incompletely blocked in import and which associate with ER and Golgi elements	87
4.7.2 Protein with carboxyl-terminal C ₃ HC ₄ domains are important for organelle biogenesis	89
4.7.3 Possible role of Pex2p in membrane biogenesis	90
4.7.4 Evolutionary conservation of peroxisomal membrane targeting signals	90
5. Overexpression of the <i>Y. lipolytica</i> <i>PEX16</i> gene encoding the peroxin Pex16p, an intraperoxisomal peripheral membrane protein, results in fewer but enlarged peroxisomes	92
5.1 Isolation of the <i>YIPEX16</i> gene	92
5.2 <i>pex16</i> mutant cells lack normal peroxisomes but do show evidence of vesicular structures containing peroxisomal proteins	97
5.3 Pex16p is an intraperoxisomal peripheral membrane protein	107
5.4 The carboxyl terminus of Pex16p is not essential for its function or targeting	111
5.5 Oversynthesis of Pex16p results in cells with a reduced number of enlarged peroxisomes	112
5.6 Summary and discussion	120
5.6.1 <i>pex16</i> mutant strains contain abnormal peroxisomal structures	120
5.6.2 The carboxyl-terminal tripeptide, Ser-Thr-Leu, of Pex16p is not essential for its targeting to peroxisomes	121
5.6.3 A function for Pex16p in peroxisome growth and fission?	122
6. PERSPECTIVES	124
7. BIBLIOGRAPHY	136

LIST OF TABLES

Table 2.1	Antibody, animal source and dilution used for immunoblot analyses presented in this study.	16
Table 2.2	Oligonucleotides used to amplify and clone various genetic products.	24
Table 2.3	<i>Yarrowia lipolytica</i> strains and genotype used in this study.	26
Table 3.1	Distribution of peroxisomal and mitochondrial marker enzymes in the 20KgS and 20KgP fractions isolated from cell homogenates of the <i>E122</i> , <i>pex9</i> , <i>P9-KO</i> and <i>PEX9</i> strains.	58
Table 4.1	Amino acid sequence alignment of the putative Pmp47 internal PTS motif and the corresponding Pex2p region.	92
Table 6.1	Description of yeast peroxins and <i>PEX</i> genes.	127

LIST OF FIGURES

1.1	Peroxisomal β -oxidation of fatty acids.	5
2.1	Identification of the <i>Y. lipolytica</i> ICL protein as an anti-SKL immunoreactive peptide.	33
2.2	Immunoblot showing cross-reactivity of anti-(<i>Y. lipolytica</i>) thiolase antibodies.	48
3.1	Growth of various <i>Yarrowia lipolytica pex9</i> strains on oleic acid medium.	52
3.2	Ultrastructure of the <i>pex9</i> mutant (<i>panels A and B</i>) and wild-type <i>E122</i> (<i>panels C and D</i>) strains.	53
3.3	Peroxisomal thiolase and a PTS1-immunoreactive polypeptide are mislocalized to the 20KgS fraction of the <i>pex9</i> mutant strain.	55
3.4	Ultrastructure of the <i>P9-KO</i> mutant (<i>panels A and B</i>) and the <i>PEX9</i> transformant (<i>panels C and D</i>).	57
3.5	Cloning and analysis of the <i>YIPEX9</i> gene.	60
3.6	Hydropathy analysis of Pex9p.	61
3.7	Pex9p is a peroxisomal integral membrane protein.	63
3.8	Pex9p mRNA and peroxisomal thiolase mRNA are induced by growth of <i>Y. lipolytica</i> in oleic acid.	65
3.9	Pex9p is induced by growth of <i>Y. lipolytica</i> in oleic acid.	66
4.1	Growth of various <i>Y. lipolytica pex2</i> strains on oleic acid medium.	70
4.2	Ultrastructure of the wild-type, <i>pex2</i> mutant and <i>PEX2</i> transformant strains.	72
4.3	Cloning and analysis of the <i>YIPEX2</i> gene.	73
4.4	Hydropathy analysis of Pex2p.	74

4.5	Pex2p and peroxisomal thiolase mRNA are induced by growth of <i>Y. lipolytica</i> in oleic acid.	76
4.6	Alignment of <i>Y. lipolytica</i> Pex2p with human, <i>P. pastoris</i> and <i>P. anserina</i> homologues.	78
4.7	Pex2p is a peroxisomal integral membrane protein.	80
4.8	<i>YIPex2p</i> is targeted to peroxisomes of CHO cells.	81
4.9	Peroxisomal proteins are synthesized normally but are mislocalized to the 20KgS fraction to varying extents in <i>pex2</i> mutant cells.	83
4.10	Peroxisomal proteins are mislocalized to cytosolic and light particulate fractions in <i>pex2</i> mutant cells.	85
4.11	Density gradient analysis shows the accumulation of ER and Golgi associated light peroxisomes in <i>pex2</i> mutant cells.	87
5.1	Growth of various <i>Y. lipolytica pex16</i> strains on oleic acid medium.	94
5.2	Cloning and analysis of the <i>YIPEX16</i> gene.	96
5.3	Hydropathy profile of Pex16p.	97
5.4	Ultrastructure of wild-type and <i>pex16</i> mutant strains.	99
5.5	Peroxisomal proteins are mislocalized to the 20KgS to varying extents in <i>pex16</i> mutants.	101
5.6	Peroxisomal matrix proteins localized to the 20KgP fraction of the <i>pex16-1</i> mutant reside within vesicles.	103
5.7	Immunofluorescence microscopy shows small vesicular structures in <i>pex16</i> mutant strains.	104
5.8	Immunocytochemical analysis of <i>E122</i> and <i>pex16-1</i> cells with anti-SKL and gold conjugated antibodies.	105
5.9	Isopycnic density gradient analysis of 20KgP fractions of the wild-type and <i>pex16</i> strains.	107
5.10	Immunocytochemical analysis of wild-type and <i>pex16-1</i> subcellular fractions.	109

5.11	Pex16p is a peripheral protein preferentially associated with the matrix face of the peroxisomal membrane.	111
5.12	Pex16p-HA is targeted to peroxisomes and associates with the matrix face of the peroxisomal membrane.	114
5.13	Pex16p is oversynthesized in the strain <i>pex16-TH</i> .	117
5.14	Oversynthesis of Pex16p results in cells with a reduced number of enlarged peroxisomes.	118
5.15	Ultrastructure of the <i>PEX16</i> overexpression strain <i>pex16-TH</i> .	119
5.16	Characterization of the enlarged peroxisomes of the <i>pex16-TH</i> strain.	120
6.1	A model of peroxisome biogenesis.	134

LIST OF ABBREVIATIONS

20KgS	supernatant of a 20,000 x <i>g</i> PNS lysate
20KgS	pellet of a 20,000 x <i>g</i> PNS lysate
avg	average
AOX	acyl-CoA oxidase
ATP	adenosine triphosphate
bp	base pair
BSA	bovine serum albumin
<i>C.</i>	<i>Candida</i>
C	Celsius
CAT	catalase
CCO	cytochrome <i>c</i> oxidase
CHO	chinese hamster ovary
Ci	Currie
CoA	coenzyme A
cpm	counts per min
d	day
Da	Dalton
DNA	deoxyribonucleic acid
DTT	dithiothrietol
<i>E.</i>	<i>Escherichia</i>
ECL	enhanced chemiluminescence
EDTA	ethylenediamine tetraacetic acid
ER	endoplasmic reticulum
g	gram
<i>g</i>	gravitational force
<i>H.</i>	<i>Hansenula</i>
h	hour
HA	influenza hemmagglutinin antigen (epitope tag)
HRP	horseradish peroxidase
ICL	isocitrate lyase
IgG	immunoglobulin G
k	kilo
kbp	one thousand base pairs
L	litre
m	milli
M	molar
μ	micro
MES	2-morpholinoethane sulfonic acid
min	minute
MLS	malate synthase
MOPS	4-morpholinopropane sulfonic acid
mRNA	messenger RNA

n	nano
OD	optical density at $\lambda = x$ nm
ole-	deficient in oleic acid metabolism
ORF	open reading frame
<i>P.</i>	<i>Pichia</i>
p	protein
PAGE	polyacrylamide gel electrophoresis
PCR	polymerase chain reaction
Pay#p	protein involved in peroxisome assembly in <i>Y. lipolytica</i>
Pex#p	peroxin (protein) involved in peroxisome assembly
<i>PAY#</i>	gene encoding Pay#p
<i>PEX#</i>	gene encoding peroxin Pex#p
<i>pay#</i>	<i>PAY#</i> mutant strain
<i>pex#</i>	<i>PEX#</i> mutant strain
pH	-(log[H ⁺])
PNS	post nuclear supernatant
PTS	peroxisomal targeting signal
RNA	ribonucleic acid
<i>S.</i>	<i>Saccharomyces</i>
s	second
SDS	sodium dodecyl-sulfate
SKL	carboxyl-terminal PTS1 motif: serine-lysine-leucine
THI	thiolase
U	unit of enzyme activity
V	volt
vol	volume
wt	weight
<i>Y.</i>	<i>Yarrowia</i>
<i>Yl</i>	<i>Yarrowia lipolytica</i>
YEPD	rich yeast growth media containing glucose
YPBO	rich yeast growth media containing oleic acid
YND	minimal yeast growth media containing glucose
YNO	minimal yeast growth media containing oleic acid

1. INTRODUCTION

1.1 Overview

Eukaryotic cells have evolved a complex set of organelles, with each organelle possessing a specific complement of enzymes required for its particular metabolic or biosynthetic role. The maintenance of this cellular organization requires the coordination of a number of processes. Proteins destined to reside within a particular organelle must be specifically recognized, efficiently transported to the organelle, translocated across or into the organelle membrane that serves as a barrier, and assembled into a biologically active conformation. Secondly, organelles must replicate and segregate in conjunction with the cell cycle. Thirdly, organelles must respond to changes in their environment. Organelle biogenesis is the study of the mechanisms of these processes. The mechanisms of biogenesis have largely been defined for organelles such as the endoplasmic reticulum, mitochondrion, chloroplast and nucleus. In contrast, comparatively little is known about peroxisome biogenesis, perhaps because of its relatively recent discovery as a subcellular compartment (de Duve and Baudhuin, 1966). However, in the last few years, investigations have begun to uncover the components that underlie peroxisome assembly. This thesis describes a combined genetic, biochemical and cell biological approach to the study and characterization of the molecular mechanisms involved in peroxisome biogenesis, using the yeast *Yarrowia lipolytica* as a model organism.

1.2 Organelle biogenesis

All eukaryotic cells contain many functionally distinct membrane-enclosed organelles. The functional identity of an organelle is largely defined by the unique set of proteins it contains. Accurate and efficient delivery of proteins to a given organelle is therefore crucial for the maintenance of this functional identity.

Two intracellular delivery mechanisms exist for newly synthesized polypeptides. Cotranslational delivery of proteins into the endoplasmic reticulum lumen or membrane serves as an entry point for most proteins destined for compartments along the secretory pathway (Palade, 1975). In contrast, delivery of nuclear encoded proteins to mitochondria, chloroplasts and peroxisomes is posttranslational, following synthesis on free polysomes in the cytosol (Pfanner and Neupert, 1990; de Boer and Weisbeek, 1991; Lazarow and Fujiki, 1985). One method used for the accurate delivery of proteins to their correct organelles is through targeting signals encoded in the primary sequences of proteins (Blobel, 1980). Signal sequence receptors exist as part of intracellular transport mechanisms that ensures efficient protein delivery by recognition of and binding to targeting signals. Such receptors can be strictly organelle-bound, but in most cases are likely a combination of cytosolic factors working in conjunction with organelle-bound receptors. Protein targeting to and import into organelles are complex phenomenon, often involving divergent pathways that converge at a common site for protein translocation across the organelle membrane. Targeting to and import into the endoplasmic reticulum, mitochondria, chloroplasts and peroxisomes have been the subject of several recent reviews (Walter and Johnson, 1994; Schnell, 1995; Lill et al., 1996; Rachubinski and Subramani, 1995).

Under normal circumstances, cells do not synthesize organelles *de novo*. Instead, templates or mature organelles are inherited during cell division, and new organelles are formed by the proliferation of preexisting organelles (Warren and Wickner, 1996). Organelle composition is not fixed and must be able to respond to changes in the environment or to the demands placed upon a cell. Signals that regulate organelle biogenesis are often in response to nutritional needs and activate a complex transcriptional network that modulates the expression of genes encoding organellar proteins (Nunnari and Walter, 1996).

1.3 The functions of peroxisomes

Peroxisomes are members of the microbody family that includes glyoxysomes of plants and glycosomes of trypanosomes (Lazarow and Fujiki, 1985). Peroxisomes are roughly spherical, bounded by a single unit membrane, range in diameter from 0.1 - 1 μm and sediment to a buoyant density of 1.21 - 1.25 g/cm^3 in sucrose (a density greater than that of mitochondria or plasma membrane). This high buoyant density reflects the extremely high protein content of the peroxisome matrix, which often results in the formation of a paracrystalline core in the matrix.

The term “peroxisome” was coined by de Duve whose early tissue fractionation studies led to the identification of this organelle as the site of oxidative metabolism with the production of H_2O_2 as a by-product and the presence of catalase to degrade peroxides (de Duve and Baudhuin, 1966). Significant progress has since been made in delimiting the diverse catabolic and anabolic functions that peroxisomes perform (van den Bosch et al., 1992). Peroxisomes perform several essential metabolic tasks, mainly those that require oxidative

catabolism of nutrients such as fatty acids, glycolate, lactate, amino acids, alcohols, and complex polyamines. In mammals, peroxisomes also participate in bile acid, cholesterol, and plasmalogen synthesis and in the pentose phosphate pathway (Tolbert, 1981).

In yeast, peroxisomes are the exclusive site of fatty acid β -oxidation (Tanaka et al., 1982). When yeast cells are grown in medium containing fatty acids as the sole carbon source, peroxisomes are fundamental for the production of energy by supplying acetyl-CoA units to the TCA cycle (Fig 1.1). In the methylotrophic yeasts, *Hansenula polymorpha*, *Candida boidinii* and *Pichia pastoris*, peroxisomes also harbour the enzymes methanol oxidase and dihydroxyacetone synthase, required for methanol utilization (Gleeson and Sudbery, 1988).

1.4 Protein import into peroxisomes

Some fundamental features of peroxisomal import have recently emerged from studies in yeast (for a review, see Rachubinski and Subramani, 1995). Peroxisomes do not contain DNA or protein synthetic machinery (Kamiryo et al., 1982). Nuclear encoded proteins are synthesised in the cytosol and imported posttranslationally by a process that is sensitive to the alkylating agent, N-ethylmaleimide (Wendland and Subramani, 1993a). Two peroxisomal targeting signals (PTSs) have been shown to deliver matrix proteins. PTS1 is a carboxyl-terminal tripeptide motif with the consensus sequence Ser-Lys-Leu (SKL), or conserved variants thereof, that has been found in many different peroxisomal matrix proteins from

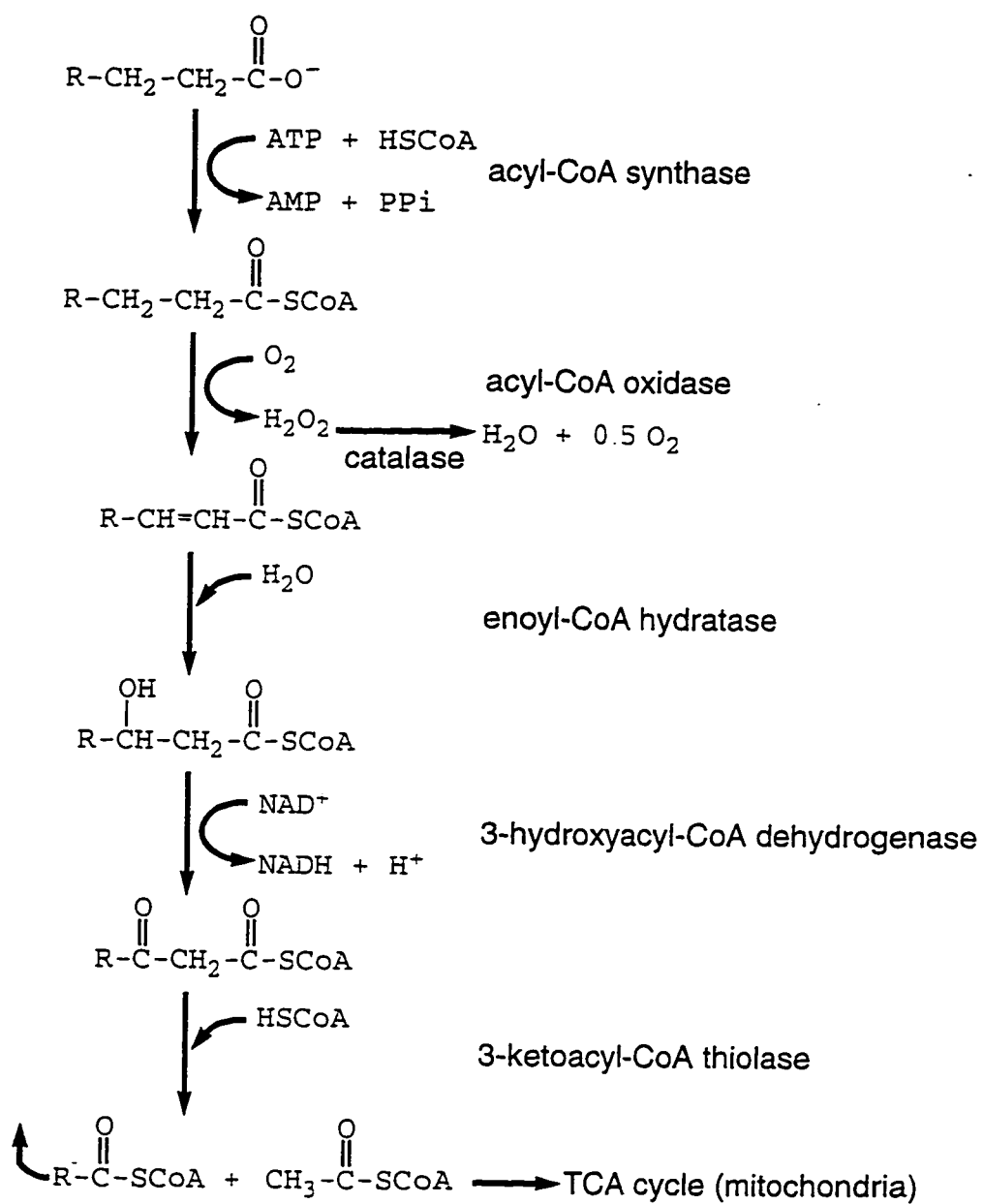


Figure 1.1 Peroxisomal β -oxidation of fatty acids.

several evolutionarily divergent organisms (Gould et al., 1989, 1990; Aitchison et al., 1991). PTS2 is an amino-terminal motif first identified as a cleavable presequence in rat 3-ketoacyl-CoA thiolase (Swinkels et al., 1991). Similar sequences have been found in yeast thiolases, amine oxidase and Pex8p, and in watermelon glyoxysomal malate dehydrogenase and trypanosomal aldolase (de Hoop and AB, 1992; Waterham et al., 1994). The minimal consensus sequence was delineated to be (Arg/Lys)-(Leu/Val/Ile)-X₅-(His/Gln)-(Leu/Ala) (Glover et al., 1994a). Other peroxisomal matrix proteins exist that contain neither of these topogenic signals. Internal regions are thought to encode PTSs in a small number of matrix proteins (Small et al., 1988). Recently, an internal targeting motif has been reported for PMP47, a major peroxisomal membrane protein of *C. boidinii*, comprising a cluster of basic amino acids in a short, 20 amino acid hydrophilic loop between two hydrophobic domains (Dyer et al., 1996). The peroxisomal import machinery, unlike that of the endoplasmic reticulum and mitochondrion, can translocate folded and oligomeric proteins and other large particles such as 9 nm colloidal gold particles decorated with PTS1 peptides (Glover et al., 1994b; McNew and Goodman, 1994; 1996; Walton et al., 1992; 1995).

Using genetic screens, PTS receptors have been identified in several yeast species. These receptors seem to function selectively in the import of matrix proteins targeted by either PTS1 or PTS2 motifs. Pex5p from several yeasts specifically affects the import of proteins containing PTS1 (van der Leij et al., 1993; McCollum et al., 1993; Szilard et al., 1995; van der Klei et al., 1995). Likewise, Pex7p of *Saccharomyces cerevisiae* specifically functions to target proteins containing PTS2 (Marzioch et al., 1994; Zhang and Lazarow, 1995). In some instances, Pex5p and Pex7p have been shown to physically interact with the

amino acid sequences that comprise the PTS1 and PTS2 motifs, respectively (Terlecky et al., 1995; Rehling et al., 1996). More recently, the peroxisomal integral membrane protein, Pex13p, has been shown to function as a docking factor for the mobile PTS1 receptor, Pex5p (Gould et al., 1996; Elgersma et al., 1996; Erdmann and Blobel, 1996). Many yeast peroxisome assembly mutant strains are affected in the import of both PTS1- and PTS2-containing proteins, and therefore, it is likely that these two pathways converge for protein translocation (McNew and Goodman, 1996).

1.5 Human genetic disorders of peroxisome assembly

The importance of peroxisomes for normal human development and physiology is demonstrated by the lethality of various peroxisome biogenesis disorders. Human peroxisomal disorders have been classified into three groups based on the biochemical loss of peroxisome function (Moser, 1993).

Group 1 disorders are the most severe and are characterized by generalized peroxisome assembly defects. Several peroxisomal matrix proteins are mislocalized, some of which are found in the cytosol. Peroxisomes are either non-existent or consist of membrane ghosts, which contain some integral membrane proteins and migrate to aberrant density upon density gradient centrifugation (Schram et al., 1986; Santos et al., 1988a; Gartner et al., 1991). Diseases in this class include the classical Zellweger (cerebrohepatorenal) syndrome, neonatal adrenoleukodystrophy, infantile Refsum disease and hyperpipecolic acidemia.

Group 2 encompasses peroxisomal disorders that result from the loss of a limited set of peroxisomal proteins, but morphologically intact peroxisomes are present (Roscher and Rolinski, 1992). These disorders may reflect a deficiency in a particular targeting pathway used to import a subset of peroxisomal proteins as in rhizomelic chondrodysplasia punctata, which seems to be the result of a PTS2 disorder (Heikoop et al., 1992)

Group 3 disorders have defects in the activity of a single peroxisomal enzyme. Diseases in this category include deficiencies in individual β -oxidation enzymes such as acatalasemia (catalase) and X-linked adrenoleukodystrophy (acyl-CoA synthetase) and Refsum disease (phytanic oxidase) (Wilson et al., 1988). However, the clinical distinctions between groups 2 and 3 are not always obvious. For example, rhizomelic chondrodysplasia punctata was manifested by a lack of peroxisomal dihydroxyacetonephosphate (DHAP) acyl transferase, alkyl DHAP synthase, phytanic acid oxidase and thiolase in one patient, while only thiolase was lacking in another (Heikoop et al., 1992). Therefore, groups 2 and 3 disorders may be distinguishable biochemically but lead to the same clinical manifestations.

1.6 Peroxisome assembly using a genetic approach in yeast

Much remains to be determined about the mechanisms of peroxisome biogenesis. Peroxisomes were first detected in electron microscopic sections of *S. cerevisiae* glucose-grown cells as small single-membrane organelles containing catalase (Avers and Federman, 1968). It was later discovered that peroxisome proliferation could be induced by growth of yeast in media containing fatty acids (Osumi et al., 1974; Veenhuis et al., 1987).

While a great deal is now known about the nature of protein targeting to peroxisomes, little is known about the mechanisms of how new peroxisomes arise. Results from early ultrastructural studies suggested that peroxisomes arise by budding directly from the endoplasmic reticulum (de Duve and Baudhuin, 1966). It is now proposed that new peroxisomes derive from preexisting peroxisomes. However, the delivery of components to peroxisomes from the endoplasmic reticulum and physical interconnections between these two organelles are supported by morphological and biochemical observations (Fahimi et al., 1993; Titorenko et al., 1996). *De novo* peroxisome formation still remains a formal possibility (Waterham et al., 1993).

Peroxisome proliferation can be induced in response to nutritional conditions. For the yeasts *S. cerevisiae*, *C. tropicalis* and *Y. lipolytica*, growth in oleic acid as a carbon source can elicit a peroxisome proliferative response. Growth in methanol acts a proliferator for methylotrophic yeasts such as *C. boidinii* and *H. polymorpha*. Either oleic acid- or methanol-containing medium induces peroxisome formation in *P. pastoris*. Shifting yeast cells from glucose-containing medium to a peroxisome induction medium results in the upregulation of peroxisomal protein synthesis, accompanied by a rapid increase in peroxisome number (Goodman and Veenhuis, 1990; this thesis), whereas the opposite occurs when cells are shifted back to glucose (Osumi et al., 1974; 1975). Therefore, peroxisomes are truly adaptive organelles that can proliferate or decrease in number, and can alter their contents in response to environmental conditions and needs.

Two distinct mechanisms of peroxisome proliferation have been described in detail. In *H. polymorpha*, peroxisome enlargement occurs first until a critical size is reached, and

then small peroxisomes bud off large peroxisomes (Veenhuis et al., 1979). Similar studies in *C. boidinii* showed that the initial proliferation response entails the formation of clusters of small peroxisomes that enlarge at a later stage (Veenhuis and Goodman, 1990). Observations in *S. cerevisiae*, *P. pastoris* and *Y. lipolytica* have shown that the mechanism used by *C. boidinii* is probably the more common one (Veenhuis et al., 1987; Subramani, 1993; Rachubinski, unpublished).

In yeast, functional peroxisomes can be completely disposed of without compromising the viability of cells in glucose-containing medium (conditional lethal mutations). This fact has facilitated the isolation of a large collection of peroxisome assembly mutants, collectively termed *pex* mutants, in the yeasts *S. cerevisiae*, *H. polymorpha*, *P. pastoris* and *Y. lipolytica* (Erdmann et al., 1989; Cregg et al., 1990; Gould et al., 1992; Nuttley et al., 1993). *PEX* genes can be isolated by functional complementation of *pex* mutants with DNA libraries. *PEX* genes encode peroxins, which are proteins involved in peroxisome biogenesis. To date, this genetic approach has elucidated 17 (or more) peroxins (see Table 6.1).

1.7 Focus of this thesis

Peroxisome proliferation is rather poor in *S. cerevisiae*, which does not grow well in fatty acid-containing medium. Thus, other experimental organisms have been widely used to study peroxisome biogenesis. Yeasts such as *H. polymorpha*, *P. pastoris* and *C. boidinii* massively proliferate peroxisomes in response to methanol; however, their response to fatty-

acids is limited. *Candida tropicalis* markedly proliferates peroxisomes when grown in fatty acids, but a genetic system is not available (Aitchison and Rachubinski, 1990). Therefore, the Rachubinski laboratory has turned its efforts to studying peroxisome biogenesis in *Y. lipolytica*. As its name implies, this yeast grows well when oleic acid is the sole carbon source (~1 h doubling time), a condition that requires the presence of functional peroxisomes (Nuttley et al., 1994). Peroxisome assembly mutants can be selected by screening for lack of growth on oleic acid medium (requiring peroxisomal β -oxidation for the production of acetyl-CoA), while maintaining growth on acetate medium (directly supplying the TCA cycle with acetyl-CoA and bypassing the need for β -oxidation) to eliminate mitochondrial mutants (see Fig. 1.1). *Y. lipolytica* strains containing auxotrophic markers and appropriate shuttle vectors for their transformation are available (Gaillardin et al., 1973), making this organism a suitable choice for our genetic approach to peroxisome biogenesis. Peroxisomes can be isolated readily and reproducibly from *Y. lipolytica*. Subcellular morphology is very characteristic, and peroxisomes and other organelles can be identified in electron microscopic sections (this thesis).

The focus of this thesis is the characterization of the peroxisome assembly pathway in *Y. lipolytica* and the description and analysis of some of the factors involved in this process. Specifically, three *pex* mutants have been characterized morphologically and biochemically for their defects in peroxisome biogenesis. The complementing *PEX* genes have been isolated, and their sequences along with those of their encoded peroxins are reported. Analysis of the peroxins has allowed us to propose functional roles for them in the peroxisome assembly pathway.

2. MATERIALS AND METHODS

2.1 Materials

The following sections list the suppliers of some key materials. All reagents were of the highest quality available.

2.1.1 *Reagents and chemicals*

agar	Difco Laboratories
agarose (GTG)	FMC BioProducts
albumin (bovine serum; BSA)	Boehringer-Mannheim
L-amino acids	Sigma Chemical Company
ampicillin	Sigma Chemical Company
antipain	Boehringer-Mannheim
Bio-Rad protein assay dye reagent	Bio-Rad Laboratories
Brij-35 (polyoxyethylene 23-lauryl ether)	Sigma Chemical Company
chymostatin	Sigma Chemical Company
Coomassie Brilliant Blue (R-250)	Gibco/BRL
cytochrome <i>c</i> , horse heart	Sigma Chemical Company
dithiothreitol (DTT)	Boehringer-Mannheim
ethylenediaminetetraacetic acid (EDTA)	Sigma Chemical Company
film (X-ray)	Kodak/Fuji
Freund's adjuvant (complete & incomplete)	Sigma Chemical Company
formamide	BDH Chemicals
formaldehyde	BDH Chemicals
5-bromo-4-chloro-3-indolyl- β -D-galactoside (X-gal)	Sigma Chemical Company
hydrogen peroxide	Sigma Chemical Company
β -hydroxybutyryl-CoA	Sigma Chemical Company
isopropyl β -D-thiogalactoside (IPTG)	Sigma Chemical Company
leupeptin	Boehringer-Mannheim
malic acid	Sigma Chemical Company
malt extract	Difco Laboratories
1-methyl-3-nitro-1-nitrosoguanidine (NTG)	BDH Chemicals
2-(<i>N</i> -morpholino)ethane sulfonic acid (MES)	Sigma Chemical Company
morpholino propane sulfonic acid (MOPS)	Sigma Chemical Company
nitrocellulose	Amersham Life Sciences
oleic acid	Fisher Scientific
ovalbumin	Sigma Chemical Company

pepstatin A	Sigma Chemical Company
peptone	Difco Laboratories
phenol, buffer saturated	Gibco/BRL
Sephadex G-50	Pharmacia
sodium dodecyl sulfate (SDS)	Sigma Chemical Company
sodium sulfite	Sigma Chemical Company
sorbitol	Fisher Scientific
sucrose	BDH Chemicals
trichloroacetic acid	BDH Chemicals
tris(hydroxymethyl)aminomethane (Tris)	Boehringer-Mannheim
Triton X-100	Sigma Chemical Company
Tween 20 (polyoxyethylene sorbitan monolaurate)	Sigma Chemical Company
Tween 40 (polyoxyethylene sorbitan palmitate)	Sigma Chemical Company
yeast extract	Difco Laboratories
yeast nitrogen base without amino acids (YNB)	Difco Laboratories

2.1.2 *Enzymes*

calf intestinal alkaline phosphatase (CIP)	New England Biolabs
DNA ligase, T4	Gibco/BRL
DNA polymerase, Klenow fragment	New England Biolabs
DNA polymerase, T4	New England Biolabs
DNA polymerase, T7 sequenase (version 1.0)	United States Biochemicals
restriction endonucleases	New England Biolabs;
	Boehringer-Mannheim
ribonuclease A (RNase A)	Boehringer-Mannheim
trypsin	Boehringer-Mannheim
zymolyase 100T	ICN

2.1.3 *Molecular size standards*

1 kb DNA ladder	Gibco/BRL
Dalton Mark VII for SDS-PAGE (14.2, 20.1, 24, 29, 36, 45, 66 kDa)	Sigma Chemical Company
phosphorylase b (97.4 kDa)	
β -galactosidase (116 kDa)	Sigma Chemical Company
Prestained markers for SDS-PAGE (18.5, 27.5, 32.5, 49.5, 80, 106 kDa)	Sigma Chemical Company
Prestained markers for SDS-PAGE (6.5, 16.5, 25, 32.5, 47.5, 62, 83, 175 kDa)	Bio-Rad Laboratories
	New England Biolabs

2.1.4 *Radiochemicals and detection kits*

¹²⁵ I-protein A (30 mCi/mg, 0.1 Ci/μL, total protein A)	Amersham Life Sciences
α[³² P]-dATP (3000 Ci/mmol, 10 μCi/μL)	Amersham Life Sciences/ICN
random primer DNA labelling kit	Boehringer-Mannheim
Enhanced chemiluminescence (ECL), horseradish peroxidase detection kit	Amersham Life Sciences

2.1.5 *Plasmids*

i) *E. coli* vectors

pGEM5Zf(+)	Promega
pGEM7Zf(+)	Promega
pSP73	Promega
pBLUESCRIPT SKII(-)	Stratagene
pMAL-c2	New England Biolabs

ii) *Y. lipolytica* shuttle vectors

pINA 445	Dr. Claude Gaillardin (INRA, Grignon, France)
pINA 443	Dr. Claude Gaillardin (INRA, Grignon, France)
pTEC	Ms. Jennifer Smith (University of Alberta, Canada)
pSU	Mr. Arjuna Thiagarajah (U. of Alberta, Canada)
p37	Mr. Arjuna Thiagarajah (U. of Alberta, Canada)

iii) Mammalian shuttle vectors

pSG5	Dr. Steven Green (ZENECA, Cheshire, Great Britain)
pRSVCAT	Dr. Bruce H. Howard (NIH, Bethesda, MD, USA)

2.1.6 *Antibodies*

Table 2.1 lists the primary and secondary antibodies used in this study, the animal in which they were raised and the dilution used for immunoblot analysis. Development of antibodies against *Y. lipolytica* Pex9p, Pex2p, Pex16p, thiolase and isocitrate lyase and *S.*

cerevisiae acyl-CoA oxidase is described in *Section 2.7*. *Y. lipolytica* anti-Pex5p antibodies were raised in guinea pig and rabbit against a maltose-binding protein (MBP)-Pex5p fusion protein by Ms. Rachel Szilard (Szilard et al., 1995). Antibodies raised in rabbit against *S. cerevisiae* malate synthase were a gift from Dr. Andreas Hartig (Institute of Biochemistry and Molecular Cell Biology, Vienna, Austria). Anti-SKL antibodies were raised in rabbit against the peptide NH₂-CRYHLKPLQSKL-CO₂H linked to keyhole limpet hemocyanin (Gould et al., 1990) by Dr. John Glover (McMaster University, Hamilton, ON). Anti-AKI antibodies were raised in guinea pig against the carboxyl-terminal 12 amino acids of *Candida tropicalis* multifunctional enzyme (the peptide NH₂-CAIKLVGDKAKI-CO₂H) linked to keyhole limpet hemocyanin by Dr. John Aitchison (Aitchison, 1992). 12CA5 monoclonal antibodies against the influenza virus hemagglutinin antigen (HA) derived from mouse ascites fluid were purchased from the Berkeley Antibody Company (Berkeley, CA).

Secondary antibodies conjugated to horseradish peroxidase specific for rabbit, guinea pig and mouse IgG were purchased from Amersham Life Sciences and Sigma Chemical Company. Antigen-antibody complexes were detected by enhanced chemiluminescence (ECL) or ¹²⁵I-protein A (Amersham Life Sciences). For immunofluorescence microscopy, primary antibodies were diluted to concentrations 10-fold less than in Table 2.1. Fluorescein (FITC) and rhodamine (TRITC) conjugated secondary antibodies specific for rabbit or guinea pig IgG were purchased from Jackson ImmunoResearch Laboratories (West Grove, PA). For immunocytochemical staining of electron microscopic sections, 10 nm gold-conjugated antibodies specific for rabbit IgG were purchased from Sigma Chemical Company.

Table 2.1 Antibody, animal source and dilution used for immunoblot analysis.

antibody	animal ^a	name ^b	dilution
Primary:			
<i>Y. lipolytica</i> Pex2p	gp	Pay5-NN	1:2,000
	gp	Pay5-N	1:1,000
	rb	D260	1:500
	gp	P42-NN	1:10,000
	gp	P42-N	1:2,000
<i>Y. lipolytica</i> Pex5p	rb	Q2	1:1,000
	gp	P32-N	1:10,000
<i>Y. lipolytica</i> Pex9p	gp	Pay2-#2	1:500
	gp	Pay2-#1	1:300
	rb	Pay2-ONE	1:200
	rb	Pay2-TWO	1:300
<i>Y. lipolytica</i> Pex16p	gp	SOAP	1:4,000
	rb	H1	1:500
<i>Y. lipolytica</i> thiolase	rb	D646	1:10,000
	rb	D645	1:10,000
	gp	THI-N	1:25,000
	gp	THI-NN	1:25,000
<i>Y. lipolytica</i> isocitrate lyase	rb	E408	1:5,000
	gp	ICL-N	1:2,000
	gp	ICL-NN	1:2,000
<i>S. cerevisiae</i> acyl-CoA oxidase	gp	POX1-N	1:1,000
	gp	POX1-NN	1:1,000
	rb	E261	1:1,000
<i>S. cerevisiae</i> malate synthase	rb	MLS	1:1,000
SKL (peptide)	rb	Steve	1:1,000
AKI (peptide)	gp	AKI-#1	1:1,000
12CA5 (HA)	ms	HA	1:2,000
Secondary:			
anti-rabbit IgG:HRP	dk		1:30,000
anti-guinea pig IgG:HRP	rb		1:50,000
anti-mouse IgG:HRP	sh		1:10,000
anti-rabbit IgG:FITC	dk		1:200
anti-guinea pig IgG:TRITC	dk		1:200
anti-rabbit IgG:10 nm gold	gt		1:20

^arb, rabbit; gp, guinea pig; ms, mouse; dk, donkey; sh, sheep; gt, goat^bpreferred antibody is listed first

2.2 DNA manipulation

2.2.1 *Cultivation of Escherichia coli*

E. coli DH5 α was used for propagation of plasmid DNA. Cells were grown in LB medium (1% tryptone, 0.5% yeast extract, 1% NaCl (pH 7.5)) containing 100 μ g ampicillin/mL for plasmid maintenance. To introduce plasmid DNA into bacteria, DH5 α were transformed according to the manufacturer's (Gibco/BRL) protocol and plated onto LB-agar (2%) containing 100 μ g ampicillin/mL.

2.2.2 *Isolation of nucleic acids*

i) *E. coli*

Plasmid DNA was isolated from small scale bacterial cultures (2 mL) by the rapid alkaline lysis method (Ausubel et al., 1996). Purification of DNA from contaminating proteins was achieved by extraction with an equal volume of phenol/chloroform/isoamyl alcohol (25:24:1), followed by extraction with chloroform/isoamyl alcohol (24:1), prior to ethanol precipitation. Plasmid DNA was purified from contaminating genomic DNA and RNA by CsCl density centrifugation (Maniatis et al., 1982).

ii) *Y. lipolytica*

Total nucleic acids (DNA, RNA and plasmid where applicable) were isolated from *Y. lipolytica* by glass bead disruption in yeast NA buffer (10 mM Tris-HCl, pH 8.0, 100 mM NaCl, 1 mM EDTA, 2% (wt/vol) Triton X-100, 1% SDS). Cell debris was removed by

centrifugation, and the supernatant was extracted twice with phenol/chloroform/isoamyl alcohol (25:24:1) and once with chloroform/isoamyl alcohol (24:1). Total nucleic acids were precipitated by addition of 2.5 volumes absolute ethanol, incubation at -20°C for 30 min, and centrifugation at $16,000 \times g_{\text{max}}$ 4°C for 30 min. Salts were removed by a 70% ethanol wash. Plasmid DNA was rescued by dissolving the pellet in 10 μL of TE (10 mM Tris-HCl, pH 8.0, 1 mM EDTA) containing 25 μg RNaseA/mL and transformation of *E. coli*. High molecular weight genomic DNA was obtained by adding 50 μL TE/RNaseA to the nucleic acid pellet and allowing the pellet to slowly dissolve by warming and gentle agitation at 42°C for 30 min. A 10 mL overnight culture typically yielded 50 - 100 μg genomic DNA with an average size >12 kbp. For RNA, pellets were dissolved in 100 μL diethyl pyrocarbonate-treated water containing 0.1 U RNase-free DNase I/ μL to digest genomic DNA.

2.2.3 Restriction endonuclease digestion

Restriction endonuclease digestions were performed using the manufacturers' supplied buffer systems at the recommended temperatures. Occasionally, double digests with two enzymes of incompatible buffer systems or temperatures were required. In these cases, the enzyme requiring the lower salt concentration or temperature was performed first. After approximately 1 h, this enzyme was heat killed by incubation at 75°C for 15 min. The second enzyme was then added, and the buffer and temperature optimized.

2.2.4 Generation of blunt-ended DNA

Filling in of 5' overhangs and removal of 3' overhangs left after DNA restriction

digestion were performed by incubation with T4 DNA polymerase in the presence of 100 μ M dNTPs. Incubation at 37°C for 15 min was used to optimize the fill in reaction, while incubation at 11°C for 30 min was used to optimize the removal reaction. Both reactions were carried out simultaneously by incubation at room temperature for 1 h.

2.2.5 *Purification of DNA fragments*

DNA fragments were purified by agarose gel (1%) electrophoresis in 1 x TBE buffer (89 mM Tris-borate (pH 8.0), 89 mM boric acid, 2 mM EDTA, 5 μ g/mL ethidium bromide). Samples were loaded in gel dye (0.01% bromophenol blue, 0.01% xylene cyanol, 5% (wt/vol) glycerol) and run at ~10 V/cm using a Hoefer submarine gel apparatus (Hoefer Scientific Instruments, San Francisco, CA).

Bands of interest were excised from gels and electroeluted for 30 min in 0.5 x TBE using an International Biotechnology Instruments (IBI) (New Haven, CO) unidirectional electroelution apparatus. Two 175 μ L aliquots were removed from the salt trap, precipitated with 1 mL of -20°C absolute ethanol for 30 min, washed with 70% ethanol and dissolved in water.

2.2.6 *Ligation of DNA fragments*

The concentration of purified DNA fragments and cloning vectors was estimated by visual comparison of band intensity with molecular size standards of known concentration (1kb ladder, Gibco/BRL). 50 ng of vector was combined with a 3- to 5-fold molar excess of insert in ligase buffer (66 mM Tris-HCl, pH 7.5, 5 mM MgCl₂, 1 mM DTT, 1 mM ATP)

containing 0.1 U T4 DNA ligase/ μ L. For cases where fragments had identical 5' and 3' "sticky" ends or blunt ends (except for PCR amplified products), cloning vectors were treated with 0.1 U calf intestinal phosphatase (CIP)/ μ L at 37°C for 15 min, followed by heat inactivation at 75°C for 15 min. This treatment effectively minimized reclosure of vector. Sticky-end ligations were performed at 25°C for 2 h. Blunt-end ligations were performed at 16°C for 16 h.

2.2.7 *Labelling of DNA probes*

25 ng of the DNA fragment to be used as a probe for Southern or northern blot analysis was denatured by boiling for 5 min, followed by rapid cooling on wet ice. The denatured fragments were radioactively labelled with α [³²P]-dATP using a random primer labelling kit (Boehringer-Mannheim). After incubation for 1 h at 37°C, unincorporated label was removed by separation on a Sephadex G-50 spun column (Maniatis et al., 1982). Typically, probes were labelled to a specific activity of 10⁶ cpm/ng DNA, as determined by liquid scintillation counting.

2.2.8 *Southern blot analysis*

Southern blot analysis of yeast genomic DNA was performed by a protocol adapted from Ausubel et al. (1996). Genomic DNA was digested with the appropriate restriction endonuclease for >6 h. DNA fragments were separated by agarose gel electrophoresis (see *Section 2.2.3*), denatured by penetration with 0.5 M NaOH, 1.5 M NaCl for 30 min and neutralized by two 15 min washes in 0.5 M Tris-HCl, pH 8.0, 1.5 M NaCl. The DNA was

transferred in 5 X SSC (75 mM trisodium citrate, pH 7.0, 750 mM NaCl) to nitrocellulose by capillary action using a 2 cm stack of paper towels carefully cut to fit just inside the nitrocellulose so as not to short circuit the transfer. Successful transfers were performed within 30 min. DNA was fixed to the nitrocellulose by ultraviolet crosslinking at 1200 J/cm² using a UV Stratalinker 1800 (Stratagene, La Jolla, CA). Blots were prehybridized for 3 h at 60°C in 1 X hyb-buffer (1.25 X SSC, 0.2 X Denhart's solution (0.02% Ficoll, 0.02% polyvinylpyrrolidone, 0.02% BSA), 0.01% SDS, 20 mM sodium phosphate, pH 7.0, 4 µg denatured salmon sperm DNA/mL). Hybridization was carried out in the same buffer containing 30% (vol/vol) deionized formamide (Maniatis et al., 1982) and heat denatured probe (5 X 10⁵ cpm/mL) for 16 h at 42°C. Blots were washed at 50°C, 4 X 15 min in 1 X SSC, 0.1% SDS, wrapped in cellophane and exposed to film.

2.2.9 Northern blot analysis

To isolate RNA samples, *Y. lipolytica* E122 was grown overnight in YEPD, pelleted by centrifugation, washed in sterile water, and transferred to YPBO. Samples were removed at various times after transfer to YPBO, and nucleic acids were isolated by disruption of cells with glass beads as described in Section 2.2.1. 3 µL of RNA sample buffer (900 µL deionized formamide, 300 µL formaldehyde, 180 µL 20 X borate, 0.01% bromophenol blue, 0.01 % xylene cyanol) was combined with 1 µL of RNA sample and heated to 65°C for 5 min. RNA (10 µg per lane) was separated by electrophoresis on a 1% formaldehyde-agarose gel (1 g agarose, 5 mL 20 X borate, 86 mL water, 9 mL formaldehyde) in 1 X borate buffer (0.02 M boric acid (pH 8.3), 0.2 mM EDTA) containing 1.1 % (vol/vol) formaldehyde. Gels were run

at ~5 V/cm in a Hoefer submarine gel apparatus until the bromophenol blue migrated 75% of the gel length. Formaldehyde was removed from gels by washing 4 X 15 min in water. 5 µg ethidium bromide/mL was added to the first 15 min wash to visualize size markers and RNA. Gels were soaked 30 min in 10 X SSC, and transferred to nitrocellulose by capillary action (see *Section 2.2.8*) in 20 X SSC (0.3 M trisodium citrate, pH 7.0, 3 M NaCl) for 16 h. RNA was crosslinked, prehybridized, hybridized (northern hybridization buffer: 5 mL deionized formamide, 2.5 mL 20 X SSC, 1 mL 50 X Denhardt's, 0.25 mL 20% SDS, 0.1 mL 10 mg salmon sperm DNA/mL, 1.15 mL water) and washed as described in *Section 2.2.8*.

2.2.10 DNA sequencing

Various restriction endonuclease fragments of the *Y. lipolytica* *PEX9*, *PEX2* and *PEX16* genes were cloned into the vectors pGEM-7Zf(+), pGEM-5Zf(+) (Promega, Madison WI) and pBLUESCRIPT SKII(-) (Stratagene) for dideoxynucleotide sequencing of both strands from double-stranded templates (Sanger *et al.*, 1977; Zhang *et al.*, 1988) using the Sequenase system (United States Biochemicals). Reaction products were resolved on 5% Long Ranger™ acrylamide gels (J.T. Baker, Toronto, ON), containing 8 M urea and 1.2 X TBE. Gels were run on a Gibco/BRL sequencing gel apparatus in 0.6 X TBE at 60 watts per gel, dried and exposed to film.

The deduced Pex9p, Pex2p and Pex16p amino acid sequences were determined with the aid of the PC/GENE program (IntelliGenetics, Inc., Mountain View, CA) and compared to other protein sequences using the GENINFO(R) BLAST Network Service (Blaster) of the National Center for Biotechnology Information (Bethesda, MD).

2.2.11 Epitope-tagging of *Pex16p*

Various *YIPEX16* expression plasmids were constructed as follows. The *YIPEX16* gene, along with 965 bp and 16 bp of genomic DNA 5' and 3', respectively, to the open reading frame (ORF), was amplified by the polymerase chain reaction (PCR) from p16N1 (see Fig. 5.2 A) using primers 222 (5') and 224 (3') (Table 2.2) and inserted as a blunt-ended fragment into the *Sma*I site of pGEM7Zf(+) (Promega). The insert was excised with *Hind*III and ligated into a *Y. lipolytica* shuttle vector (pSU) to yield p16CN, which expresses mRNA for the full-length Pex16p. The *YIPEX16* gene was also amplified by PCR from p16N1 using primers 222 (5') and 261 (3') (Table 2.2) and inserted into pGEM7Zf(+), as above. The insert was excised and cloned into a shuttle vector, as above, to give p16Δ, which expresses mRNA for a Pex16p lacking the carboxyl-terminal amino acids Ser-Thr-Leu. p16Δ was cleaved with *Bgl*II, which cuts immediately prior to the stop codon, and the double-stranded oligonucleotide 7-HA (Table 2.2) encoding the HA-epitope (Wilson et al., 1984) was ligated into this site, creating p16HA, which expresses mRNA for a Pex16p fused near its carboxyl terminus to two copies of the HA-epitope (Pex16p-HA). p16CN, p16Δ, and p16HA were used to transform the *pex16-1* and *P16KO-8A* mutant strains.

2.2.12 Overexpression of the *YIPEX16* gene

For *YIPEX16* overexpression studies, the promoter and terminator regions of the *Y. lipolytica* thiolase gene were amplified by PCR from plasmid pS106 (Berninger et al., 1993) using the oligonucleotide pairs THpr5'/THpr3' and THtr5'/THtr3', respectively (Table 2.2). Amplified products were cloned into the plasmid pGEM7Zf(-) to create the expression

cassette vector pTEC with a unique *EcoRI* cloning site between the promoter and terminator regions. The ORF of the *YIPEX16* gene was amplified by PCR from p16N1 using oligonucleotides 249 (5') and 224 (3') (Table 2.2) and cloned into pGEM7Zf(+) as a blunt-ended fragment. The insert was excised by digestion with *EcoRI* and ligated into the *EcoRI* site of pTEC. The *YIPEX16* ORF flanked by the thiolase gene promoter and terminator regions was excised by digestion with *BglII* and cloned into the pSU shuttle vector to make the plasmid p16TH.

Table 2.2 Oligonucleotides used to amplify and clone various genetic products.

oligo	sequence	gene
Y1ICL-1	5' -ATT GAA TTC AGC ATC CAA GTG TCA CAT CAA AC-3'	<i>Y1ICL1</i>
Y1ICL-2	5' -ATT GAA TTC TAA AGC TTG GAC TTG AAC TG-3'	<i>Y1ICL1</i>
53	5' -CTC CCA AGC TTC TTA ATC TTT CAT AAG CTG-3'	<i>Y1PEX2</i>
55	5' -TAA AAG CTT ACC ATG GCT TCG GTT CTA CGA C-3'	<i>Y1PEX2</i>
222	5' -TCA TAA GCT TTG AGA ACC CCG AAG A-3'	<i>Y1PEX16</i>
224	5' -GCT TAA GCT TCC AAT CAT CAA TCG CTT AGA-3'	<i>Y1PEX16</i>
249	5' -TAC GAA TTC ATG ACG GAC AAG CTG GTC AA-3'	<i>Y1PEX16</i>
261	5' -TTA AGC TTA AAG ATC TGC GGT GAA GTA GTA CCG AT-3'	<i>Y1PEX16</i>
THpr5'	5' -CAG ATC TAA CCT ACC GG-3'	thiolase
THpr3'	5' -TGA ATT CGG TCC AAA GTG-3'	thiolase
THtr5'	5' -GAG TGA ATT CAC ATA CAA G-3'	thiolase
THtr3'	5' -GAG ATC TAC GAC CTG G-3'	thiolase
7-HA ^a	5' -GAT CCG CTA GCC ATG TAC CCA TAC GAC GTC CCA GAC GC GAT CGG TAG ATG GGT ATG CTG CAG GGT CTG D P L A M <u>Y P Y D V P D</u> TAC GCT GCC ATG TAC CCA TAC GAC GTC CCA GAC TAC ATG CGA CGG TAC ATG GGT ATG CTG CAG GGT CTG ATG <u>Y A A M Y P Y D V P D Y</u> GCT GCC ATG GGT AAG GGT GAA TAG AAG AGG AAG ATCT-3' CGA CGG TAC CCA TTC CCA CTT ATC TTC TCC TTC A A M G K G E -	HA- epitope- tag

^aThe hemagglutinin antigenic peptide sequence is *underlined*

2.3 Yeast cultivation and strain generation

2.3.1 Yeast strains and culture conditions

Y. lipolytica wild-type parental strains *E122* (*MatA*) and *22301-3* (*MatB*) (Table 2.3) used in this study were supplied by Dr. Claude Gaillardin, INRA, Grignon, France. Mutant, transformed, gene-disruption and diploid strains generated in these investigations (Table 2.3) are reported in the appropriate results sections. Strains not harbouring plasmids were grown for 15 h in YEPD medium (1% yeast extract, 2% peptone, 2% glucose) to an OD₆₀₀ of ~1.5, harvested by centrifugation at 2000 x g_{max} and then diluted 1:4 in YPBO medium (0.3% yeast extract, 0.5% peptone, 50 mM potassium phosphate, pH 6.7, 1% Brij-35 (polyoxyethylene 23-lauryl ether), 1% (wt/vol) oleic acid) and grown usually for 8 h to induce peroxisome proliferation. Strains transformed with plasmid were selected and maintained on YND-agar plates and were similarly grown as above in YND minimal medium (0.67% yeast nitrogen base without amino acids, 2% glucose) to an OD₆₀₀ of ~1.5 and then shifted to YNO medium (0.67% yeast nitrogen base without amino acids, 0.05% (wt/vol) Tween 40, 0.1% (wt/vol) oleic acid) for 8 h to induce peroxisome proliferation. Media were supplemented with uracil, leucine, lysine and histidine at 50 µg/mL as required. Growth was at 30°C.

2.3.2 Mutagenesis and genetic screening

Random mutagenesis of yeast cells with 1-methyl-3-nitro-1-nitrosoguanidine (NTG) (Nuttley et al., 1993) was performed on *Y. lipolytica* essentially as described by Gleeson and Sudbery (1988). Strain *E122* was grown in YEPD medium to an OD₆₀₀ of ~0.6. 50 mL of

Table 2.3 *Yarrowia lipolytica* strains and genotype used in this study.

Strains	Genotype
<i>E122</i>	<i>MatA, ura3-302, leu2-270, lys8-11</i>
<i>22301-3</i>	<i>MatB, ura3-302, leu2-270, his1</i>
<i>D1-AB</i>	<i>MatA/MatB, ura3-302/ura3-302, leu2-270/leu2-270, lys8-11 +, +his1</i>
<i>pex9</i>	<i>MatA, ura3-302, leu2-270, lys8-11, pex9-1</i>
<i>PEX9</i>	<i>MatA, ura3-302, leu2-270, lys8-11, pex9-1, pO2-2.2(LEU2)</i>
<i>P9KO</i>	<i>MatA, ura3-302, leu2-270, lys8-11, pex9::LEU2</i>
<i>P9KO-3</i>	<i>MatB, ura3-302, leu2-270, his1, pex9::LEU2</i>
<i>D9-22</i>	<i>MatA/MatB, ura3-302/ura3-302, leu2-270/leu2-270, lys8-11 +, -his1, pex9::LEU2 +</i>
<i>D9-301</i>	<i>MatA/MatB, ura3-302/ura3-302, leu2-270/leu2-270, lys8-11 +, +his1, pex9::LEU2/pex9::LEU2</i>
<i>pex2-1</i>	<i>MatA, ura3-302, leu2-270, lys8-11, pex2-1</i>
<i>PEX2</i>	<i>MatA, ura3-302, leu2-270, lys8-11, pex2-1, pBH7(LEU2)</i>
<i>P2KO-8A</i>	<i>MatA, ura3-302, leu2-270, lys8-11, pex2::LEU2</i>
<i>P2KO-9B</i>	<i>MatB, ura3-302, leu2-270, his1, pex2::LEU2</i>
<i>D2-OB</i>	<i>MatA/MatB, ura3-302/ura3-302, leu2-270/leu2-270, lys8-11 +, -his1, pex2-1 +</i>
<i>D2-O9</i>	<i>MatA/MatB, ura3-302/ura3-302, leu2-270/leu2-270, lys8-11 +, -his1, pex2-1, pex2::LEU2</i>
<i>D2-A9</i>	<i>MatA/MatB, ura3-302/ura3-302, leu2-270/leu2-270, lys8-11 -, -his1, -pex2::LEU2</i>
<i>D2-8B</i>	<i>MatA/MatB, ura3-302/ura3-302, leu2-270/leu2-270, lys8-11 -, -his1, pex2::LEU2 -</i>
<i>D2-89</i>	<i>MatA/MatB, ura3-302/ura3-302, leu2-270/leu2-270, lys8-11 -, -his1, pex2::LEU2 pex2::LEU2</i>
<i>pex16-1</i>	<i>MatA, ura3-302, leu2-270, lys8-11, pex16-1</i>
<i>P16TR</i>	<i>MatA, ura3-302, leu2-270, lys8-11, pex16-1, p16HC2(LEU2)</i>
<i>P16KO-8A</i>	<i>MatA, ura3-302, leu2-270, lys8-11, pex16::LEU2</i>
<i>P16KO-8B</i>	<i>MatB, ura3-302, leu2-270, his1, pex16::LEU2</i>
<i>D16-E1x8B</i>	<i>MatA/MatB, ura3-302/ura3-302, leu2-270/leu2-270, lys8-11 -, -his1, +pex16::LEU2</i>
<i>D16-8Ax22</i>	<i>MatA/MatB, ura3-302/ura3-302, leu2-270/leu2-270, lys8-11 -, -his1, pex16::LEU2 -</i>
<i>D16-P16x8B</i>	<i>MatA/MatB, ura3-302/ura3-302, leu2-270/leu2-270, lys8-11 -, -his1, pex16-1 pex16::LEU2</i>
<i>D16-P16x22</i>	<i>MatA/MatB, ura3-302/ura3-302, leu2-270/leu2-270, lys8-11 -, -his1, pex16-1 -</i>
<i>pex16-HA</i>	<i>MatA, ura3-302, leu2-270, lys8-11, pex16-1::PEX16HA-URA3</i>
<i>pex16-TH</i>	<i>MatA, ura3-302::PEX16TH-URA3, leu2-270, lys8-11, pex16-1</i>
<i>ΔICL1</i>	<i>MatA, ura3-302, leu2-270, lys8-11, icl1::LEU2</i>

this culture was washed twice with 50 mL of 0.1 M sodium citrate (pH 5.5) and incubated 30 min at 25°C in 50 mL of 0.1 M sodium citrate (pH 5.5), 25 µg NTG/mL with gentle agitation. Cells were then washed with five changes of water.

To isolate peroxisome assembly mutants, 0.1 volume of mutagenized cells was grown in 25 mL of YEPD for 3 h. This culture was diluted 1:100 into fresh YEPD, and 50 µL aliquots were plated onto YEPD agar plates. Plates were incubated until small (< 1 mm) colonies were visible (approximately 2 d). Colonies were replica plated onto YNO-(leucine, uracil, lysine)-agar plates and YNA-(leucine, uracil, lysine)-agar plates (YNA; 0.67% yeast nitrogen base without amino acids, 2% sodium acetate). Colonies that could grow on glucose and acetate-containing media but not on oleic acid-containing media (ole⁻ for oleic acid non-utilization) were recovered and stored on YEPD-agar plates for further analysis (*performed by Mr. Anthony Brade for pex9, and Ms. Rachel Szilard for pex2-1 and pex16-1*).

Secondary screens for selection of the *pay* phenotype (peroxisome assembly mutant of *Y. lipolytica*, now known as the *pex* phenotype) included mislocalization of catalase from a 20KgP fraction (enriched for peroxisomes and mitochondria) to a 20KgS fraction (enriched for cytosol) and the absence of normal peroxisomes as detected by electron microscopy and immunofluorescence microscopy.

2.3.3 Mating and genetic analysis

Mutants were characterized by standard genetic techniques for *Y. lipolytica* (Gaillardin et al., 1973). To generate diploid strains, haploid strains were pregrown on PSM-agar (0.5% yeast extract, 0.5% (NH₄)₂SO₄, 0.2% KH₂PO₄, 2% glucose) overnight at 30°C.

Haploid strains of opposite mating type were mixed and grown on YM-agar (0.3% yeast extract, 0.5% peptone, 0.3% malt extract) 4 d at 25°C. Diploids were selected on YND-(ura, leu)-agar and tested for growth on oleic acid media.

Diploid strains of *Y. lipolytica* were transferred to malt extract-agar (0.5% malt extract) for spore formation. Sporulating cultures turn brown after growing 8 d at 25°C. Random spore analysis was performed by removing a loop of brown culture and incubating in 5 mL of 50 mM sodium citrate (pH 5.5), 0.5 mg zymolyase 20T overnight at 30°C with vigorous shaking. Spores were washed with 4 x 10 mL sterile water, resuspended in 10 mL water, sonicated for 1 min and plated onto YEPA-agar (10 - 50 µL per plate). Cosegregation of the auxotrophic marker used for gene disruption and the ole⁻ phenotype was checked in haploid cells.

2.3.4 Transformation of *Y. lipolytica*

Y. lipolytica strains were grown overnight in YEPA (1% yeast extract, 2% peptone, 2% sodium acetate), diluted 1:10 in fresh YEPA and grown with vigorous shaking to an OD₆₀₀ of 0.8 - 1.0. 30 mL of this culture was harvested by centrifugation, resuspended in 10 mL of 10 mM Tris-HCl (pH 7.5), 1 mM EDTA, 100 mM lithium acetate and incubated for 30 min at 30°C with gentle agitation. 100 µL of 1 M DTT was added, and the culture was incubated for 15 min more. Cells were washed once with water at room temperature, once with water at 4°C and once with 1 M sorbitol at 4°C. The volume of cells was determined, and an equal volume of 1 M sorbitol (4°C) was added. A 20 µL aliquot of the cell suspension was combined with 1 µL DNA, placed between the bosses of a chilled microelectroporation

chamber and subjected to electroporation in a Gibco/BRL Cell-Porator™ set to 16 k Ω , 330 μ F, low resistance and 250 V. A discharge of 1.6 kV across the sample was typically observed. Cells were transferred to 100 μ L cold 1 M sorbitol and immediately spread on YNA-agar containing 1 M sorbitol and appropriate amino acids. Colonies were observed after 3 d of growth at 30°C.

2.3.5 Construction of yeast gene-deletion-conversion strains

Various gene-deletion and gene-conversion strains were generated by targeted integrative disruption as described by Rothstein (1991). For gene-deletion, DNA constructs were made that contained an auxotrophic marker (*e.g.* *LEU2*) flanked on both sides by fragments of the genes to be deleted. For gene-conversion, DNA constructs were made that contained a copy of the *URA3* auxotrophic marker in tandem with the gene of interest. Linear fragments were used to transform *Y. lipolytica* wild-type strains (gene-deletion) and mutant strains (gene-conversion). Integration by homologous recombination was selected for by growth on minimal media. Transformants (*i.e.* leucine or uracil prototrophic colonies) were replica plated onto YNO-(plus appropriate amino acids)-agar to screened for the ole⁻ phenotype (typically ~1%). Integration into the correct genomic locus was also checked by Southern blot analysis.

2.3.5.1 Integrative disruption of the *YlPEX9* gene

Integrative disruption of the *Y. lipolytica* *PEX9* gene was done with the *LEU2* gene of *Y. lipolytica*. The plasmid pINA445 was cleaved into two fragments with *Bgl*II. The ends

were made blunt with T4 DNA polymerase. The fragment containing the *LEU2* gene was isolated by electroelution after agarose gel electrophoresis. The isolated DNA fragment was cleaved with *Eco47III*. The *Eco47III*/blunt-*BglII* fragment containing the *LEU2* gene was inserted into the *YIPEX9* gene cleaved with *EagI* and *HindIII* made blunt with the Klenow fragment of DNA polymerase I. This construction replaced 222 bp in the coding region of the *YIPEX9* gene ORF with an approximately 2.1 kbp fragment. A construct with the ORF of the *LEU2* gene transcribed in the direction opposite to that of the *YIPEX9* gene was selected. This construct was digested with *SalI* and *BamHI* to liberate the *LEU2* gene flanked by 697 bp and 1224 bp of the *YIPEX9* gene at its 5' and 3' ends, respectively. This linear molecule was used to transform *Y. lipolytica* wild-type strains *E122* and *22301-3* to leucine prototrophy, yielding strains *P9-KO* and *P9KO-3*, respectively.

2.3.5.2 Integrative disruption of the *YIPEX2* gene

Integrative disruption of the *Y. lipolytica* *PEX2* gene was accomplished by replacing a 1480 bp *SnaBI/BglII* fragment, which included most of the ORF of the *YIPEX2* gene, with a 2.1 kbp *Eco47III/BglII* fragment from pINA445 containing the *LEU2* gene of *Y. lipolytica*. The construct was digested with *BamHI* and *HindIII* to liberate the *LEU2* gene flanked by 125 bp and 423 bp of the *YIPEX2* gene at its 5' and 3' ends respectively. This linear DNA fragment was used to transform *Y. lipolytica* *E122* and *22301-3* to leucine prototrophy to make the strains *P2KO-8A* and *P2KO-9B* respectively.

2.3.5.3 Integrative disruption of the *YIPEX16* gene

Targeted integrative disruption of the *Y. lipolytica* *PEX16* gene was performed with the *LEU2* gene of *Y. lipolytica*. A 2.2 kbp *Sph*I fragment containing the *LEU2* gene was ligated into the *YIPEX16* gene cleaved with *Sph*I, replacing an 850 bp fragment. This construct was digested with *Cla*I and *Bam*HI to liberate the *LEU2* gene flanked by 485 bp and 135 bp of the *YIPEX16* gene at its 5' and 3' ends, respectively. Integrative transformation of *Y. lipolytica* *E122* and *22301-3* was shown by leucine prototrophy, and selection of *YIPEX16* gene deletion was indicated by the inability to metabolize oleic acid in the strains *P16KO-8A* and *P16KO-8B*, respectively.

2.3.5.4 Integrative disruption of the *Y. lipolytica* isocitrate lyase gene (*ICL1*)

The gene encoding *Y. lipolytica* isocitrate lyase (ICL) was previously cloned, and ICL was shown to contain a carboxyl-terminal SKL (Barth and Scheuber, 1993). Therefore, it is likely to reside in the peroxisomal matrix. The *ICL1* gene was amplified from *Y. lipolytica* genomic DNA using the primers *YIICL-1* and *YIICL-2* (Table 2.2) for the 5' and 3' ends, respectively. These primers were engineered with *Eco*RI sites near their 5' ends. The PCR fragment (1668 bp) was gel purified and cloned into the *Sma*I site of pGEM7Zf(+) as a blunt-end fragment. A blunt-end fragment containing the *LEU2* gene (see Section 2.3.5.1) was ligated into the *ICL1* gene cleaved with *Eco*RV, replacing 346 bp of the *ICL1* gene. This construct was digested with *Eco*RI which liberates the *LEU2* gene flanked by 732 bp and 590 bp of the *ICL1* gene on its 5' and 3' ends respectively. Integrative transformation of *Y. lipolytica* *E122* was shown by leucine prototrophy. *ICL1* gene deletion strains were selected

by the inability to grow on oleic acid (strain $\Delta ICL1$). Immunoblot analysis of wild-type lysates shows two polypeptides (62 and 64 kDa) that react with anti-SKL antibodies. The 64 kDa anti-SKL reactive band is absent in lysates of the $\Delta ICL1$ strains, suggesting that this protein is ICL (Fig. 2.1).

2.3.5.5 Integration of the construct encoding Pex16p-HA

The *YIPEX16* construct encoding Pex16p-HA (see Section 2.2.11) was integrated into the *Y. lipolytica* genome by gene conversion (Rothstein, 1991) to control for gene copy number and to ensure stability of recombinant gene expression. The p16HA insert, along with the *URA3* gene, was cloned into the plasmid pSP73 (Promega), creating plasmid p16HA-int. Plasmid p16HA-int was digested with *Cla*I, which cuts in the *YIPEX16* promoter region. This construction will target integration to the *pex16* locus. Linearized DNA was introduced into the *pex16-1* mutant by electroporation, and Ura⁺/ole⁺ transformants were selected, yielding strain *pex16-HA*.

2.3.5.6 Integration of the *Y. lipolytica* PEX16 overexpression construct

The *YIPEX16* overexpression construct (the *PEX16* ORF flanked by the thiolase promoter/terminator regions (see Section 2.2.12)) was integrated into the *Y. lipolytica* genome by gene conversion (Rothstein, 1991) to control for gene copy number and to ensure stability of recombinant gene expression. The p16TH insert, along with the *URA3* gene, was cloned into the plasmid pSP73 creating plasmid p16TH-int. Plasmid p16TH-int was digested with *Pst*I, which cuts in the *URA3* coding region. This construct will target integration

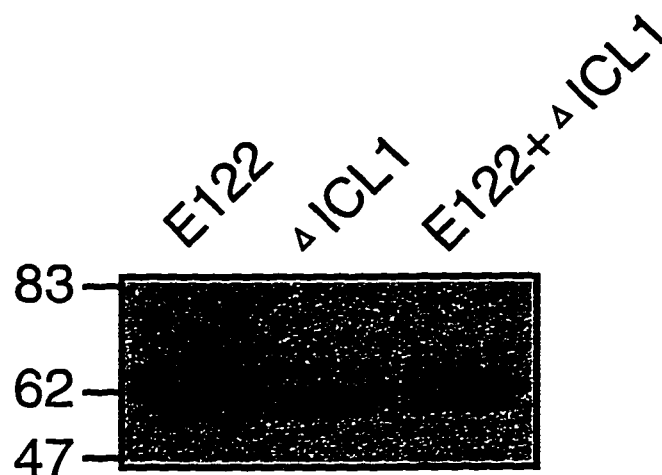


Figure 2.1 **Identification of the *Y. lipolytica* ICL protein as an anti-SKL immunoreactive peptide.** Wild-type *E122* and $\Delta ICL1$ gene-deletion strains were grown in YEPD to an $OD_{600} \sim 1.5$, transferred to YPBO (1:4 dilution) and grown for an additional 8 h. Total cell lysates were prepared (see *Section 2.4.1*), and 30 μ g of protein was subjected to SDS-PAGE, blotted to nitrocellulose and probed with anti-SKL antibodies. The *numbers* at the left indicate the migration of molecular weight standards in kDa. Of the two bands in *lane* $\Delta ICL1$, the upper 62 kDa band, corresponds to the lower band in *lane* *E122*. The lower band in *lane* $\Delta ICL1$ is a commonly observed degradation product of the 62 kDa anti-SKL polypeptide. A direct comparison by mixing 25 μ g of $\Delta ICL1$ lysate with 5 μ g of *E122* lysate is shown in *lane* $\Delta ICL1 + E122$. Therefore, the upper 64 kDa band is ICL.

to the *ura3-302* locus. Linearized DNA was introduced into the *pex16-1* mutant by electroporation, and Ura⁺/ole⁺ transformants were selected to give strain *pex16-TH*.

2.4 Preparation of subcellular fractions

2.4.1 Whole cell lysates

Total cellular protein was isolated by glass bead (425-600 microns) disruption of cells in 25 mM Tris-HCl (pH 7.5), 100 mM KCl, 1 mM EDTA, 10% (wt/vol) glycerol, 0.1 mM DTT plus protease inhibitors (1 mM phenylmethylsulfonyl fluoride (PMSF), 1 µg pepstatin/mL, 1 µg chymostatin/mL, 1 µg antipain/mL and 1 µg leupeptin/mL). Suspensions were vortexed 2 X 30 s. Unbroken cells and glass beads were pelleted by centrifugation (16,000 × g_{\max} for 5 min), and the supernatant was carefully removed.

2.4.2 Organelle isolation

Subcellular fractions were prepared from *Y. lipolytica* strains by homogenization of spheroplasts and differential centrifugation. Spheroplasts were prepared by treatment of cultures with 1 mg zymolyase 100T in 4 mL zymolyase buffer (0.5 M KCl, 5 mM MOPS (pH 7.2), 10 mM Na₂SO₃) per g of cells at 30°C for 30 min with gentle agitation. All subsequent manipulations were performed at 4°C. Spheroplasts, collected by centrifugation in a Beckman JS13.1 rotor at 2500 × g_{\max} for 8 min. were mechanically homogenized (Potter-Elvehjem homogenizer, 20 strokes, 1000 rpm) in 3 mL of MES/Sorb buffer per g of cells

(MES/Sorb: 5 mM MES (pH 5.5), 1 M sorbitol, 1 mM PMSF, 1 μ g pepstatin/mL, 1 μ g chymostatin/mL, 1 μ g antipain/mL and 1 μ g leupeptin/mL). Postnuclear supernatant (PNS) fractions were prepared by centrifugation of lysates in a Beckman JS13.1 rotor at $1000 \times g_{\max}$ for 10 min. Organellar pellets (20KgP) enriched for peroxisomes and mitochondria and a supernatant (20KgS) enriched for cytosol were prepared by centrifugation of PNS fractions in a Beckman JS13.1 rotor at $20,000 \times g_{\max}$ for 30 min. High speed particulate fractions (200KgP) containing all remaining membranes and vesicles were separated from the cytosol (200KgS) by centrifugation of 20KgS fractions in a Beckman Type 80 rotor at $200,000 \times g_{\max}$ for 30 min.

20KgP fractions were subjected to isopycnic centrifugation on a discontinuous sucrose (25%, 35%, 42%, 53%, (wt/wt)) gradient in 5 mM MES (pH 5.5) at $84,500 \times g_{av}$ for 1 h in a Beckman VTi50 rotor. Some samples were also subjected to centrifugation on a linear 16-56% (wt/wt) sucrose gradient in 50 mM MES (pH 5.5) at $84,500 \times g_{av}$ for 1 h in a Beckman VTi50 rotor or at $197,000 \times g_{av}$ for 16 h in a Beckman SW41Ti rotor. Gradient fractions were taken from the bottom of punctured tubes. 18 fractions of either 2 mL (VTi50 rotor) or 0.72 mL (SW41Ti rotor) were collected. Sucrose concentration was determined by refractometry and density (specific gravity) was calculated from these values. Samples were immediately prepared for SDS-PAGE by boiling in sample buffer for 5 min (Laemmli, 1970).

Isolation of the complex formed by peroxisomes, endoplasmic reticulum and Golgi in *pex2-1* and *P2KO-8A* cells was performed by flotation on a two-step sucrose gradient (performed by Dr. Vladimir Titorenko). Samples were loaded at the bottom of ultracentrifuge tubes and overlaid with 2.3 mL of 60% (wt/vol) sucrose and then with 2.3 mL of

35% (wt/vol) sucrose. Samples were subjected to centrifugation in a Beckman SW50.1 rotor at $200,000 \times g_{av}$ for 16 h. 18 fractions of 250 μ L were collected from the bottoms of tubes.

2.4.3 *Membrane extraction*

Peroxisomal membrane fractions were prepared by extraction of purified peroxisomes (0.1 mg protein/mL) isolated from sucrose gradients (1 mL final volume, frozen and thawed once) with various high pH buffers at 4°C for 30 min with occasional agitation, followed by centrifugation at $200,000 \times g_{max}$ at 4°C for 30 min in a Beckman TLA 120.2 rotor. Ti8 buffer (10 mM Tris-HCl, pH 8.5, 5 mM EDTA, 0.5 mM PMSF) was used to lyse peroxisomes. Centrifugation of Ti8-treated peroxisomes creates a membrane pellet of integral and peripheral membrane-associated proteins. TS buffer (Ti8 containing 0.5 M KCl) extracts loosely associated proteins from membranes and is more stringent than Ti8 buffer (Erdmann and Blobel, 1995). CO3 buffer (0.1 M Na_2CO_3 , pH 11.5, 0.5 mM PMSF) extracts all peripheral membrane proteins leaving only integral membrane proteins (Fujiki et al., 1982). Protein in soluble fractions was precipitated by the addition of trichloroacetic acid to 10% (vol/vol) and bovine serum albumin to 0.1 mg/mL final concentration, incubation at 4°C for 1 h with occasional agitation, and centrifugation at 4°C for 30 min at maximum speed in a microfuge. Samples were washed with 80% (vol/vol) acetone, briefly air dried, dissolved in SDS-PAGE sample buffer (62.5 mM Tris-HCl (pH 6.8), 2% SDS, 10% sucrose, 10 mM DTT, 0.001% bromophenol blue) (Laemmli, 1970), boiled and subjected to SDS-PAGE and immunoblot analysis.

2.4.4 *Protease protection*

Protease protection experiments were performed on 20KgP fractions (100 µg of protein in a 50 µL volume) isolated in the absence of protease inhibitors. 0, 2, 10, or 25 µg of trypsin was added to the fractions, with or without 0.5% (vol/vol) Triton X-100 to disrupt membranes. Reactions were incubated at 4°C for 30 min and terminated by addition of hot SDS-PAGE sample buffer and immediate boiling. Samples were subjected to SDS-PAGE, followed by immunoblotting.

2.5 **Analysis of proteins**

2.5.1 *Electrophoresis and protein blotting*

Protein samples denatured by boiling 5 min in SDS-PAGE sample buffer were separated by discontinuous 8% or 10% SDS-PAGE systems (Laemmli, 1970). Bio-Rad 10 well, 0.75 mm, mini-gel apparatus were mainly used and run at 50 - 200 V in running buffer (50 mM Tris-HCl, pH 8.8, 0.4 M glycine, 0.1% SDS). Proteins were directly visualized by staining gels in 0.1% Coomassie Brilliant Blue (R-250), 10% (vol/vol) acetic acid, 35% (vol/vol) methanol. Proteins were electrophoretically transferred to nitrocellulose (1 h at 250 mA or 16 h at 100 mA) in transfer buffer (20 mM Tris-HCl (pH 7.5), 150 mM glycine, 20% (vol/vol) methanol) using a Bio-Rad Western Transblotter apparatus with plate electrodes (Burnette, 1981).

2.5.2 *Immunoblot analysis*

For immunoblot analysis, protein-nitrocellulose blots (*Section 2.5.1*) were blocked in TBST (20 mM Tris-HCl, pH 7.5, 150 mM NaCl, 0.05% (wt/vol) Tween 20) containing 1% skim milk powder or bovine serum albumin for 1 h. Blocking solution was replaced by primary detection antibodies diluted in TBST-1% skim milk (see Table 2.1) and incubated 1.5 h. Blots were washed 4 X 15 min with TBST and incubated with secondary detection antibodies or ^{125}I -protein A (0.5 $\mu\text{Ci/mL}$) diluted in TBST for 30 min. Blots were washed 4 X 15 min with TBST. ^{125}I -protein A blots were exposed to film (Kodak XAR-5) with an intensifying screen. Blots probed with HRP-conjugated secondary antibodies were processed by ECL (Amersham Life Sciences) and exposed to film (Fuji RX). Quantitation of immunoblots was performed as described (Szilard et al., 1995). Densitometry was performed using a LKB Ultrosan XL laser densitometer (Bromma, Sweden).

2.5.3 *Protein determination*

Total protein was measured as described by Bradford (1976) using BioRad protein assay dye and known concentrations of ovalbumin for comparison. Samples were mixed by vortexing, incubated 5 min at room temperature and quantitated in a Beckman DU-60 spectrophotometer at 595 nm.

2.5.4 *Enzymatic assays*

Enzymatic activities of the peroxisomal markers catalase (Luck, 1963; Baudhuin et al., 1964) and β -hydroxyacyl-CoA dehydrogenase (Osumi and Hashimoto, 1979); the mitochondrial markers cytochrome *c* oxidase (Douma et al., 1985; Cooperstein and Lazarow, 1951) and fumarase (Tolbert, 1974); the endoplasmic reticulum marker NADPH:cytochrome *c* reductase (Roberts et al., 1991); the Golgi marker guanosine diphosphatase (Abeijon et al., 1989); the vacuolar marker alkaline phosphatase (Thieringer et al., 1991) and the plasma membrane marker vanadate-sensitive ATPase (Roberts et al., 1991) were determined by established methods and described here briefly.

Catalase activity was measured by combining 10 μ L of sample and 940 μ L of 50 mM potassium phosphate buffer (pH 7.5). The OD₂₄₀ of the mixture was set to 0 and 50 μ L of 0.3% H₂O₂ was added. The consumption of H₂O₂ was measured for 1 min as a change in OD₂₄₀.

β -hydroxyacyl-CoA dehydrogenase activity was measured by combining 10 μ L of sample and 990 μ L of buffer containing 0.1 M Tris-HCl (pH 10.2), 0.1 M KCl, 0.1% (wt/vol) Triton X-100, 1 mM NaN₃, 0.1 M NAD⁺, and 10 μ M β -hydroxybutyryl-CoA as substrate. The production of NADH was measured at 340 nm for 5 min.

Cytochrome *c* oxidase activity was measured by combining 10 μ L of sample and 2.5 mL of buffer containing 0.38 mg/mL reduced horse heart cytochrome *c* in 0.3 M ammonium acetate (pH 7.4), 1% (wt/vol) Triton X-100. Cytochrome *c* was reduced by the addition of a minimal amount of sodium hydrosulfite. Excess sodium hydrosulfite was removed by gel filtration on Sephadex G-50 in ammonium acetate buffer. Oxidation of cytochrome *c* was

monitored as a decrease in OD₅₅₀ for 1 min.

Fumarase activity was measured by combining 50 μ L of sample and 950 μ L of buffer containing 50 mM potassium phosphate (pH 7.5) and 15 mM L-malate as substrate. The production of fumarate was measured as an increase in OD₂₄₀.

NADPH:cytochrome *c* reductase activity was measured by combining 50 μ L of sample and 900 μ L of buffer containing 25 mM potassium phosphate (pH 7.5), 1 mM KCN and 0.1 mg/mL oxidized cytochrome *c*. The NADPH-independent rate was measured at 550 nm for 1 min, followed by measurement of the NADPH-dependent rate for 1 min after addition of 50 μ L of 15 mM NADPH.

Alkaline phosphatase activity was measured by combining 50 μ L of sample and 950 μ L of buffer containing 0.1 M glycine (pH 8.4), 10 mM MgCl₂, 0.1% (wt/vol) Triton X-100 and 6 mM *p*-nitrophenylphosphate as substrate. The production of *p*-nitrophenyl was monitored at 405 nm.

Guanosine diphosphatase activity was measured by combining 25 μ L of sample and 25 μ L of buffer containing 20 mM imidazole-HCl (pH 7.4), 2 mM CaCl₂, 0.1% (wt/vol) Triton X-100 and 7 mM GDP as substrate. Reactions were incubated at 30°C for 1 h and stopped by addition of 5 μ L of 10% SDS and 445 μ L water. Inorganic phosphate was measured by the addition of 100 μ L of the reaction mixture to 800 μ L of 4.2% ammonium molybdate, 0.045% malachite green and 0.1% (wt/vol) Triton X-100, incubation for 1 min at room temperature, addition of 100 μ L of 34% sodium citrate-dihydrate, incubation for 30 min at room temperature and measurement of OD₆₆₀.

Vanadate-sensitive (azide-resistant) ATPase activity was measured by combining 25

μL of sample and 25 μL of buffer containing 10 mM MES (pH 6.0), 5 mM NaN_3 , 5 mM MgCl_2 , 5 mM Na_2ATP , 5 mM phosphoenolpyruvate and 25 μg pyruvate kinase. Reactions were incubated at 30°C for 1 h, stopped by the addition of 5 μL 10% SDS and 445 μL water. Inorganic phosphate was measured as previously described.

2.6 Microscopy

2.6.1 *Immunofluorescence Microscopy*

i) Yeast Cells: Immunofluorescence microscopy of yeast cells was performed essentially as described (Pringle et al., 1991). Cultures were pre-fixed for 3 min by direct addition of formaldehyde to a final concentration of 3.7% (vol/vol). Cells were harvested and resuspended in 30 mM Tris-HCl (pH 6.5), 1.5 mM MgCl_2 , 3.7% formaldehyde and fixed for 1 h at room temperature. These cells could be stored overnight at 4°C or immediately used. Cells were permeabilized by digestion in 100 mM potassium phosphate (pH 7.5), 1.2 M sorbitol, 28 mM β -mercaptoethanol, 1 mg zymolyase 100T/mL for 1 h at 30°C. Cells were post-fixed by incubation for 6 min in -20°C methanol and for 30 s in -20°C acetone.

Guinea pig anti-thiolase and rabbit anti-isocitrate lyase antibodies were used for primary hybridizations (1 h in TBST, 1% milk). Fluorescein-conjugated anti-rabbit IgG and rhodamine-conjugated anti-guinea pig IgG were used for secondary hybridizations (1 h in TBST 1% milk). 10 washes with TBST were performed after each hybridization. Slides were viewed on an Olympus BX50 microscope. Photographs were taken with an Olympus PM20 automated camera and Kodak Tmax-400 film.

ii) Mammalian cells (*performed by Ms. Jennifer Smith*): Chinese hamster ovary (CHO) strains K1 and ZR02p66 (obtained from Dr. Yukio Fujiki, Kyushu University, Japan) were maintained in F-12 medium (Gibco/BRL) containing 10% (vol/vol) fetal calf serum. The *YIPEX2* gene was amplified by PCR from pHDO4 using primers #55 and #53 (Table 2.2) at the 5' and 3' ends, respectively. The amplified fragment was gel purified, cloned into pGEM7Zf(+), and subjected to partial digestion with *EcoRI* and complete digestion with *BamHI*. The appropriate fragment was subcloned into plasmid pSG5 digested with *EcoRI* and *BamHI*. Transcription of *YIPEX2* is therefore under the control of the constitutive SV40 early promoter (Green et al., 1988). Transfections (performed as described by Tsukamoto et al. (1991)) contained 1.7 µg of the expression plasmid pSG5-*YIPEX2* and 0.3 µg of pRSVCAT expressing bacterial chloramphenicol acetyl transferase (Gorman et al., 1982) or 2 µg of pRSVCAT. Immunofluorescence microscopy was performed as described by Walton et al. (1992).

2.6.2 Electron Microscopy

Electron microscopy was performed on whole cells harvested 8 h after shifting cells from glucose- to oleic acid-containing medium. Cells were fixed for 20 min at room temperature in 1.5% KMnO₄, dehydrated in a graded ethanol series (60, 80, 95, 98, 100 %, (vol/vol)), incubated 1 h in 50% ethanol/50% Taab 812, and embedded in Taab 812 resin (Merivac, Halifax, NS). Ultrathin sections were cut (*performed by Mrs. Honey Chan*) and viewed with a Philips 410 electron microscope. Electron microscopic examination of

organelles was performed on 20KgP and sucrose gradient fractions. Sucrose fractions were fixed for 30 min at 4°C by direct addition of glutaraldehyde to a final concentration of 0.5% (wt/vol), and organelles were isolated by centrifugation in a microfuge for 30 min at 4°C at maximum speed. Samples were fixed in 6% (wt/vol) glutaraldehyde and postfixed in 0.5% (wt/vol) OsO₄, 2.5% K₂Cr₂O₇ in 0.1 M sodium cacodylate buffer (pH 7.2), for 1 h each, at 4°C. Samples were poststained in uranyl acetate and prepared for electron microscopic sectioning as before.

For immunocytochemical staining of electron microscopic sections, whole cells or organelle fractions were fixed in 3% (wt/vol) paraformaldehyde, 0.2% (wt/vol) glutaraldehyde in 0.1 M sodium cacodylate (pH 7.2) for 1 h at 4°C. Samples were washed once in 0.1 M sodium cacodylate, dehydrated in a graded methanol series (50, 70, 90% (vol/vol)) at -20°C and embedded in LR Gold resin according to the manufacturer's instructions (Electron Microscopy Sciences, Fort Washington, PA). Ultrathin sections were cut and mounted onto carbon-coated nickel grids. Grids were sequentially incubated in phosphate buffered saline (PBS) (137 mM NaCl, 2.7 mM KCl, 4.3 mM Na₂HPO₄, 1.4 mM KH₂PO₄, pH 7.4)-1% BSA, PBS-1% gelatin and PBS-20 mM glycine (pH 8.3) for 10 min each, and then incubated for 90 min with primary antibody diluted in PBS-1% BSA at 10 times strength (see Table 2.1). After 90 min, grids were washed with 5 exchanges of PBS-1% BSA (1 min each) and incubated for 1 h with goat anti-rabbit IgG antibodies conjugated to 10 nm gold, diluted 1:20 in PBS-1% BSA. Grids were washed with 5 exchanges of PBS (1 min each), postfixed for 10 min in PBS-2.5% (wt/vol) glutaraldehyde, washed with 5 exchanges of water (1 min each) and poststained with uranyl acetate and lead citrate.

2.7 Antibody production

Polyclonal antibodies were elicited against proteins synthesized as fusions with the maltose-binding protein (MBP) of *E. coli*. Fusions were made by inserting fragments of genes encoding the various proteins, in-frame and downstream of the ORF encoding MBP in the vector pMAL-c2 (New England Biolabs). *E. coli* (strain DH5 α) transformed with these fusion constructs was pregrown to an OD₆₀₀ of ~0.5 in LB-ampicillin. Fusion protein synthesis was induced by addition of IPTG to 0.1 M. After 2.5 h of induction, fusion proteins were affinity purified on an amylose resin column according to the manufacturer's instructions. MBP-fusion proteins were further purified by SDS-PAGE on 10% preparative gels (Fujiki et al., 1984). Bands of the appropriate molecular weight were excised, and the protein was electroeluted by placing gel slices into dialysis tubing containing 10 mL buffer (0.2 M Tris-Acetate, pH 7.4, 1% SDS, 10 mM DTT). Electrophoresis was performed in a large Hoefer submarine gel apparatus in 50 mM Tris-Acetate (pH 7.4), 0.1% SDS, at 60 V, 4°C for 4 h. Eluted proteins were dialyzed against several changes of 50 mM ammonium bicarbonate, lyophilized and dissolved in a minimal amount of distilled, deionized water. 1 mL injections, enough for one rabbit or two guinea pigs, contained 250 μ g fusion protein, 0.01 % SDS and 50% Freund's adjuvant. Animals were injected subcutaneously at six week intervals, and sample bleeds were taken 10 d after third and subsequent injections. Serum was cleared of cells by clotting at room temperature for 1 h and at 4°C for >1 h, followed by centrifugation at 2000 \times g_{max} for 15 min at room temperature. Details of fusion protein constructs and antisera titres are described in the next five sections.

2.7.1 *Anti-Pex9p antibodies*

To produce antibodies to Pex9p, a 732 bp fragment of the *YIPEX9* ORF encoding amino acid residues 76 to 318 of Pex9p was excised with *SlyI*, made blunt with T4 DNA polymerase, and inserted into the *XmnI* site of pMAL-c2. In-frame fusions downstream of the ORF encoding the maltose-binding protein were checked by boiling cells from induced cultures in 1 X SDS-PAGE sample buffer and looking for induced bands of the correct size on coomassie stained SDS-PAGE gels. Fusion protein purification and antibody production in two rabbits (PAY2-ONE, PAY2-TWO) and two guinea pigs (PAY2-#1, PAY2-#2) were performed as described above. Antibodies produced by guinea pig PAY2-#2 (used at 1:500 dilution) or rabbit PAY2-TWO (1:300 dilution) were preferentially used.

2.7.2 *Anti-Pex2p antibodies*

To produce antibodies to Pex2p, a 1648 bp *EcoRI/BamHI* fragment encoding amino acid residues 49-380 of Pex2p was excised from plasmid pHD04. This fragment was purified and cloned into the *EcoRI/BamHI* sites of pMAL-c2. Fusion protein purification and antibody production in one rabbit (E260) and two guinea pigs (Pay5-N, Pay5-NN) were performed as described. Antiserum from guinea pig Pay5-NN (1:2,000 dilution) was preferentially used. Antiserum from rabbit was used at a 1:500 dilution.

Antibodies were also produced against a 577 bp *EcoRI/PstI* fragment encoding amino acids 49-240 of Pay5p. This fragment was cloned into the *EcoRI/PstI* sites of pMAL-c2. Fusion protein purification and antibody production in two guinea pigs (P42-N, P42-NN)

were as described. Guinea pig P42-NN produced a highly specific serum which was used at a 1:10,000 dilution.

2.7.3 *Anti-Pex16p antibodies*

To produce antibodies to Pex16p, the *YIPEX16* ORF was amplified from plasmid p16N1 (Fig. 2 A) by PCR using primers 249 and 224 for the 5' and 3' ends, respectively (Table 2.2). Primers 249 and 224 have *EcoRI* and *HindIII* sites near their 5' ends, respectively. The product was digested with *EcoRI* and *HindIII* and ligated into pMAL-c2 cut with *EcoRI* and *HindIII*. This created an in-frame fusion of Pex16p downstream of the ORF of MBP. Fusion protein purification and antibody production in one rabbit (H1) and two guinea pigs (SOAP, 63I) were as described. Antiserum produced by guinea pig SOAP was used at 1:4,000 dilution. Rabbit H1 antiserum was used at 1:500 dilution.

2.7.4 *Anti-thiolase antibodies*

To produce antibodies to *Y. lipolytica* peroxisomal 3-ketoacyl-CoA thiolase, a 1916 bp *XhoI/SalI* fragment encoding amino acid residues 11-414 of thiolase was excised from plasmid pS106 (Berninger et al., 1993). This fragment was purified and ligated into pMAL-c2 digested with *SalI*. A construct was selected that encoded an in-frame fusion of thiolase downstream of the MBP coding region. Fusion protein purification and antibody production in two rabbits (D645, D646) and two guinea pigs (THI-N, THI-NN) were performed as described. All antisera showed very high titres of monospecific thiolase antibody. Rabbit sera

were used at 1:10,000 dilution and guinea pig sera were used at 1:25,000 dilution. Guinea pig THI-N serum crossreacted with thiolases from other yeast species (Fig. 2.2).

2.7.5 *Anti-isocitrate lyase antibodies*

To produce antibodies against peroxisomal ICL, the *Y. lipolytica ICL1* gene (Barth and Scheuber, 1993) was amplified from genomic DNA by PCR using primers *YIICL-1* and *YIICL-2* (Table 2.2) for the 5' and 3' ends, respectively. A 801 bp *SalI/HindIII* fragment, encoding amino acid residues 288-555 of ICL, was subcloned from the full length PCR product and ligated into pMAL-c2 digested with *SalI* and *HindIII*. Fusion protein purification and antibody production in one rabbit (D408) and two guinea pigs (ICL-N, ICL-NN) were performed as described. Antiserum from rabbit D408 was used at 1:5,000 dilution. Guinea pig sera were used at 1:2,000 dilution.

2.7.6 *Anti-(S. cerevisiae)acyl-CoA oxidase antibodies*

To produce peroxisomal anti-acyl-CoA oxidase (AOX) antibodies, we used the *S. cerevisiae POX1* gene (which encodes AOX) since a *Y. lipolytica* clone was not available. A 1644 bp *EcoRV/BglII* fragment of pAD17 (Dmochowska et al., 1990) encoding amino acid residues 93-641 was subcloned into pMAL-c2 digested with *XmnI/BamHI*. Fusion protein purification and antibody production in one rabbit (E261) and two guinea pigs (POX1-N, POX1-NN) were performed as described. Guinea pig POX1-N antiserum was preferentially used at 1:1000 dilution. All other sera were used at 1:1000 dilution.

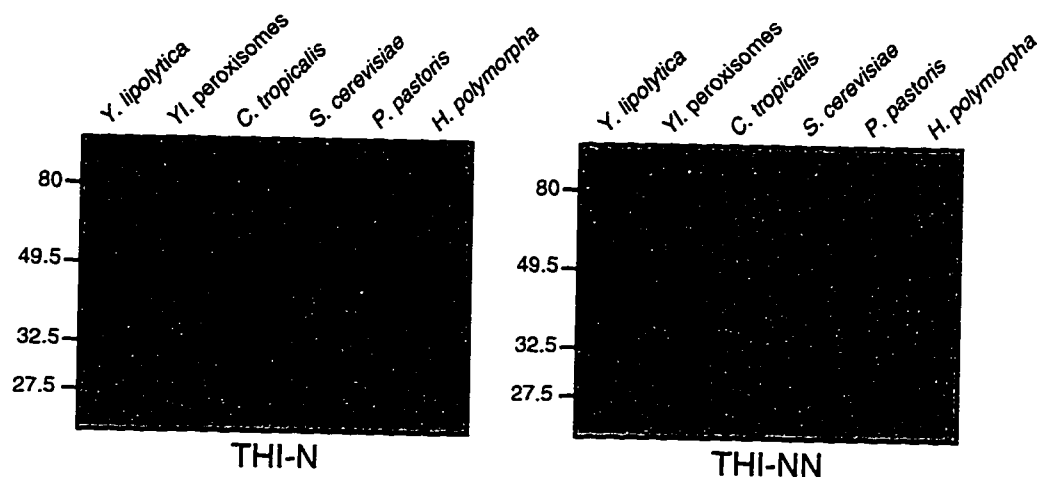


Figure 2.2 Immunoblot showing cross-reactivity of anti-(*Y. lipolytica*)thiolase antibodies. *Y. lipolytica*, *C. tropicalis*, *S. cerevisiae*, *P. pastoris* and *H. polymorpha* were grown in YEPD to an $OD_{600} \sim 1.5$, transferred to YPBO and grown for an additional 8 h. Total cell lyastes were prepared (see Section 2.4.1) and 50 μ g of protein was subjected to SDS-PAGE, blotted to nitrocellulose and probed with anti-(*Y. lipolytica*)thiolase antibodies raised in two guinea pigs (*THI-N*, *THI-NN*). The numbers at the left indicate the migration of molecular mass standards in kDa.

RESULTS AND DISCUSSION

The question of how peroxisomes assemble has received a great deal of attention in recent years. Although much is known about protein targeting to peroxisomes, little is known about other cellular events that govern peroxisome biogenesis. This thesis is aimed at elucidating some of the steps of peroxisome assembly.

Yeast represent an excellent experimental system to identify genes encoding proteins required for peroxisome assembly. We chose the yeast *Yarrowia lipolytica* as our model organism, since a genetic system has been developed (Gaillardin, 1973) and a very good peroxisome proliferative response is induced by growth in oleic acid-containing medium (Nuttley et al., 1993). We have made a large collection of peroxisome assembly mutants of *Y. lipolytica*, collectively called *pay* mutants. The following three sections report the morphological and biochemical characterizations of the *pay2*, *pay5* and *pay6* mutant strains. Functional complementation of these mutant strains with a *Y. lipolytica* genomic DNA library (Brade, 1992) has allowed us to isolate the corresponding *PAY* genes that encode proteins essential for peroxisome biogenesis. Portions of this work have been published (Eitzen et al., 1995; 1996; 1997; Titorenko et al., 1996).

During the course of this study, a unified nomenclature for peroxisome assembly mutant was established. Peroxisome assembly mutants isolated in different yeast and mammalian systems were collectively renamed and numbered based on amino acid homology. Mutants with defects in peroxisome biogenesis are now referred to as *pex* mutants. The corresponding *PEX* genes encode proteins referred to as peroxins (Distel et al., 1996).

The unified nomenclature is used throughout this thesis. The following name changes have occurred for *Y. lipolytica* *pay* strains published prior to the unified nomenclature: *pay2* = *pex9*; *pay5* = *pex2*; *pay6* = *pex16*; *pay32* = *pex5*, *pay4* = *pex6*. Where appropriate, or for clarification, a two letter code is used to designate genus and species (e.g. *Ylpex9* = *Y. lipolytica pex9* strain; *YIPEX9* = *Y. lipolytica PEX9* gene).

3. The *Y. lipolytica* *PEX9* gene encodes a 42 kDa peroxisomal integral membrane peroxin essential for matrix protein import and peroxisome enlargement but not for peroxisome membrane proliferation*

This chapter reports the characterization of the peroxisome assembly mutant strain, *pex9*, and the peroxin Pex9p. The results presented show that this strain cannot import most peroxisomal matrix proteins and fails to assemble normal peroxisomal structures. However, electron microscopy of *pex9* cells revealed the presence of small peroxisomal "ghosts", similar to the vesicular structures found in fibroblasts of patients with the human peroxisome assembly disorder, Zellweger syndrome. Functional complementation of the *pex9* strain identified a gene, *YIPEX9*, that restores growth of *pex9* on oleic acid, import of peroxisomal matrix proteins, and formation of wild-type peroxisomes. The *YIPEX9* gene encodes the peroxin, Pex9p, a peroxisomal integral membrane protein of 404 amino acid residues (44,913 Da), with no known homologues. Our results suggest that Pex9p is essential for the activity of the peroxisomal import machinery but does not affect the initial steps of peroxisomal membrane proliferation.

*Portions of this chapter are reproduced from The Journal of Biological Chemistry (Eitzen et al., 1995, 270:1429-1436) with copyright permission of The American Society of Biochemistry and Molecular Biology Inc.

3.1 *pex9* cells can proliferate peroxisome-like structures but are deficient for peroxisome growth

The *Y. lipolytica* mutant strain, *pex9*, was isolated from randomly mutagenized cells by its inability to utilize oleic acid as a carbon source (Fig. 3.1). *pex9* is a mutant of peroxisome assembly, as it aberrantly localized the peroxisomal marker enzymes, catalase and multifunctional enzyme (measured as β -hydroxyacyl-CoA dehydrogenase activity), to the 20KgS fraction (Table 3.1, page 57). Examination of the wild-type *E122* and mutant *pex9* strains by electron microscopy (*performed by Dr. Marten Veenhuis, University of Groningen, The Netherlands*) supports the classification of the *pex9* strain as being compromised in peroxisome assembly. *E122* cells grown in oleic acid medium showed peroxisomes scattered throughout the cytosol (Figs. 3.2 C and 3.2 D). In contrast, *pex9* cells grown in oleic acid show many small peroxisome-like vesicular structures (Figs. 3.2 A and 3.2 B), reminiscent of the peroxisomal "ghosts" seen in Zellweger cells (Santos et al., 1988a; 1988b). These peroxisome-like structures (Figs 3.2 A and B, *arrows*) appear less granular than wild-type peroxisomes, are often clustered, and have an average diameter of less than 0.2 μm , in contrast to the average diameter of 0.4 μm of peroxisomes in the *E122* strain. Therefore, *pex9* cells appear to be able to proliferate peroxisome-like structures but are deficient for subsequent growth of the organelle.

3.2 *pex9* cells mislocalize PTS1- and PTS2-containing proteins to a subcellular fraction enriched for cytosol

20KgP (enriched for peroxisomes and mitochondria) and 20KgS (enriched for cytosol)

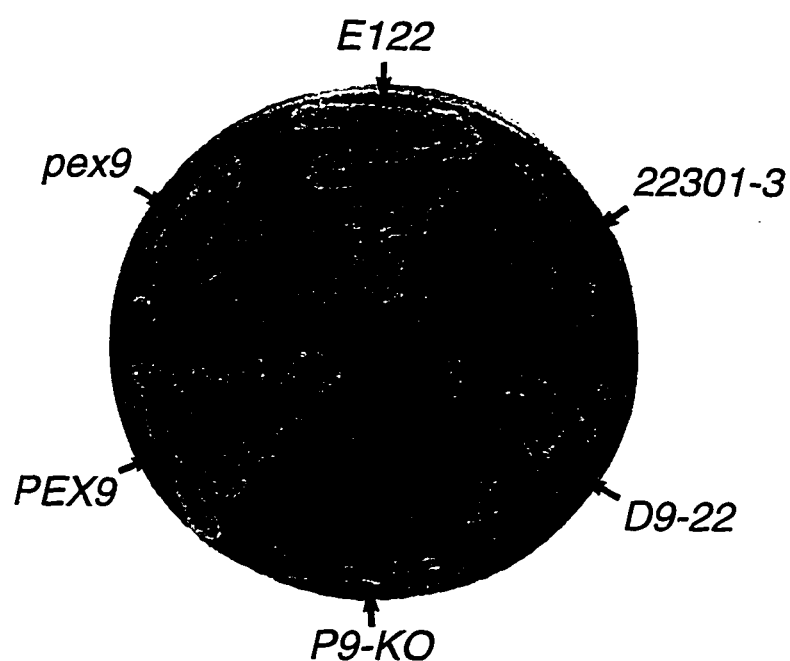


Figure 3.1 **Growth of various *Yarrowia lipolytica pex9* strains on oleic acid medium.** Appearance of the complemented strain *PEX9* in comparison to the parental strain *E122*, the mutant strain *pex9*, the gene disruption strain *P9-KO*, the diploid strain *D9-22* (*P9-KO* X *22301-3*), and a second parental strain *22301-3* (the plate was not supplemented to satisfy the auxotrophic requirements of this strain). Growth was for 4 d on YNO-agar.

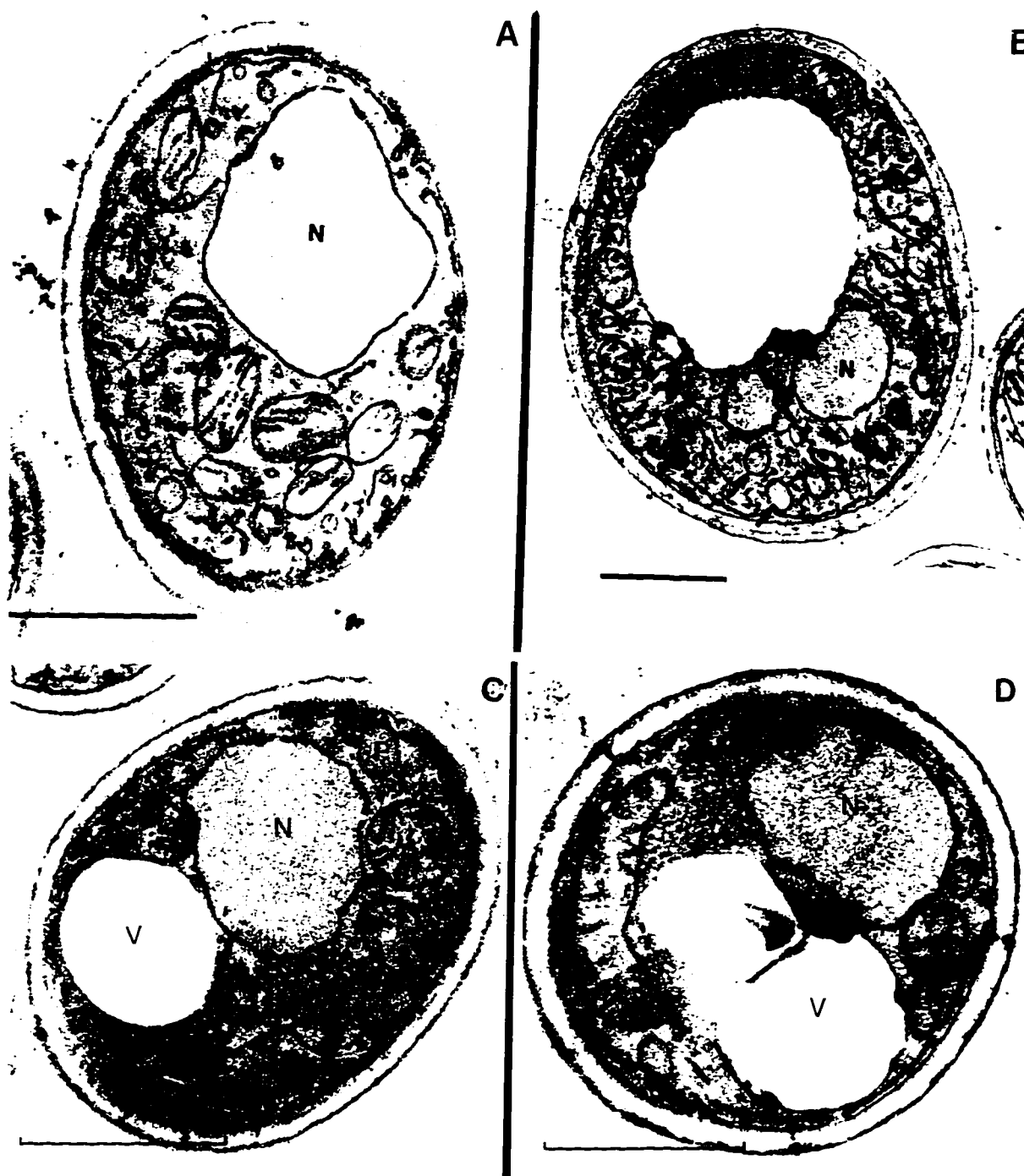


Figure 3.2 Ultrastructure of the *pex9* mutant (panels A and B) and wild-type *E122* (panels C and D) strains. Cells were grown 16 h in YEPD medium to an OD_{600} of ~ 1.6 , diluted 1:4 into YPBO medium and grown for an additional 8 h in YPBO. Cells were then fixed in $KMnO_4$ and processed for electron microscopy. Arrows, vesicular structures similar to the peroxisomal "ghosts" of Zellweger fibroblasts. P, peroxisome; N, nucleus; V, vacuole. Bar = 1 μm .

fractions were prepared from the wild-type *E122* and *pex9* mutant strains grown in oleic acid medium, as described in *Section 2.4.2*. Immunoblot analysis showed that proteins that are normally localized to the 20KgP fraction of *E122* cells were mislocalized to the 20KgS fraction of the *pex9* mutant (Fig. 3.3). In *E122*, a 42 kDa polypeptide is detected by anti-(*S. cerevisiae*)-thiolase antibodies (Nuttley et al., 1994). Thiolase, which is targeted to peroxisomes by a PTS2 (Swinkels et al., 1991), was localized exclusively to the 20KgP fraction in *E122* cells (Fig. 3.3 A, *E122*). However, in *pex9* cell, thiolase was not localized to the 20KgP but was mislocalized to the 20KgS (Fig. 3.3 A, *pex9*). Moreover, the majority of the thiolase in the *pex9* 20KgS fraction was the larger, precursor form of the protein (Nuttley et al., 1994), although some mature thiolase was also detected. Proteins of intermediate size were also detected in the *pex9* 20KgS. The origins of these intermediate forms are unknown, but they could represent non-specific degradation products or specific intermediates of thiolase precursor cleavage (Authier et al., 1995). Fractions probed with anti-AKI serum, which reacts with PTS1-containing proteins (Aitchison, 1992), showed that a 64 kDa polypeptide band normally localized to the 20KgP fraction of *E122* (Fig. 3.3 B, *E122*) was mislocalized to the 20KgS fraction of *pex9* (Fig. 3.3 B, *pex9*). The ~30 kDa anti-AKI reactive band present in the 20KgS of the *pex9* strain is most probably a degradation product.

3.3 Isolation of the *YIPEX9* gene

Transformation of the *pex9* strain with a plasmid library containing *Y. lipolytica* genomic DNA yielded 4 transformants capable of restored growth on oleic acid (*performed*

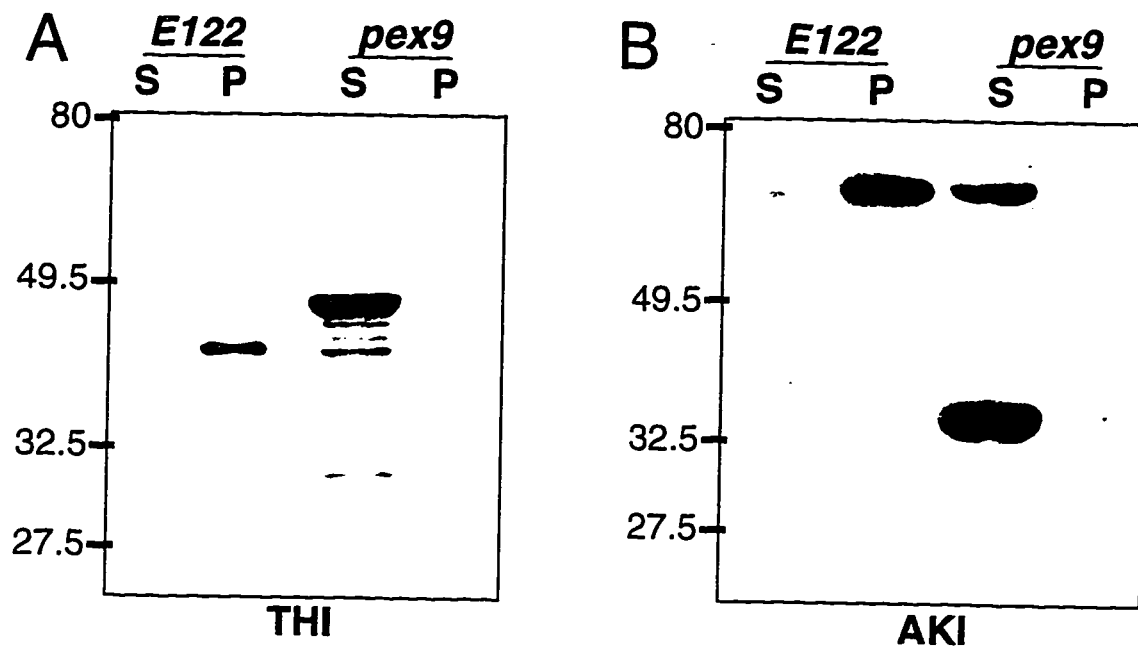


Figure 3.3 Peroxisomal thiolase and a PTS1-immunoreactive polypeptide are mislocalized to the 20KgS fraction of the *pex9* mutant strain. Wild-type *E122* and *pex9* mutant strains were grown for 8 h in YPBO, as described in the legend to Figure 3.2. Equivalent cellular fractions (0.5%) of the supernatant (S) and pellet (P) fractions from a $20,000 \times g_{\max}$ centrifugation of postnuclear supernatants were separated by SDS-PAGE, transferred to nitrocellulose, and probed with anti-thiolase antibodies (panel A) and anti-AKI antibodies (panel B). The numbers at left indicate the migrations of molecular mass markers in kDa.

by Dr. John Aitchison). Four independent recombinant plasmids, designated p02-A to p02-D, were rescued into *E. coli*. Restriction analysis of p02-A and p02-B, followed by subcloning and transformation of the *pex9* mutant, showed the complementing activity of the inserts was localized to a common minimal 2.2 kbp segment (Fig 3.5 A). A transformant, hereafter called *PEX9* (Fig. 3.1; Table 2.3), harbouring the plasmid pO2-2.2 containing the common 2.2 kbp segment, was used for further study.

The putative *YIPEX9* gene was used for gene disruption experiments with the *Y. lipolytica* *LEU2* gene, as described in Section 2.3.5.1. A *Leu*⁻/*ole*⁻ transformant, designated *P9-KO*, was isolated (Table 2.3; Fig. 3.1). The recessive nature of the *ole*⁻ phenotype was shown by the ability of the *P9-KO* x *22301-3* diploid strain, *D9-22*, to grow on oleic acid (Fig. 3.1). Sporulation of the diploid *D9-22* showed cosegregation of the *ole*⁻ and *Leu*⁻ phenotypes. When the *ole*⁻, *MatB* strain, *P9KO-3* (Table 2.3), was back-crossed to the original *pex9* strain, the resultant diploid strain, *D9-301*, was unable to grow on oleic acid, thereby confirming that the authentic *YIPEX9* gene had been cloned.

Electron microscopic examination (performed by Dr. Marten Veenhuis) of *PEX9* transformant cells grown in oleic acid medium showed peroxisomes like those found in the wild-type *E122* strain (Figs. 3.4 C and 3.4 D). In contrast, the *P9-KO* strain (Figs. 3.4 A and 3.4 B) showed vesicular peroxisomal ghosts like those seen in the original *pex9* mutant.

Transformation of *pex9* with pO2-2.2 to yield *PEX9* also restored the correct localization of peroxisomal marker enzyme activities. In the parental strain *E122*, approximately 50% of the catalase activity and 60% of the multifunctional β -hydroxyacyl-CoA dehydrogenase activity were found in the 20KgP fraction (Table 3.1), reflecting the

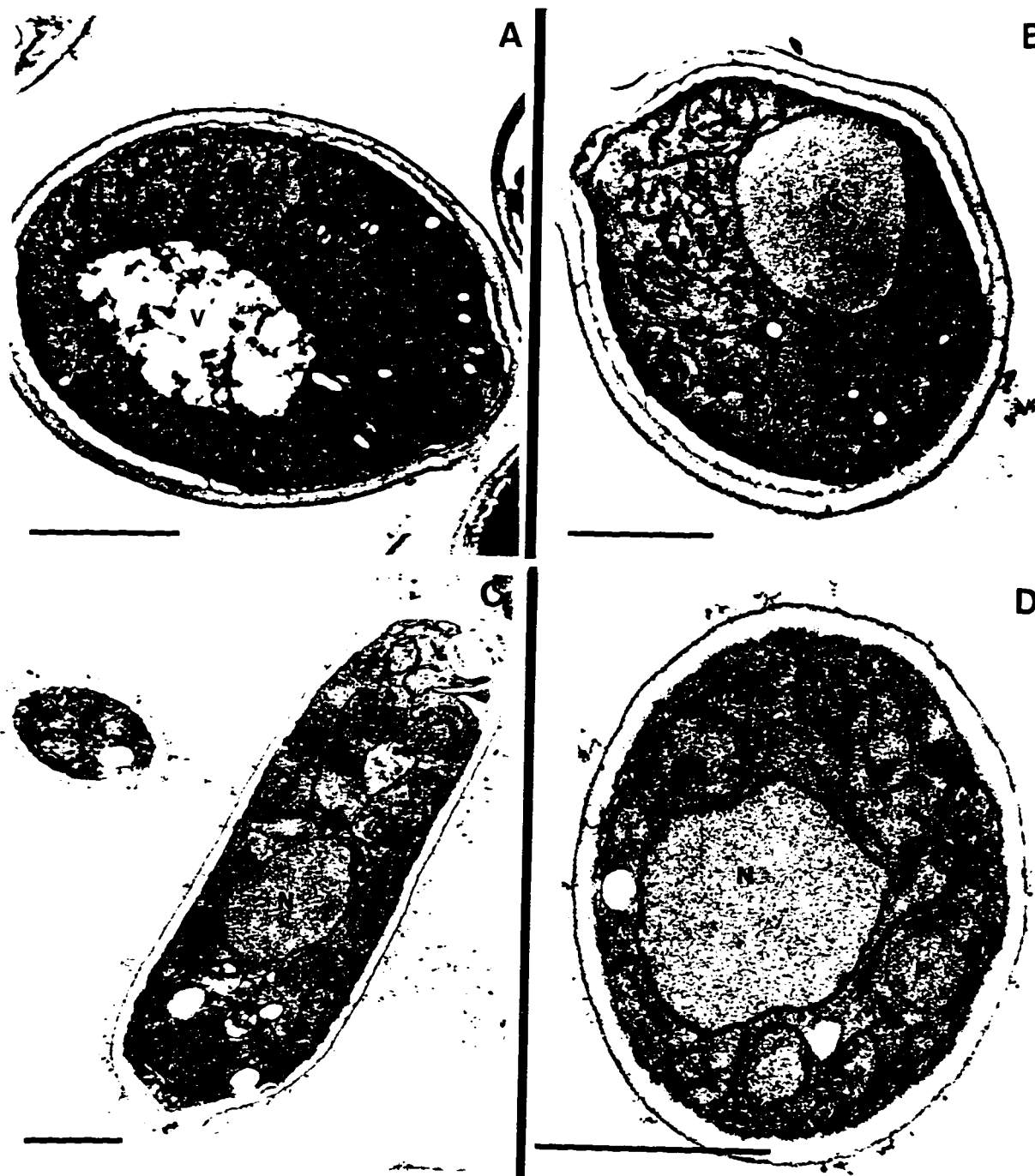


Figure 3.4 Ultrastructure of the *P9-KO* mutant (panels *A* and *B*) and the *PEX9* transformant (panels *C* and *D*). Strains were grown for 8 h in YPBO, as described in the legend to Figure 3.2, fixed with KMnO_4 and processed for electron microscopy. The electron micrographs show the morphology of the *P9-KO* mutant to be similar to that of the original *pex9* mutant. The *PEX9* transformant contains normal peroxisomes. Arrows, vesicular structures similar to the peroxisomal "ghosts" of Zellweger fibroblasts. *P*, peroxisome; *N*, nucleus; *V*, vacuole. Bar = 1 μm .

peroxisomal location of these enzymes. The activities of these enzymes recovered in the 20KgS fraction were due, at least in part, to leakage from peroxisomes broken during the fractionation procedure (Aitchison et al., 1991). In the *pex9* mutant strain, as well as in the gene-disruption strain *P9-KO*, less than 5% of catalase activity and 10% of multifunctional (dehydrogenase) activity were recovered in the 20KgP. Transformation of *pex9* with pO2-2.2 corrected this defect, resulting in recoveries of catalase and dehydrogenase activities in the 20KgP fraction at levels similar to those found in the *E122* strain. The distribution of the mitochondrial marker cytochrome *c* oxidase was not affected by the *pex9* mutation, as comparable levels of cytochrome *c* oxidase activity were found in the 20KgP fractions of *E122*, *pex9*, *PEX9*, and *P9-KO* strains (Table 3.1).

Table 3.1 Distribution of peroxisomal and mitochondrial marker enzymes in the 20KgS and 20KgP fractions isolated from cell homogenates of the *E122*, *pex9*, *P9-KO* and *PEX9* strains.

Strain	Enzyme	Activity (U)		
		20KgS (S)	20KgP (P)	Total
<i>E122</i>	catalase	0.23	0.26	0.49
	multifunctional	5.13	7.22	12.35
	cyt. <i>c</i> oxidase	0.38	1.80	2.18
<i>pex9</i>	catalase	0.78	0.03	0.81
	multifunctional	14.38	1.47	15.85
	cyt. <i>c</i> oxidase	0.36	1.35	1.71
<i>PEX9</i>	catalase	0.18	0.34	0.52
	multifunctional	5.32	6.94	11.26
	cyt. <i>c</i> oxidase	0.35	1.52	1.87
<i>P9-KO</i>	catalase	0.86	0.02	0.88
	multifunctional	11.06	1.21	12.27
	cyt. <i>c</i> oxidase	0.44	1.81	2.25

3.4 Nucleotide sequence of the *YIPEX9* gene and the deduced amino acid sequence of Pex9p

Sequencing of the 2.2 kbp insert of the complementing plasmid pO2-2.2 revealed an open reading frame encoding a protein of 404 amino acid residues and having a predicted molecular mass of 44,913 Da (Fig. 3.5 B). This predicted molecular mass is in good agreement with the relative molecular mass determined by SDS-PAGE and immunoblot analysis (see Fig. 3.9). Three potential initiation codons are found within the first 10 amino acids of the protein encoded by the largest open reading frame. The first and the third conform to the consensus sequence for translation initiation in yeast, with a conserved A at position -3 and a conserved C at position +5 relative to the A of the initiation codon (Cigan and Donahue, 1987). The actual initiation codon is unknown. A putative TATA-element, TACAAATAA, is found between positions -117 and -109 relative to the first potential initiation codon.

3.5 Analysis of the Pex9p amino acid sequence

A search of the available protein databases using the GENINFO(R) BLAST Network Service (Blaster) of the National Center for Biotechnology Information revealed no significant homology of Pex9p to any known protein sequence. Hydropathy analysis (Fig. 3.6; Kyte and Doolittle, 1982) showed Pex9p to be extremely hydrophobic overall and most likely a membrane protein. Based on algorithms that predict membrane-spanning or -associated regions in proteins (Eisenberg et al., 1984; Klein et al., 1985; Rao and Argos, 1986), Pex9p is predicted to contain two membrane-spanning α -helices located towards the amino terminus

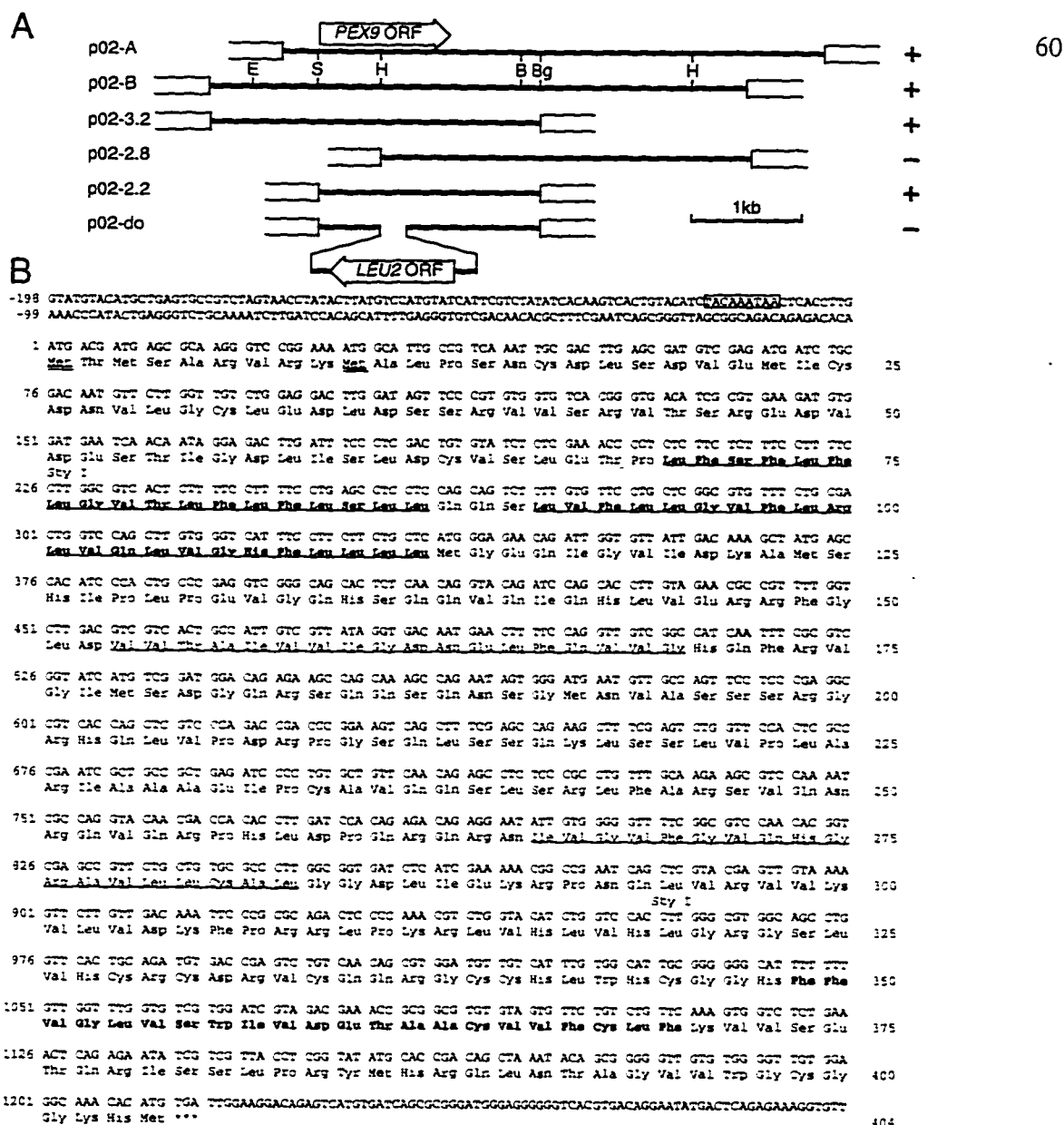


Figure 3.5 Cloning and analysis of the *YIPEX9* gene. (A) Complementing activity of inserts, restriction map analysis and targeted gene disruption strategy for the *YIPEX9* gene. Solid lines, *Y. lipolytica* genomic DNA; open boxes, vector DNA. The open reading frames of the *YIPEX9* and *LEU2* genes are indicated by the wide arrow. The (+) symbol denotes the ability and the (-) symbol denotes the inability of an insert to confer growth on oleic acid to *pex9*. B, *Bam*HI; Bg, *Bgl*II; E, *Eco*RI; H, *Hind*III; S, *Sal*I. (B) Nucleotide sequence and deduced amino acid sequence of the *YIPEX9* gene. A presumptive consensus TATA sequence is boxed. Two possible initiator methionines are doubly underlined. Two predicted membrane-spanning segments are highlighted in bold and underlined. A third potential membrane-spanning segment is highlighted in bold. Two potential membrane-associated segments are underlined. The nucleotide sequence has been submitted to GenBank with accession number U16653.

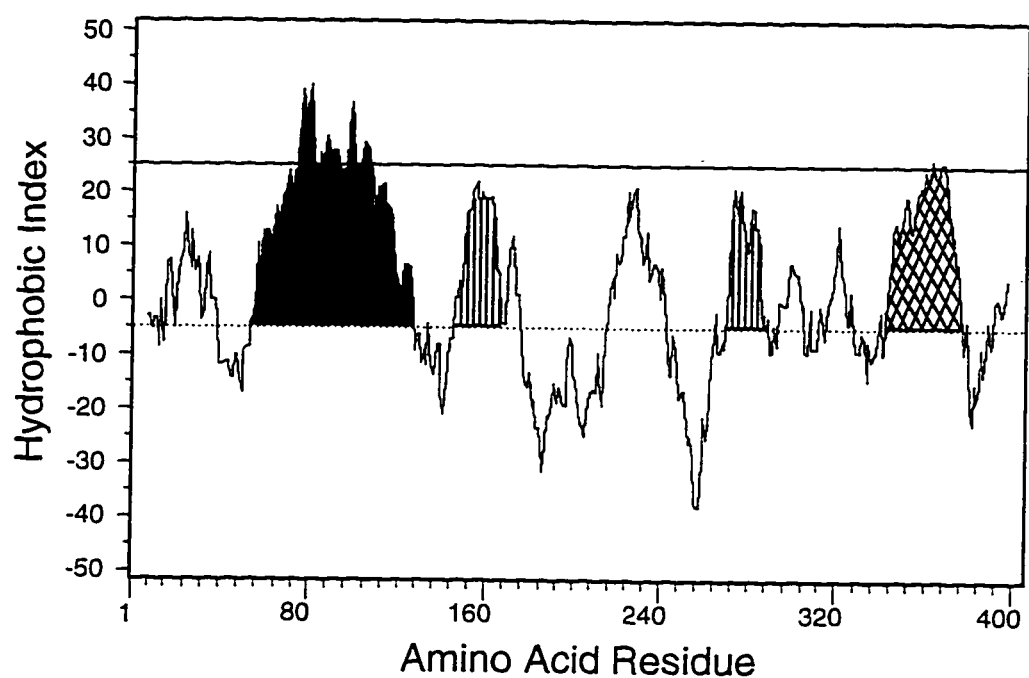


Figure 3.6 **Hydropathy analysis of Pex9p.** A hydropathy profile of the predicted amino acid sequence of Pex9p was calculated according to Kyte and Doolittle (1982) with a window size of 15 amino acids. The threshold hydrophobicity value of 25 is indicated by the *solid horizontal line*. The sequence highlighted in *black* contains the two most likely membrane-spanning domains. The sequence highlighted by *cross-hatching* also contains a putative membrane-spanning domain. The two sequences highlighted by *vertical lines* are most likely membrane-associated.

(Fig. 3.5 *B*, ***bold and underlined*** sequences). Pex9p is also predicted to contain a third membrane-spanning or membrane-associated domain (Fig. 3.5 *B*, ***bold*** sequence) and two additional membrane-associated helices (Fig. 3.5 *B*, ***underlined*** sequences).

3.6 Pex9p is a peroxisomal integral membrane protein

Since computer analysis predicted Pex9p to be a membrane protein and since the *pex9* strain is deficient in peroxisome assembly, we determined whether Pex9p is a peroxisomal membrane protein. Immunoblot analysis with anti-Pex9p antibodies of a 20K_gP fraction from oleic acid-grown *E122* cells subjected to isopycnic centrifugation on a discontinuous sucrose gradient (Fig. 3.7 *B*) showed that Pex9p was preferentially localized to the fraction of peak peroxisomal catalase activity (Fig. 3.7 *A*). Pex9p was not localized to the fraction of peak mitochondrial cytochrome *c* oxidase activity, which also contained the highest concentration of protein. Sodium carbonate (pH 11) extraction, which solubilizes all but integral membrane proteins, of the peroxisome enriched fraction followed by centrifugation at 200,000 × g_{max} , showed that Pex9p was exclusively found in the pellet, strongly indicative of Pex9p being an integral peroxisomal membrane protein (Fig. 3.7 *C*).

3.7 The levels of Pex9p mRNA and Pex9p are induced by growth on oleic acid

Growth of yeast on oleic acid leads to increased levels of mRNA coding for peroxisomal proteins and proteins involved in peroxisome assembly and to increased levels of the proteins themselves (Fujiki et al., 1986; Erdmann et al., 1991; Höhfeld et al., 1991; Nuttley et al., 1994). Growth of the wild-type strain *E122* in glucose-containing medium led

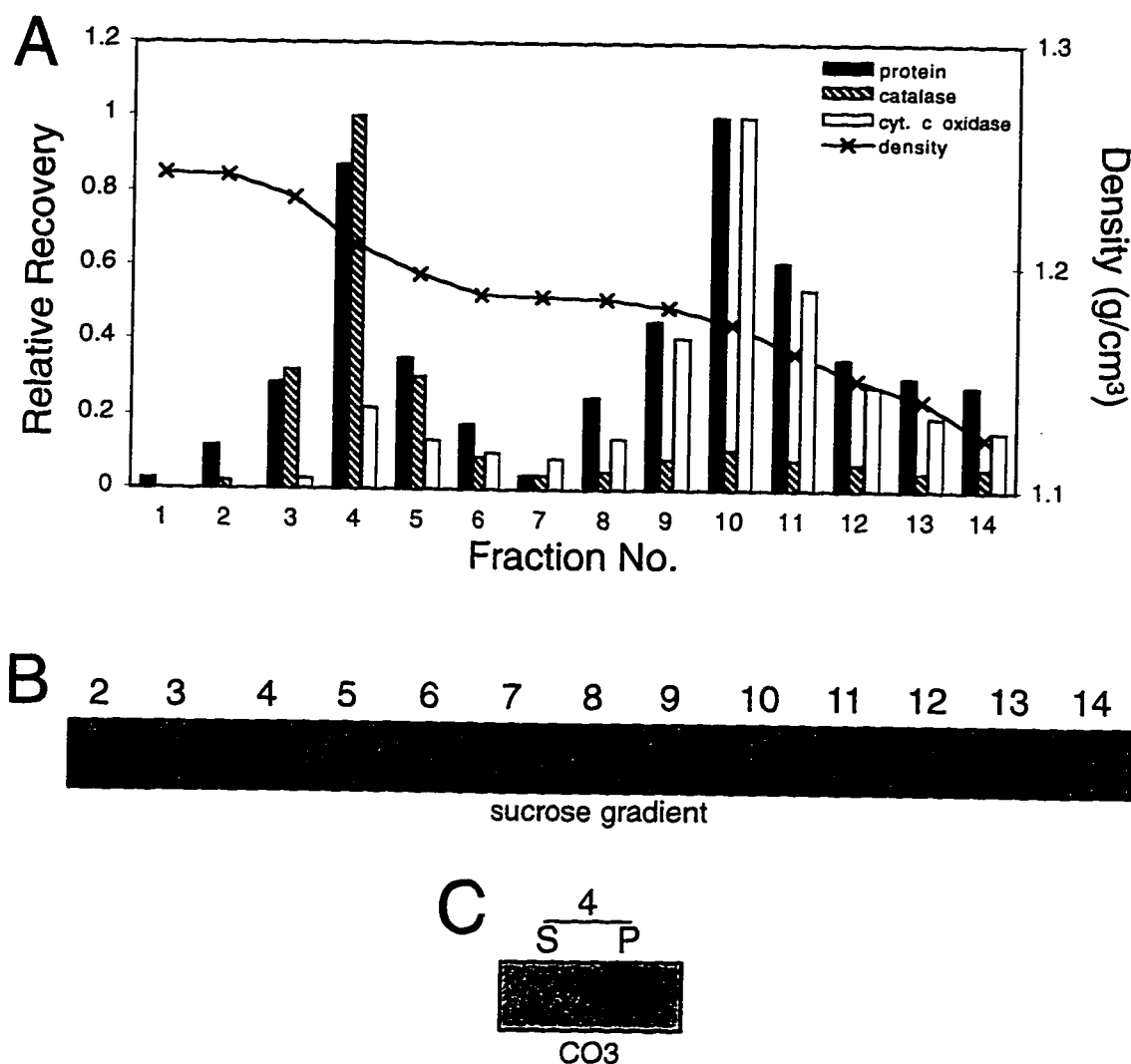


Figure 3.7 Pex9p is a peroxisomal integral membrane protein. (A) Distribution of the marker enzymes catalase (peroxisomes) and cytochrome *c* oxidase (mitochondria) on a sucrose density gradient of the 20KgP fraction (*Section 2.4.2*) from *E122* cells grown in oleic acid medium. Fractions of equal volume were collected from the bottom of the tube. (B) Immunoblot of the fractions collected in *panel A* with anti-Pex9p antibodies. (C) Fraction 4 was treated with sodium carbonate buffer (CO3) as described in *Section 2.4.3* and then subjected to ultracentrifugation to yield a supernatant (*S*) of soluble proteins and a pellet (*P*) enriched for integral membrane proteins. Equal cellular fractions were separated by SDS-PAGE, transferred to nitrocellulose, and probed with anti-Pex9p antibodies.

to a low level of Pex9p mRNA (Fig. 3.8, *left panel, lane 0*). Likewise, a low level of mRNA encoding 3-ketoacyl-CoA thiolase, a soluble peroxisomal β -oxidation enzyme, was found in the same cells (Fig. 3.8, *right panel, lane 0*). Shifting the glucose-grown cells to medium containing oleic acid, followed by continued growth in this medium, brought about an increase in the levels of both Pex9p mRNA and thiolase mRNA. Four h after the shift to oleic acid medium, Pex9p mRNA levels were increased approximately 20-fold over that found in glucose-grown cells. Pex9p mRNA levels then dropped and stabilized at 6 h after the shift at levels approximately 4 times that found in glucose-grown cells. Thiolase mRNA was maximally induced (approximately 50-fold) 2 h after shifting cells to oleic acid medium, and this high level of induction was maintained up to the final time point of 8 h of growth in oleic acid medium.

The levels of Pex9p were also increased by growth in medium containing oleic acid (Fig. 3.9). A low level of Pex9p was detected in wild-type *E122* cells grown in glucose-containing media (Fig. 3.9, *lane a*). Transfer of glucose-grown cells to oleic acid-containing medium followed by continued growth in this medium led to an increase in the level of Pex9p (*lanes a to d*), with a 10-fold induction seen by 6 h (*lane c*). Pex9p was not detected in lysates prepared from oleic acid-induced *pex9* or *P9-KO* strains (*lanes e* and *f*, respectively).

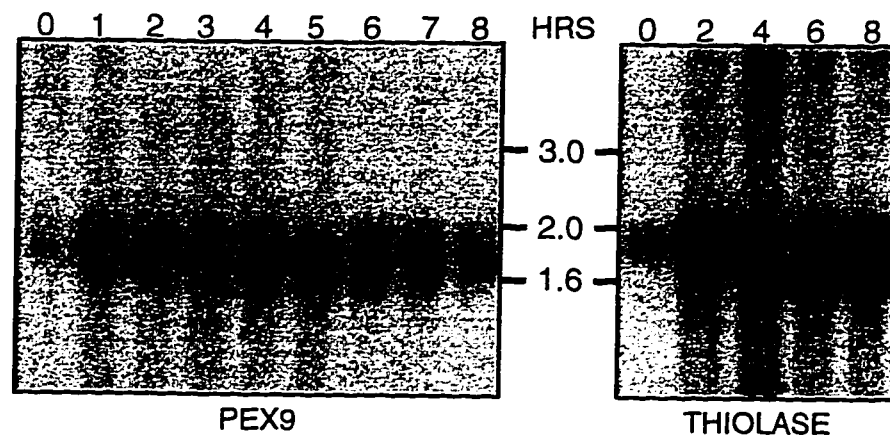


Figure 3.8 **Pex9p mRNA and peroxisomal thiolase mRNA are induced by growth of *Y. lipolytica* in oleic acid.** Total RNA was isolated from strain *E122* grown in YEPD medium (0 HRS) and after transfer to YPBO medium for different periods of time (*numbers at the top in h*). 10 μ g of RNA from each time point was run on a formaldehyde-agarose gel and transferred to nitrocellulose. The blots were hybridized with radiolabelled probes specific for the *YIPEX9* gene and the gene encoding *Y. lipolytica* peroxisomal thiolase. The *numbers* between the two panels represent the migration of DNA markers in kbp. Exposure was 5 d for the Pex9p probe and 15 h for the thiolase probe.

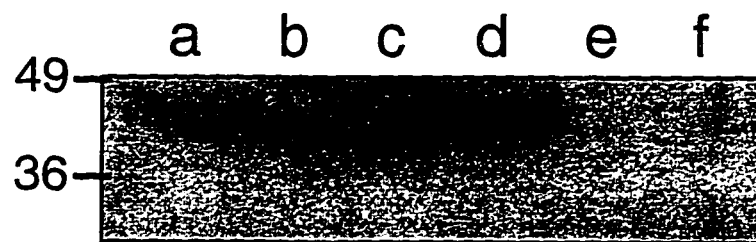


Figure 3.9 **Pex9p is induced by growth of *Y. lipolytica* in oleic acid.** *E122* cells were grown for 16 h in YEPD medium to an OD_{600} of ~ 1.6 (*lane a*), transferred to YPBO medium (1:4 dilution) and grown for 1 h (*lane b*), 6 h (*lane c*), and 12 h (*lane d*) in YPBO. The *pex9* (*lane e*) and *P9-KO* (*lane f*) strains were similarly grown in YEPD, diluted 1:4 in YPBO and grown in YPBO for 6 h. Equal amounts of protein from each sample were separated by SDS-PAGE, transferred to nitrocellulose, and probed with anti-Pex9p serum. The *numbers* at left indicate the migrations of molecular mass standards in kDa.

3.8 Summary and discussion

3.8.1 *pex9* mutant cells contain peroxisomal ghosts

The *pex9* strain is a peroxisome assembly mutant that does not contain morphologically normal peroxisomes but instead contains smaller vesicular structures reminiscent of the "peroxisomal ghosts" seen in fibroblasts of patients with Zellweger syndrome. Therefore, *pex9* appears to be a mutant in which import of proteins into the peroxisome and peroxisome enlargement, but not proliferation of the peroxisomal membrane, are disrupted. It has been shown that in most yeast species, peroxisomal membrane proliferation precedes protein import into peroxisomes (Veenhuis and Goodman, 1990; McCollum et al., 1993) and enlargement of peroxisomes is the result of protein import into initially much smaller peroxisomes (Godecke et al., 1989). In the *pex9* (Figs. 3.2 C and D) and *P9-KO* (Figs. 3.4 A and B) strains, many clusters of small peroxisome-like ghosts can be seen, however, the enlargement of these structures is retarded after the initial proliferation of peroxisomes. Therefore, peroxisomal membrane proliferation can be genetically separated from protein import into peroxisomes. These morphological results, combined with the demonstration that the *pex9* strain fails to import proteins targeted by either PTS1 or PTS2, indicate that Pex9p is required for peroxisomal matrix protein import.

3.8.2 *Role of Pex9p in a common peroxisomal import machinery*

Several proteins that are peripherally associated with the peroxisome membrane and

integral to the peroxisome membrane have now been cloned and shown to be involved specifically in protein import. Membrane-associated receptors that recognize and bind the signals encoded in PTS1 and PTS2 have been isolated (see Rachubinski and Subramani, 1995). A peroxisomal integral membrane protein, Pex13p, has been shown to function as a docking site for the mobile PTS1 receptor and thus to facilitate the import of PTS1-containing proteins (Gould et al., 1996; Elgersma et al., 1996; Erdmann and Blobel, 1996). Interestingly, disruption of the PTS1 docking factor blocks the import of proteins targeted by either PTS1 or PTS2. We can speculate that the initial events in targeting proteins with PTS1, PTS2 or other signals to peroxisomes are divergent, with each signal being recognized by a separate receptor that can shuttle between the cytosol and the peroxisomal membrane. Such cytosolic factors have been predicted to exist for all organelles and would help in the targeting of proteins to specific organelles by preventing preproteins from interacting with the incorrect membrane surface (Lithgow et al., 1993). At the peroxisomal membrane, these receptor complexes would converge and interact with a single common peroxisomal translocation machinery. Such a translocon would combine receptors and membrane docking factors with proteins that function specifically in membrane translocation. Our results suggest that Pex9p is essential for the activity of this common peroxisomal membrane translocation machinery.

4. **Mutation of the *PEX2* gene encoding a *Y. lipolytica* homologue of mammalian peroxisome assembly factor-1 results in abnormal peroxisomal structures***

The following chapter describes the characterization of the *pex2-1* peroxisome assembly mutant and the peroxin, Pex2p. When cells are shifted to oleic acid-containing medium they fail to assemble normal peroxisomes but instead form irregular vesicular structures surrounded by multiple membranes. The *pex2-1* mutant is not completely deficient in peroxisomal matrix protein import as a subset of matrix proteins continues to be localized to several peroxisomal subpopulations of unique buoyant density and protein content. The complementing gene, *YIPEX2*, encodes a peroxin, Pex2p, of 380 amino acids (41,720 Da). Pex2p is a peroxisomal integral membrane protein homologous to mammalian PAF-1 proteins, which are essential for peroxisome assembly and whose mutation in humans results in Zellweger syndrome. Pex2p is targeted to mammalian peroxisomes, demonstrating the evolutionary conservation of the targeting mechanism for peroxisomal membrane proteins. Our results suggest that mutation of *PEX2* results in a block of normal peroxisome assembly, which leads to the accumulation of the membranous structures and peroxisomal subpopulations. These structures might therefore represent a normal, intermediate step in peroxisome biogenesis.

4.1 **The *pex2-1* mutant shows abnormal peroxisome morphology**

The *pex2-1* mutant was unable to utilize oleic acid as a carbon source (Fig. 4.1) and was impaired in the targeting of a number of peroxisomal matrix proteins (see *Section 4.5*).

*Portions of this chapter are reproduced from The Journal of Biological Chemistry (Eitzen et al., 1996, 271:20300-20306; Titorenko et al., 1996, 271:20307-20314) with copyright permission of The American Society of Biochemistry and Molecular Biology Inc.

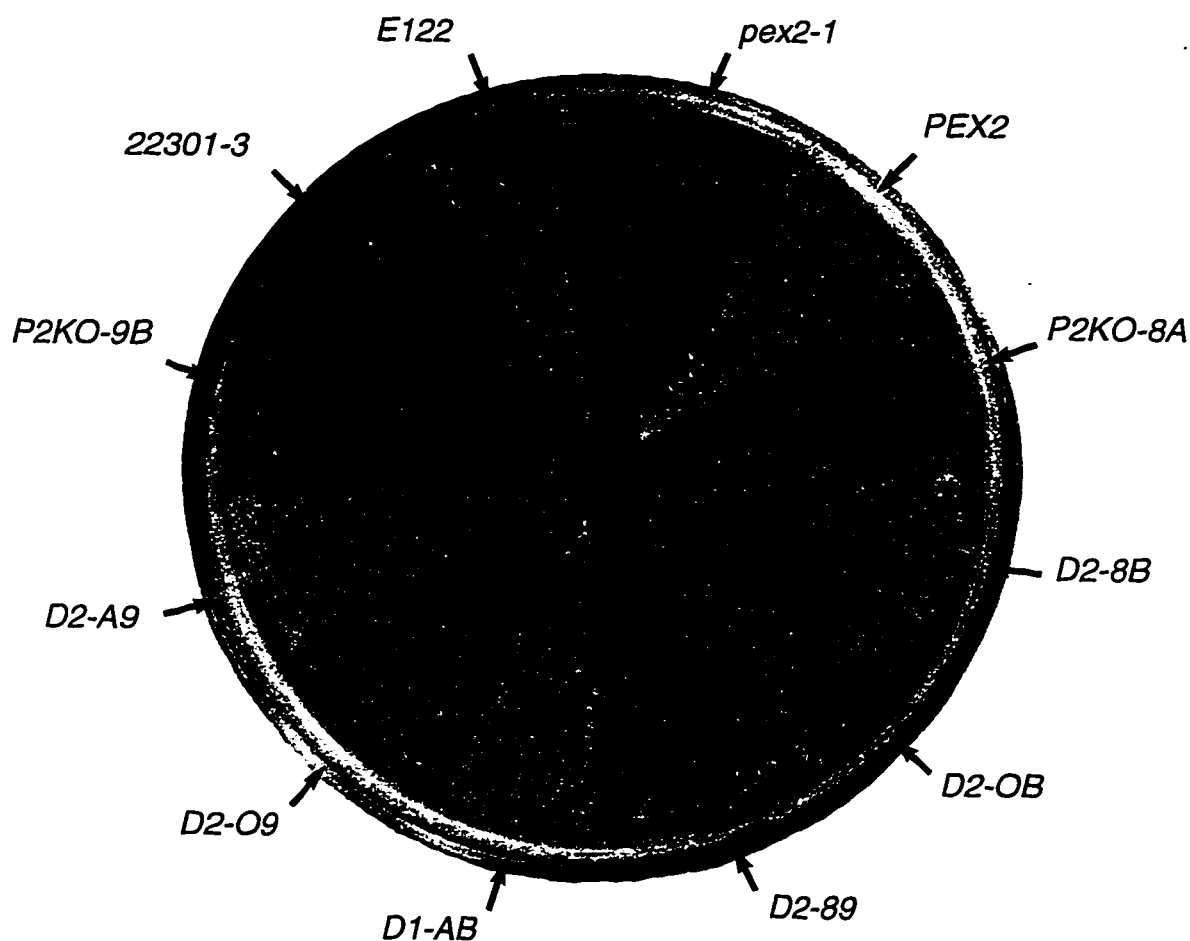


Figure 4.1 **Growth of various *Y. lipolytica* *pex2* strains on oleic acid medium.** Strains (see Table 2.3) were grown for 4 d on YNO-agar supplemented with leucine, lysine and uracil. The appearance of the complemented strain *PEX2* is compared to those of the wild-type strain *E122*, the original *pex2-1* mutant, the gene disruption strains *P2KO-8A* and *P2KO-9B*, and the diploid strains *D2-A9*, *D2-O9*, *D1-AB*, *D2-89*, *D2-OB*, *D2-8B* created by mating (see Section 4.2). The *22301-3* wild-type strain is not supplemented for its auxotrophic requirements. Growth on YNO requires at least one intact copy of the *YIPEX2* gene.

Electron microscopic sections of wild-type *E122* cells grown in oleic acid-containing medium (YPBO) showed numerous large, round peroxisomes well separated from one another and surrounded by single unit membranes (Fig. 4.2 A). In contrast, *pex2-1* cells showed irregular structures consisting of vesicular elements surrounded by closely apposed, multiple unit membranes (Fig. 4.2 B, *arrowheads*).

4.2 Isolation and characterization of the *YIPEX2* gene

The *YIPEX2* gene was isolated from a *Y. lipolytica* genomic DNA library by functional complementation of the mutation in *pex2-1* cells (*performed by Ms. Rachel Szilard*). Of the 5×10^3 transformants screened, one strain, *PEX2*, had restored growth on oleic acid (Fig. 4.1) and showed wild-type peroxisomal morphology (Fig. 4.2 C). The *PEX2* strain carried the plasmid p5S11, which contains an ~5.6 kbp insert of *Y. lipolytica* DNA (Fig. 4.3 A). Subcloning of fragments from this insert localized the ability to functionally complement the *pex2-1* mutation to an ~2.0 kbp *HindIII/BamHI* fragment. Sequencing within this fragment revealed an open reading frame of 1134 nucleotides encoding a 380 amino acid protein, Pex2p, with a predicted molecular weight of 41,720 Da (Fig. 4.3 B). Hydropathy plot analysis (Fig. 4.4) predicted one putative transmembrane domain, as well as three possible membrane-associated domains.

The putative *YIPEX2* gene was disrupted by integration of the *Y. lipolytica* *LEU2* gene to make the strains *P2KO-8A* and *P2KO-9B* in the A and B mating types, respectively (Table 2.3). These gene disruption strains were unable to grow on oleic acid (Fig. 4.1) and had the same peroxisomal morphology (Fig. 4.2 D) and peroxisomal protein targeting defects

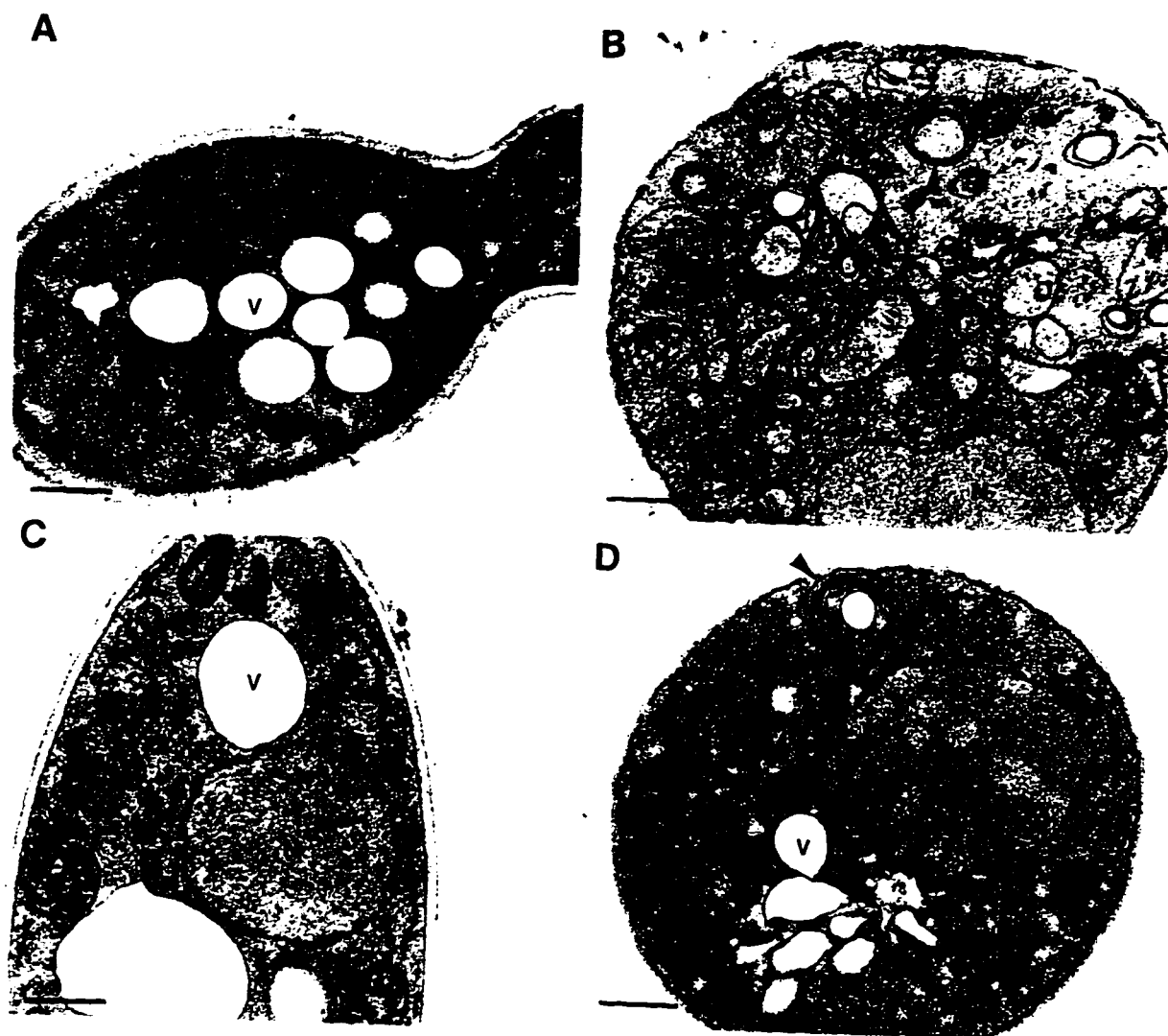


Figure 4.2 Ultrastructure of the wild-type, *pex2* mutant and *PEX2* transformant strains. The *E122* (A), *pex2-1* (B), *PEX2* (C) and *P2KO-8A* (D) strains were grown for 16 h in YEPD medium to an OD_{600} of ~ 1.6 , transferred to YPBO medium (1:4 dilution), and grown for an additional 8 h in YPBO. Cells were fixed in 1.5% $KMnO_4$ and processed for electron microscopy. Arrowheads indicate vesicular elements surrounded by multiple unit membranes. P, peroxisome; M, mitochondrion; N, nucleus; V, vacuole. Bar = 0.5 μm .

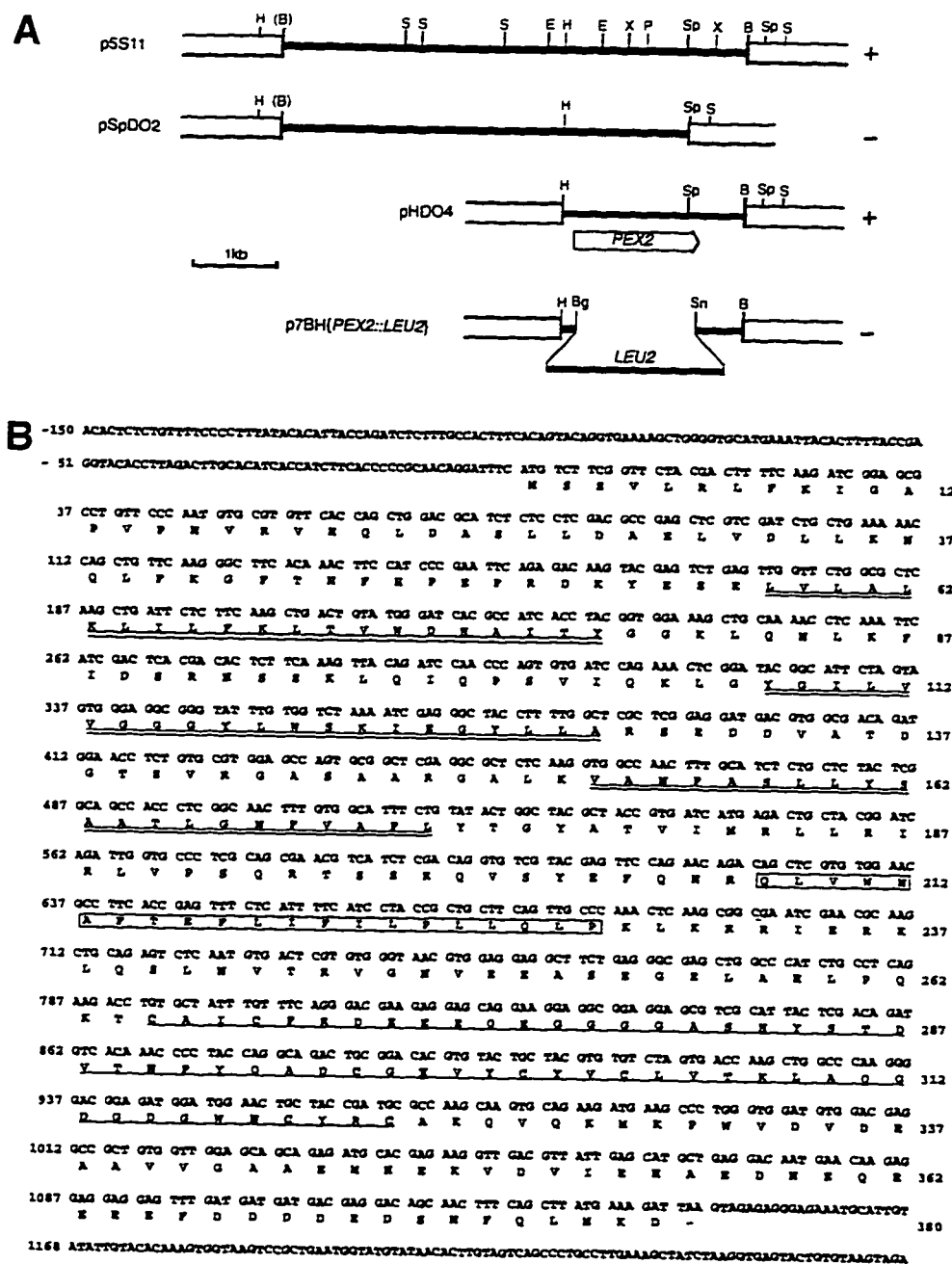


Figure 4.3 Cloning and analysis of the *YIPEX2* gene. (A) Complementing activity of inserts, restriction map analysis and targeted gene disruption strategy for the *YIPEX2* gene. Solid lines, genomic sequences; open boxes, vector sequences; *YIPEX2* open reading frame is indicated by the wide arrow. The (+) symbol denotes the ability and the (-) symbol denotes the inability of an insert to confer growth on oleic acid to *pex2-1*. B, *Bam*HI; Bg, *Bgl*II; E, *Eco*RI; H, *Hind*III; P, *Pst*I; S, *Sal*I; Sn, *Sna*BI; Sp, *Sph*I; X, *Xho*I. (B) Nucleotide sequence of the *YIPEX2* gene and deduced amino acid sequence of Pex2p. Underlined residues, C₃HC₄ RING-finger motif; boxed residues, predicted membrane-spanning α -helix; doubly underlined residues, predicted membrane-associated helices (see Section 3.5). The nucleotide sequence has been submitted to GenBank with accession number U43081.

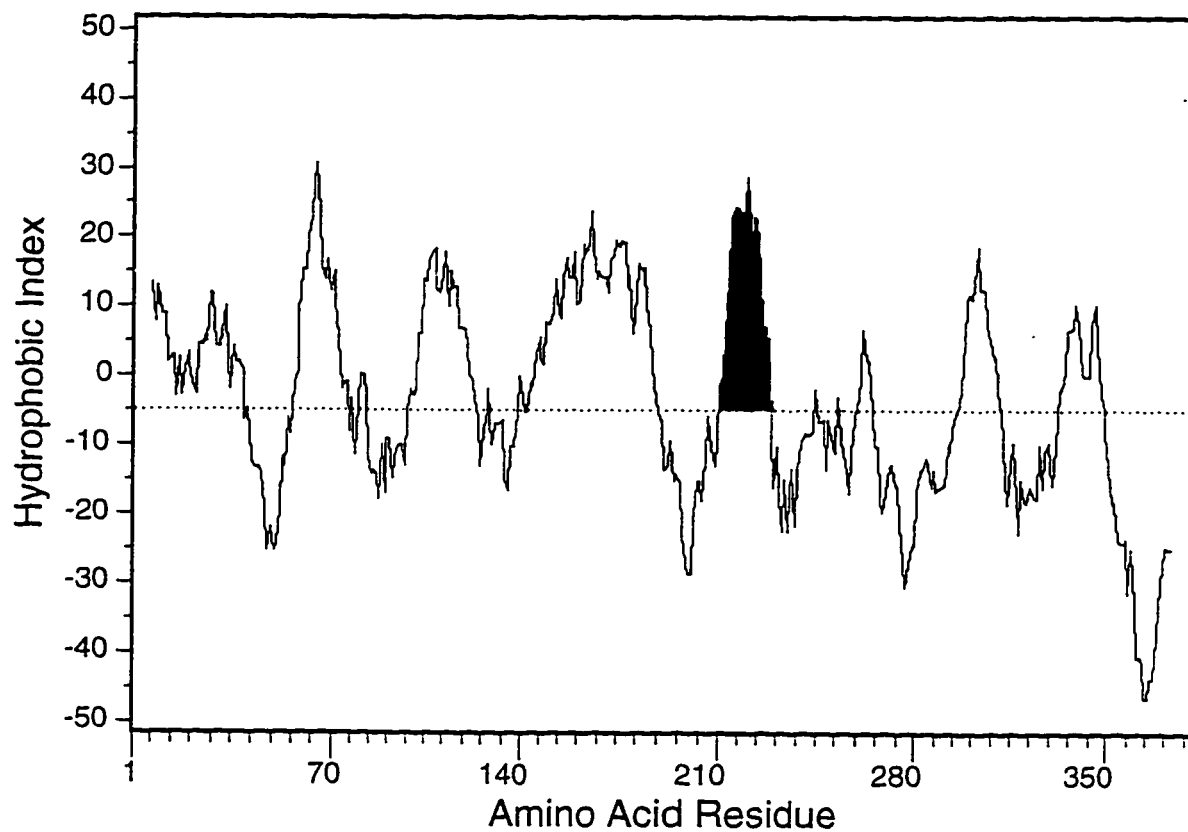


Figure 4.4 **Hydropathy analysis of Pex2p.** A hydropathy plot of the predicted amino acid sequence of the Pex2p peroxin, calculated according to Kyte and Doolittle (1982) with a window of 15 amino acids. The area *highlighted in black* contains a putative membrane-spanning α -helix.

(see *Section 4.5*) as the original *pex2-1* mutant. The diploid strains *D2-OB*, *D2-A9*, and *D2-8B* (Table 2.3), generated by mating the original mutant or gene disruption strains with wild-type strains, could grow on oleic acid (Fig. 4.1), demonstrating the recessive nature of the *pex2-1* mutation. The diploid strain *D2-O9* from the mating of *pex2-1* and *P2KO-9B* (Table 2.3) was unable to grow on oleic acid (Fig. 4.1), indicating that the authentic *YIPEX2* gene had been cloned. In all cases, the ability to utilize oleic acid as a carbon source required at least one intact copy of the *YIPEX2* gene.

Northern blot analysis showed a large induction in the level of *YIPEX2* mRNA 4 h after shifting wild-type *E122* cells from growth in glucose-containing medium to growth in oleic acid-containing medium (Fig. 4.5). Blots were hybridized with radiolabelled probes specific for the *Y. lipolytica* *PEX2* and thiolase coding regions. To allow for a qualitative comparison, these probes were of similar size, and equal amounts were labelled to comparable specific activities. Very low levels of *YIPEX2* mRNA expression were observed (blot was exposed 5 d), compared to the levels of mRNA for the peroxisomal matrix protein thiolase (blot was exposed 20 h).

4.3 Pex2p is a *Y. lipolytica* homologue of mammalian PAF-1 proteins

A C₃HC₄ RING-finger motif (Lovering et al., 1993) is found toward the carboxyl terminus of Pex2p (Fig. 4.3 B, *underlined residues*). A search of protein databases using the GENINFO(R) BLAST Network Service (Blaster) of the National Center for Biotechnology Information identified a number of proteins with homology to Pex2p within the RING-finger

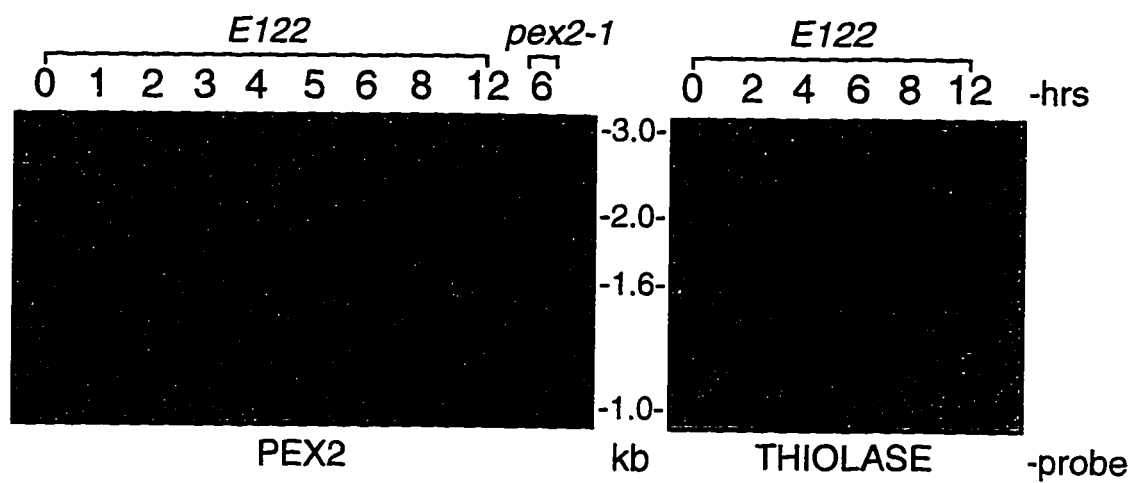


Figure 4.5 **Pex2p and peroxisomal thiolase mRNA are induced by growth of *Y. lipolytica* in oleic acid.** Total RNA was isolated from strains *E122* and *pex2-1* grown in YEPD medium (0 h) and after transfer to YPBO medium for different periods of time (*numbers* at the top in h). 10 μ g of RNA from each time point was run on a formaldehyde-agarose gel and transferred to nitrocellulose. The blots were hybridized with radiolabelled probes specific for the *Y. lipolytica* *PEX2* and thiolase genes. The *numbers* between the panels indicate the migration of size standards in kbp. Exposure time was 5 d for *PEX2* and 20 h for *THIOLASE* blots.

motif. Pex2p also showed significant sequence homology to five proteins outside this motif: human, rat and Chinese hamster ovary (CHO) PAF-1 proteins; *P. pastoris* PER6p; and the fungal *Podospira anserina* CAR-1 protein. All of these proteins are now designated Pex2p (*i.e.* *Hs*, *Rn*, CHO, *Pp* and *Pa*Pex2p respectively) (Distel et al., 1996). *Yl*Pex2p exhibits 32%, 32% and 33% identity with *Hs*, *Rn*, and CHO Pex2p, respectively. All mammalian Pex2p peroxins are integral to the peroxisomal membrane and affect peroxisome assembly when mutated (Shimozawa et al., 1992; Tsukamoto et al., 1991; 1994). Mutation of the gene encoding *Hs*Pex2p results in Zellweger (cerebrohepato renal) syndrome (Shimozawa et al., 1992). *Yl*Pex2p shows 43% and 40% identity to *Pa*Pex2p (Berteaux-Lecellier et al., 1995) and *Pp*Pex2p (Waterham et al., 1996), respectively. *Pa*Pex2p and *Pp*Pex2p show 27% identity to all mammalian Pex2p peroxins. Mutations in the gene encoding *Pa*Pex2p peroxin lead to peroxisome and sexual karyogamy defects (Berteaux-Lecellier et al., 1995). Alignment of *Yl*Pex2p with *Hs*Pex2p, *Pp*Pex2p and *Pa*Pex2p proteins (Fig. 4.6) shows several regions of strong homology outside the C₃HC₄ domain, including the amino-terminal portions of the proteins and a stretch of 39 amino acids (amino acids 198-233 of *Yl*Pex2p) encompassing hydrophobic segments within all four proteins. Both regions of strong homology are known to be essential for CHO Pex2p function (Tsukamoto et al., 1994). Additionally, yeast and fungal Pex2p peroxins contain a carboxyl-terminal hydrophilic domain rich in aspartic and glutamic acid residues. This domain is not found in the mammalian Pex2p peroxins. Therefore, it is possible that the mammalian proteins lack certain functional aspects of the yeast and fungal peroxins.

Yl	MS-----	2
Hs	MA-----	2
Pp	MP-----	2
Pa	MSDSKPPKDS SSPSAAVPDVAAAAASSTPTPAPVAITPPSNPQSAHSFAQAQQRLIARRQTRDA	64

Yl	-----SVLR-----LFGKIGAPVPN-----VRVHQLDASLLDAE	30
Hs	-----SRKE-----NAKS-ANRV-----LRISQLDALELNKA	28
Pp	-----NR-----LIPL-ANPAN-----RVLQLDAKLLDNE	26
Pa	QEAARVAAQQSESQLRARIAASQSPLLRRLGASTLSLWDTISSREGTRPAFRVGQVDAELLDEE	128

Yl	LVDLLKNQLFKGF-TNF---HPEF---RDKYSESLVLALKLILFKLTVWDEAITYGKQLNKLKFT	88
Hs	LEQLVWSQFTQCF-HGF---KPGLLAR---FEPEVKACLWVFLWRFTIYSKNATVGQSVLNLIKVK	87
Pp	ISDMLYRQLSGAFNSMR-LPSWLGRHSNYASELKLLLELLIFKVTVWNKHSSYGLTTLQNLVMY	89
Pa	LVLELMKGQVGEAVRYYGGGGGDNNIKHEWDAEISLALRAVIFKLTIWDEDATYGAALQNLKYT	192

Yl	DSR-HSSKLQIQ-PSVIQKLGYGILVVG---GYLWSKIEGYLLARSEDDVATDGTSVRGASAA	147
Hs	NDF--SPNLRYPSPSKNQKIWYAVCTIGG---RWLEER---CYDLFRN-HHLASFQKVKQCVNFV	142
Pp	DGGVBNKKFRSKQSEL-RVTKKILLSSVLLGYFVKKIQSYVYSFEDYDLETGDEDLSTLERI	152
Pa	DAR-H-TGSVLVPPSKWQKGLYGLMTVGG---RYMWSKWENWL---REQDGG-YDEPSPTVQRLS	248

Yl	RG-ALKVANFA-SLLYSAAT---LGNFVAFLYTG-YATVIMRLLRIR---LVPSQRT---SSRQ-	200
Hs	IG-LLKLGG-----LINFLIFLQRGKFATLTERLLGIH-SVFCCKPN---IRE-	187
Pp	RLKTIKLLKSQISTLEKAHSLVSNFVTVLVSGSPDLTTRILNIRFKPLVTTQVAFASNPET	216
Pa	SM-TDRL-----STLHAAASFASFLVFLQGRYRTLDRVLRM---RLAP-PTSQV---SRE-	299

Yl	VSIEFQNRQLVWMAFTEFLIFILPLLQPLKRRIERKL---QSLNVTVRVGNVEEASEGELAHL	260
Hs	VGFEYMNRELLWHGFAEFLIFLLPLINVQKLKA---KL---SSWCIPLTG---APNSDNTLAT-	240
Pp	ISYEFQNRQLVWNTLTETIVFILPALSVPKFTKSLVSSI---TGTSFKSSQVTDLEDL-VFSSL	276
Pa	VSFEYLNRLVWMAFTEFLIFVLPVGINRWRLARTWRKTRKIMSTTGEGEAEEKGEFAFL	361

Yl	PQRTCAICFRD-----EEEQEGGGGASHYSTDVTNTPYQA-DCGHVYCYVCLVTKLAQG	312
Hs	SGKECALC-----GEWP-----TMPH-TIGCEHIFCYFC---AKSSFL	273
Pp	PERVCAICFQN-----SQNSDSGAQNDISLNTFLVTNTPYET-TCGHIYCYVCILSKLQIF	330
Pa	PERTCAICYQDQNAQATNENELMAAATSKTGTVGSAQTDVTNTPYETIPCGCVYCFVCLATRIERE	425

Yl	DGDGWN-----CYRCAKQVQKMKPW-----VDVDEAAVVGA-----	343
Hs	-----FDVYFTCPKCGTEVHSLQPL-----KSGIEMSEVNAL	305
Pp	KEEGKNLPKSDPNKYWHCLRCNEPASWCRVYTGDEVDA LRQKAVEEVTEDEDA SSED EEEKRDQD	394
Pa	EGEGWN-----CLRCGELVKECKPWSGDVLEHESKSPAQKTVVFADDVKD-----	470

Yl	AEMHEKVDVIEHA-----EDNE-----QEEEE-----	365
Pp	SEGAKTVSQSFHHVNGSDYQTASFIEQAELNENEYTDGSEVEIYDAEDE-----	443
Pa	-----ASDDEQENSQVLVQQEDDDEYP EEEEGEEGEEEEEEEGSRSL EDLRTES	521

Yl	-----FDDD--DEDSNFQLMKD	380
Pp	-----YTDEEVDDDSPGFFVGAL	461
Pa	ASEESSEQEADSEGDESEDY--EAE EEEELGADLDED	554

Figure 4.6 Alignment of *Y. lipolytica* Pex2p with the human, *P. pastoris* and *P. anserina* homologues. Identical or similar residues are in *bold*. Residues identical in at least three sequences are indicated by an *asterisk*. Highly homologous domains are *boxed*. Similarity rules: I = L = V = M; A = S = T; F = Y = W; K = R; D = E; Q = N.

4.4 Pex2p is a peroxisomal integral membrane protein

Hydropathy analysis (Fig. 4.4) showed Pex2p to be hydrophobic overall and most likely a membrane protein. Based on algorithms predicting membrane-spanning regions of proteins (Eisenberg et al., 1984; Klein et al., 1985; Rao and Argos, 1986), Pex2p was predicted to contain one membrane-spanning α -helix (Fig. 4.3 A, *boxed residues*) and three membrane-associated helices (Fig. 4.3 A, *doubly underlined*). To examine the localization of Pex2p, subcellular fractions and purified peroxisomes were prepared from YPBO-grown wild-type cells. Immunoblot analysis with anti-Pex2p antibodies showed Pex2p to be localized to peroxisomes (Fig. 4.7, *lane PX*) but absent in a 20KgS fraction enriched for cytosol (Fig. 4.7, *lane S*). Lysis of peroxisomes with Ti8 buffer or treatment with sodium carbonate buffer (CO3), followed by high-speed centrifugation, showed Pex2p to be localized exclusively to pellet fractions (Fig. 4.7, compare *lanes P_{Ti8}* and *S_{Ti8}*, and *lanes P_{CO3}* and *S_{CO3}*), consistent with Pex2p being integral to the peroxisomal membrane. Pex2p was not found in either the 20KgS (*lane S*) or 20KgP (*lane P*) from the *pex2-1* mutant.

YIPEX2 was expressed in mammalian cells (*performed by Ms. Jennifer Smith*). Immunofluorescence microscopy showed that *YIPex2p* localized to peroxisomes and colocalized with anti-SKL-reactive proteins in wild-type CHO cells (strain K1) transfected with the *YIPEX2* gene (Fig. 4.8). Therefore, the mechanism of targeting integral membrane proteins to peroxisomes appears to have been conserved in both yeast and mammals.

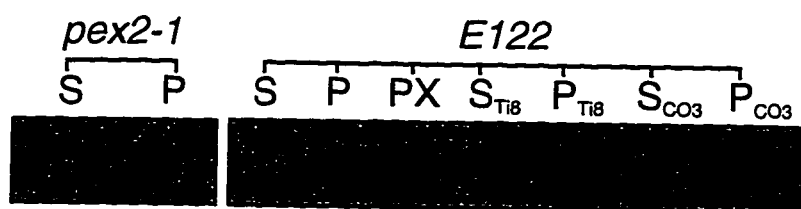


Figure 4.7 **Pex2p is a peroxisomal integral membrane protein.** Immunoblot analysis of 20KgS (*S*) and 20KgP (*P*) subcellular fractions, whole peroxisomes (*PX*) and peroxisomal subfractions (S_{Ti8} , P_{Ti8} , S_{CO3} and P_{CO3}) of the wild-type *E122* and *pex2-1* mutant strains, with anti-Pex2p antibodies. Equal portions (0.5% of total fraction volume) of the 20KgS and 20KgP fractions were analyzed. Purified peroxisomes (30 μ g of protein) were lysed with Ti8 buffer and subjected to centrifugation to yield a 245,000 $\times g_{max}$ supernatant (S_{Ti8}) and pellet (P_{Ti8}). S_{CO3} and P_{CO3} correspond to the 245,000 $\times g_{max}$ supernatant and pellet, respectively, recovered after treatment of the P_{Ti8} with 0.1 M Na_2CO_3 (pH 11).

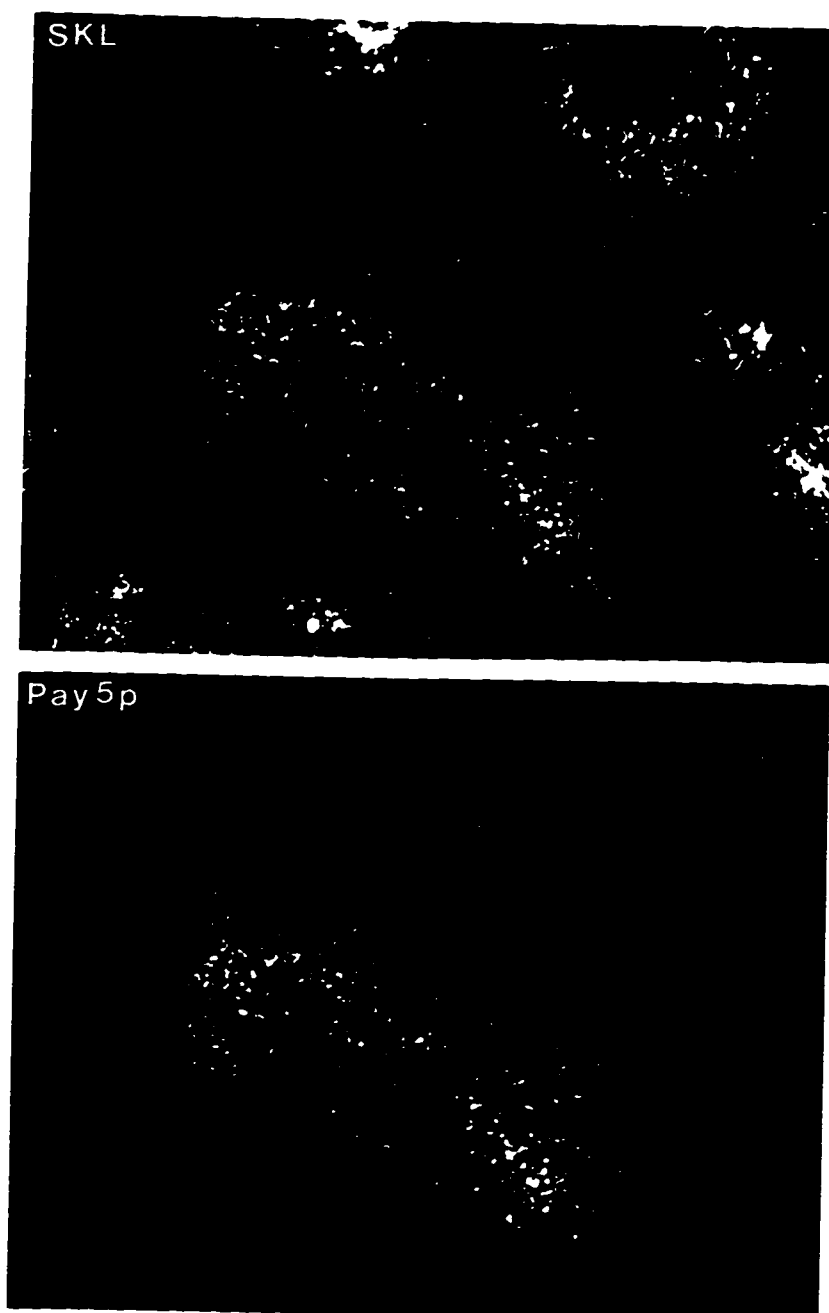


Figure 4.8 *YIPex2p* is targeted to peroxisomes of CHO cells. Double label, indirect immunofluorescence analysis of the CHO wild-type cell line, CHO-K1, transfected with the plasmid pSG5-*YIPEX2* expressing the *YIPEX2* gene. Primary antibodies were rabbit anti-SKL (*SKL*) and guinea pig anti-Pex2p (*Pex2p*). Primary antibodies were detected with fluorescein-conjugated goat anti-rabbit IgG and rhodamine-conjugated donkey anti-guinea pig IgG secondary antibodies. The transfected cell in the center of the field is decorated by both anti-SKL and anti-Pex2p antibodies. Cells surrounding this central cell were not transfected and do not show decoration by anti-Pex2p antibodies. However, these cells are still decorated by anti-SKL antibodies.

4.5 Peroxisomal proteins are mislocalized to the 20KgS enriched for cytosol to varying extents in *pex2* mutant cells

Mutations in the *YIPEX2* gene do not affect the synthesis of peroxisomal proteins. When wild-type, *pex2-1* and *P2KO-8A* strains were grown in YEPD for 15 h to an OD₆₀₀ of ~1.5 and then diluted 1:4 in YPBO and grown for a further 8 h, the levels of peroxisomal proteins were greatly induced and reached steady state in all three strains. No significant differences in the steady state levels of all peroxisomal proteins analyzed were found in the three strains (Fig. 4.9, *top panel*) (*performed by Dr. Vladimir Titorenko*). However, the distribution of these proteins between the 20KgP and the 20KgS was altered in both the original mutant and the gene disruption strains as compared to the wild-type strain (*portions of this analysis contributed by Dr. Vladimir Titorenko*). In wild-type cells, from 80 to 98% of all peroxisomal proteins analyzed were localized to the 20KgP fraction (Fig 4.9, *bottom panel*), with only 0 to 18% mislocalized to the 20KgS fraction (Fig 4.9, *middle panel*). In *pex2* mutant cells, a significant fraction of these proteins was mislocalized to the 20KgS (Fig. 4.9, *middle panel*). Furthermore, in the *pex2* mutants, the extent of mislocalization to the 20KgS varied for different peroxisomal proteins. Import of isocitrate lyase and catalase was most affected, with 81 to 91% of each protein mislocalized to the 20KgS fraction. The import of thiolase, 3-hydroxyacyl-CoA dehydrogenase and Pex5p was less affected (79 - 57 % mislocalized to the 20KgS), while the import of malate synthase, acyl-CoA oxidase and a 62 kDa anti-SKL-reactive protein was the least affected (46 - 37% mislocalized to the 20KgS).

To test whether matrix proteins were truly mislocalized to the cytosol, the 20KgS fractions of wild-type and mutant strains were subjected to a second 200,000 × *g*_{max}

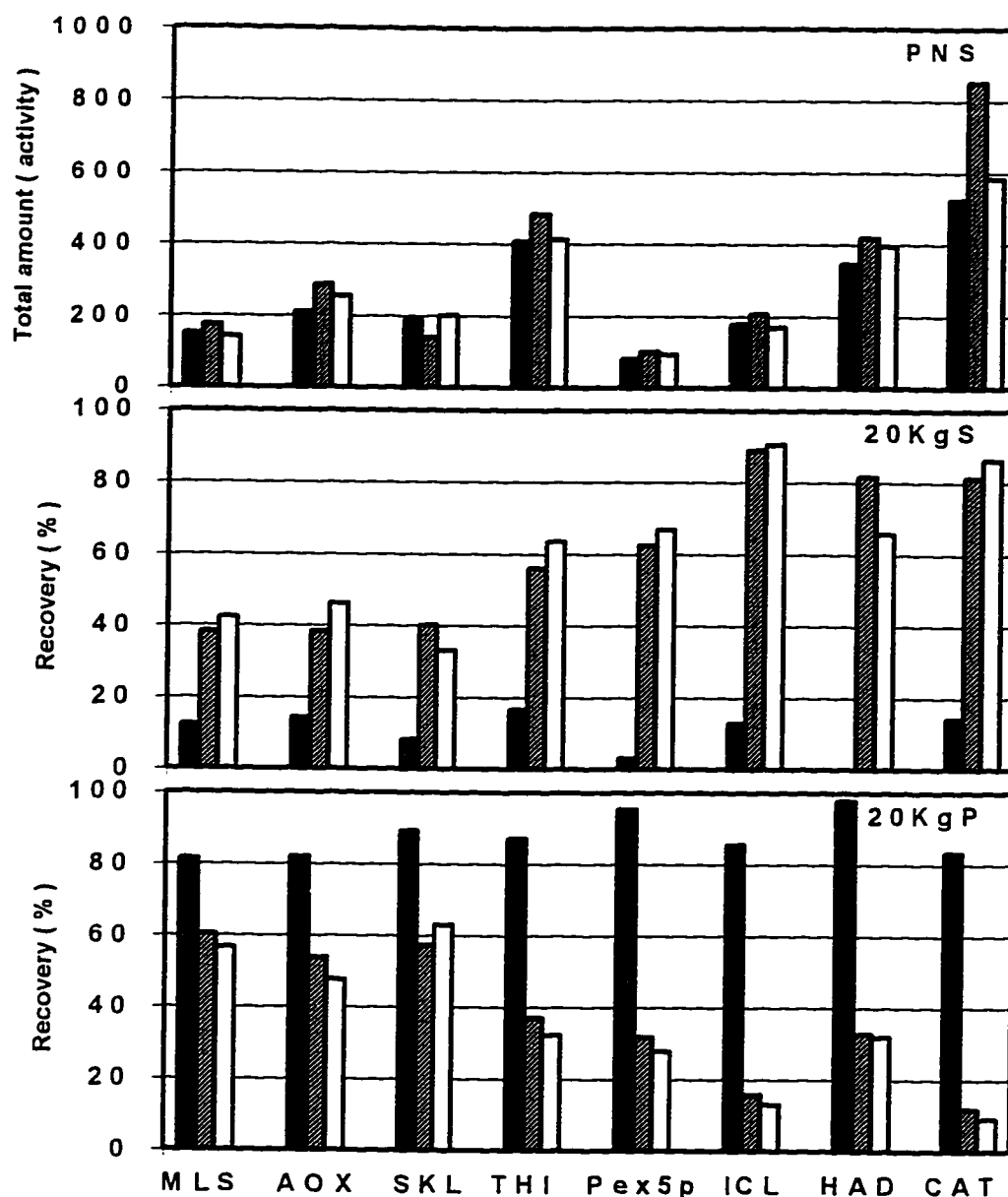


Figure 4.9 Peroxisomal proteins are synthesized normally but are mislocalized to the 20KgS fraction to varying extents in *pex2* mutants. Wild-type *E122* (solid bar), *pex2-1* (stippled bar) and *P2KO-8A* (open bar) strains were grown 8 h in YPBO as described in the legend to Figure 4.2. Cells were subjected to subcellular fractionation. The total enzymatic activities of catalase (CAT) and 3-hydroxyacyl-CoA dehydrogenase (HAD) contained in 10 mg of protein of postnuclear supernatant (PNS) are expressed either in U (CAT) or in mU x 10 (HAD) (top panel). The percentage of total enzymatic activity of CAT and HAD recovered in the 20KgS (middle panel) and 20KgP (bottom panel) are shown. Equal fractions (0.2% of the total volume) of the PNS, 20KgS and 20KgP were also analyzed by immunoblotting with anti-malate synthase (MLS), anti-acyl-CoA oxidase (AOX), anti-SKL (SKL), anti-thiolase (THI), anti-Pex5p and anti-isocitrate lyase (ICL) antibodies. Immunoblots were quantitated by densitometry (arbitrary units). SKL, quantitation was performed for the 62 kDa anti-SKL-reactive polypeptide.

centrifugation to pellet light membrane-enclosed vesicles (a high speed particulate fraction, HP), which were not pelletable by centrifugation at $20,000 \times g_{\max}$ (*performed by Dr. Vladimir Titorenko*). Immunoblot analysis showed that isocitrate lyase, which is highly mislocalized to the 20KgS in *pex2* mutant strains, was truly mislocalized to the cytosol in these strains since it was mostly present in the high speed supernatant fraction (Fig 4.10, *lane HS*). However, this was less true for thiolase and the peroxisomal membrane-associated protein Pex5p, which both showed small amounts of material in *pex2* mutant high speed particulate fractions (Fig 4.10, compare *lanes HS* and *HP*). Acyl-CoA oxidase, which is part of the least mislocalized group of peroxisomal proteins, showed a significant amount of protein localized to the the high speed particulate fraction, both in wild-type and *pex2* mutant strains (Fig. 4.10, *lane HP*). This analysis provides evidence for the presence of a heterogeneous population of peroxisomes differing in density and protein content (or differential import of peroxisomal proteins) present both in wild-type cells and to a greater extent in *pex2* mutant cells.

4.6 *pex2* mutant strains accumulate peroxisomal intermediates that are associated with endoplasmic reticulum and Golgi elements

To further investigate the cellular characteristics resulting from *YIPEX2* mutation, organelles from the 20KgP fractions of wild-type and *pex2* mutant strains were fractionated by isopycnic centrifugation on discontinuous sucrose gradients (see *Section 2.4.2*). Fractions were analyzed for density, protein, and enzymatic activity of various organelle marker proteins (Fig. 4.11 *A*) (see *Section 2.5.4*) (Franzusoff et al., 1991). Fractions were also analyzed by immunoblotting with antibodies to peroxisomal matrix (anti-SKL reactive

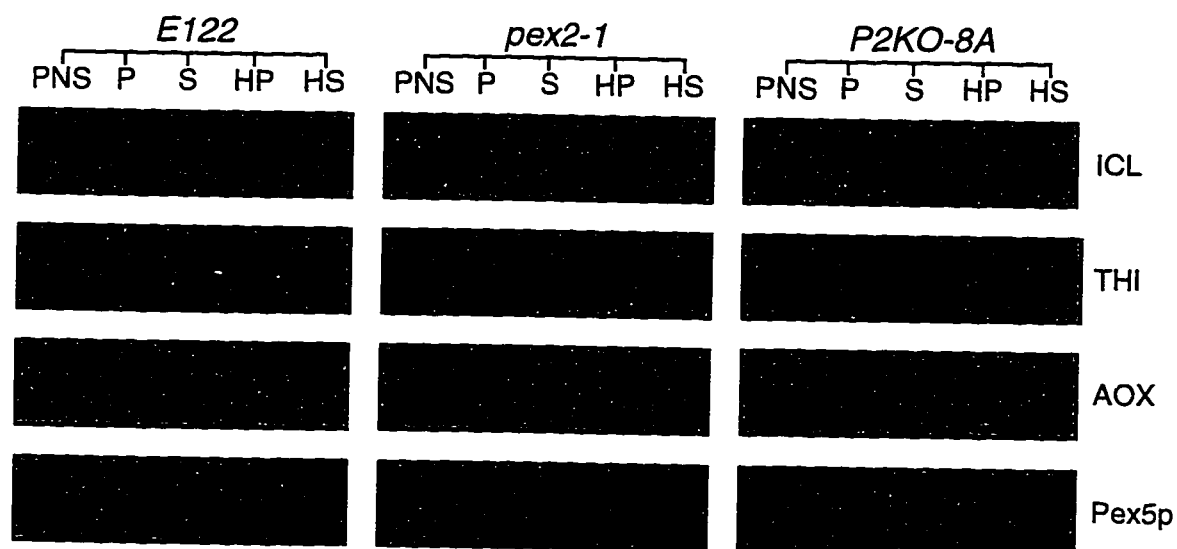


Figure 4.10 Peroxisomal proteins are mislocalized to cytosolic and light particulate fractions in *pex2* mutant cells. Wild-type *E122*, *pex2-1* and *P2KO-8A* strains were grown 8 h in YPBO, as described in the legend to *Figure 4.2*. Cells were subjected to subcellular fractionation (see *Section 2.4.2*). Equal fractions (0.2% of the total volume) of 20KgS (*S*) and 20KgP (*P*) from 20,000 $\times g_{max}$ postnuclear cell homogenates (*PNS*), and 200KgS (*HS*) and 200KgP (*HP*) from a 200,000 $\times g_{max}$ centrifugation of 20KgS fractions were analyzed by immunoblotting with anti-acyl-CoA oxidase (*AOX*), anti-thiolase (*THI*), anti-Pex5p and anti-isocitrate lyase (*ICL*) antibodies.

polypeptides, acyl-CoA oxidase, malate synthase and thiolase) and membrane (Pex5p) proteins (Fig. 4.11 B) (*portions of this analysis contributed by Dr. V. Titorenko*). In the wild-type strain *E122*, peroxisomal proteins were localized primarily to fractions 3-5, peaking in fraction 4 at a density of 1.21 g/cm³, and were essentially free of all other organelle marker enzyme activities assayed (Fig. 4.11 A). In the *pex2-1* and *P2KO-8A* mutant strains, two peaks of peroxisomal proteins were observed at densities of 1.23 g/cm³ (fraction 3) and 1.15 g/cm³ (fractions 11-13). The majority of the peroxisomal proteins peaked in fraction 12, which coincided with the peak activities of the endoplasmic reticular (ER) and Golgi marker enzymes NADPH:cytochrome *c* reductase and guanosine diphosphatase, respectively. In contrast, in the wild-type strain, ER and Golgi markers did not peak in fraction 12 but rather in fractions 10 (1.165 g/cm³) and 15 (1.10 g/cm³), respectively. The distributions of mitochondrial (cytochrome *c* oxidase), vacuolar (alkaline phosphatase) and plasma membrane (vanadate-sensitive ATPase) marker enzyme activities were comparable to those found for wild-type cells. Therefore, the biogenesis of mitochondria, vacuoles and plasma membrane was apparently not affected by the *pex2* mutation. Subsequent purification of the light peroxisomes from *pex2* mutants by flotation gradient analysis (see *Section 2.4.2*) resulted in colocalization of ER, Golgi and peroxisomal marker enzyme activities. These results show that, in the *pex2* mutants, at least three subpopulations of peroxisomes exist: a free form at 1.23 g/cm³, an ER- and Golgi-associated form at 1.15 g/cm³ and a third light, particulate form in the 200K_{gP}. Peroxisomal subpopulations have previously been observed in other yeast species (Spong and Subramani, 1993; Heyman et al., 1994), and in mammalian cells (Heinemann and Just, 1992; Lüers et al., 1993). It has been postulated that these lighter peroxisomal populations are intermediates of the peroxisome assembly pathway.

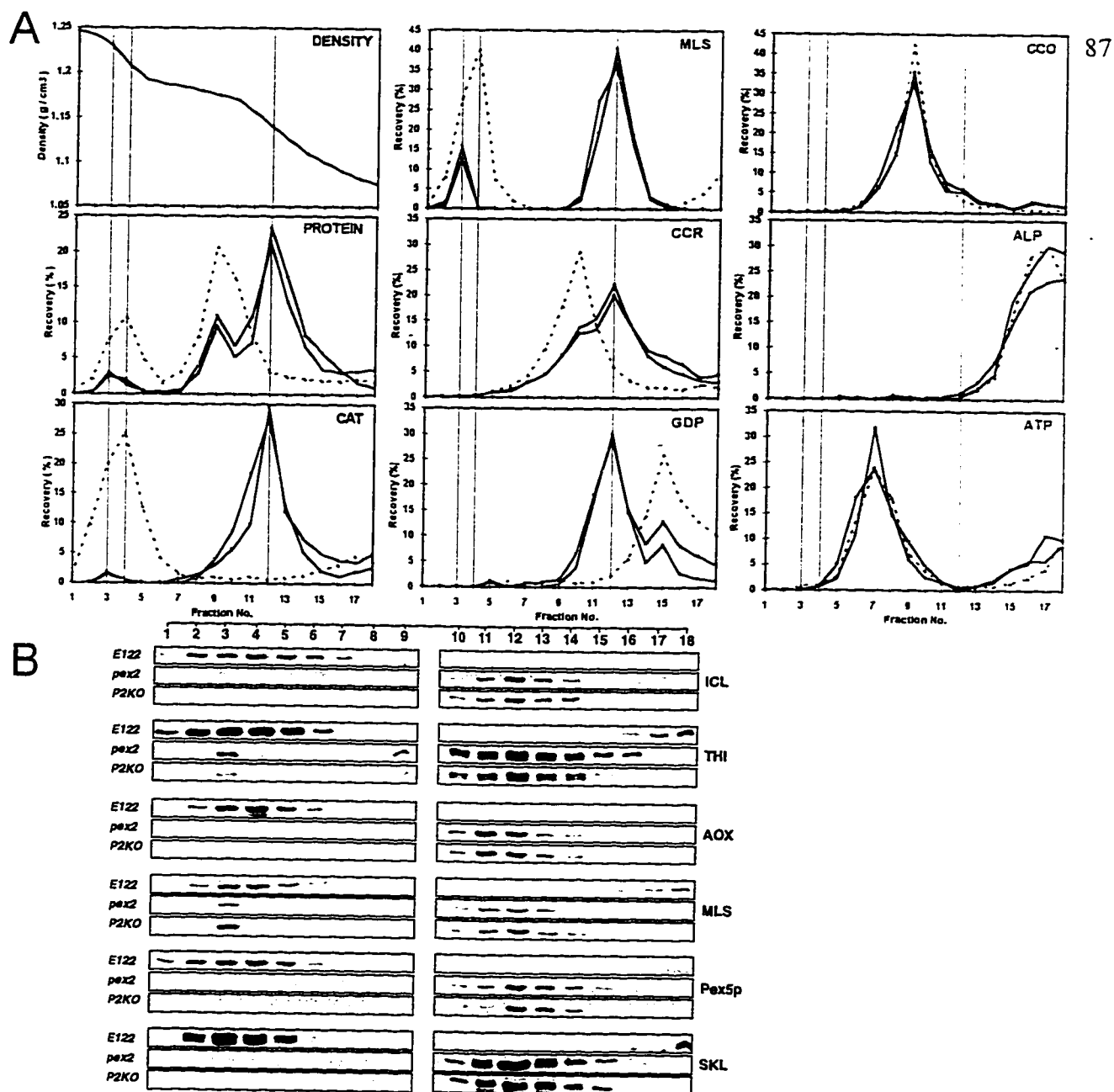


Figure 4.11 Density gradient analysis shows the accumulation of ER- and Golgi-associated light peroxisomes in *pex2* mutant cells. *E122*, *pex2-1*, and *P2KO-8A* strains were grown for 8 h in YPBO, as described in the legend to *Figure 4.2*. 20K_gP fractions were subjected to isopycnic centrifugation in discontinuous sucrose gradients (see *Section 2.4.2*). (A) Sucrose density (g/cm³) and percent recovery of protein, catalase (CAT), NADPH:cytochrome *c* reductase (CCR), guanosine diphosphatase (GDP), cytochrome *c* oxidase (CCO), alkaline phosphatase (ALP), and vanadate-sensitive ATPase (ATP) activities in 18 equal volume fractions of wild-type (—), *pex2-1* (—■—), and *P2KO-8A* (—□—) strains. For malate synthase (MLS), the immunoblot in B was quantitated by densitometry. (B) Immunoblot analysis of equal amounts of gradient fractions with anti-isocitrate lyase (ICL), anti-thiolase (THI), anti-acyl-CoA oxidase (AOX), anti-malate synthase (MLS), anti-Pex5p and anti-SKL antibodies.

4.7 Summary and discussion

Here we describe the isolation of *pex2* mutant strains, their morphological and biochemical characterizations, the cloning of the *YIPEX2* gene, and the identification and characterization of the *YIPEX2* gene product, Pex2p, which is essential for peroxisome biogenesis.

4.7.1 *pex2* mutant cells accumulate intermediate peroxisomal vesicles that are incompletely blocked in import and which associate with ER and Golgi elements

pex2 mutant strains are unable to grow on oleic acid and accumulate multiple membrane-bound vesicular structures under peroxisome-inducing conditions. We suspect that these vesicles define a peroxisomal intermediate compartment that can apparently assemble a partially active peroxisomal protein targeting and translocation machinery. This machinery seems to selectively import a subset of peroxisomal matrix proteins, since the levels of acyl-CoA oxidase, malate synthase and a 62 kDa SKL-reactive polypeptide in peroxisome-enriched fractions are only slightly less than those found in peroxisomes from the wild-type strain. In contrast, import of catalase and isocitrate lyase is severely affected in *pex2* mutant strains. Moreover, *pex2* mutant strains are not selectively affected in peroxisomal import of proteins targeted by either PTS1 or PTS2 pathways. A 62 kDa SKL-containing polypeptide (PTS1) and thiolase (PTS2) (Berninger et al., 1993) are imported with comparable efficiencies in *pex2* mutants. However, import of a second PTS1-containing protein, isocitrate lyase (Barth and Scheuber, 1993), is significantly more affected. Possible

explanations for the differences in import of the two PTS1-containing proteins is that one protein could be imported into peroxisomes by an alternative PTS (*i.e.* a second PTS) as reported for *S. cerevisiae* catalase A and *H. polymorpha* Per1p, or by a more degenerate import mechanism (Kragler et al., 1993; Waterham et al., 1994).

The glycosome biogenesis mutant, *gim1-1*, of the trypanosomatid *Leishmania* was recently reported (Flaspohler et al., 1997). Interestingly, the defective protein, Gim1p, is highly homologous to Pex2p family members (20% - 28% identity), revealing an evolutionary relationship between peroxisomes and glycosomes. Additionally, this mutant mislocalizes a subset of glycosomal proteins, a defect similar to that observed for peroxisomes in *Y. lipolytica pex2* mutants.

Mutation of *YIPEX2* results in the accumulation of at least three peroxisomal subpopulations, as shown by subcellular fractionation and density gradient analysis of *pex2* mutant cells. At the same time, maturation of functional peroxisomes is blocked. The peroxisomal subpopulations are characterized by differences in buoyant density and protein content, with vesicles that migrate to a density of 1.15 g/cm³ containing most of the peroxisomal proteins and copurifying with ER and Golgi components. These vesicular structures may represent peroxisomal remnants of an intermediate stage of the peroxisome assembly pathway, which seems to involve the delivery of components from the ER and/or the Golgi (Fig 4.11). This biochemical evidence is supported by morphological data in mammalian cells implicating such a connection (Fahimi et al., 1993). The heterogeneity of peroxisomal subpopulations accumulating in *pex2* mutant strains is further emphasized by the observation that different peroxisomal matrix proteins are localized to varying extents to a

high speed particulate fraction. Very light peroxisomal vesicles (pelletable by centrifugation at $200,000 \times g_{\max}$) have also been found in regenerating rat liver cells (Fahimi et al., 1993; Heinemann and Just, 1992).

4.7.2 *Proteins with carboxyl-terminal C₃HC₄ domains are important for organelle biogenesis*

Which structural features of Pex2p might be essential for its function in peroxisomal membrane assembly? Pex2p belongs to the newly characterized C₃HC₄-RING finger protein superfamily. This family encompasses a diverse group of proteins originally thought to mediate transcription through DNA binding via the C₃HC₄ motif (Lovering et al., 1993). More recently, this domain has been discovered in several proteins involved in organelle assembly in yeast. The proteins Pep3/Vsp18 (Preston et al., 1991, Robson et al., 1991) and Pep5/Vsp11/End1 (Woolford et al., 1990, Dulic and Riezman, 1989) that are involved in vacuole biogenesis, and the proteins Pex10p (Tan et al., 1995; Kalish et al., 1995) and Pex12p (Kunau et al., 1993; Kalish et al., 1996) that are necessary for peroxisome biogenesis, all contain C₃HC₄ domains. All of these proteins, including Pex2p, have been localized to the membranes of their respective organelles and accordingly DNA binding is not readily possible. Roles other than DNA binding have been suggested for these domains. The C₃HC₄ domains may act to stabilize tertiary protein structure (Berg, 1990), protein-protein interactions (Giedroc et al., 1987; Lillie et al., 1987) or protein-lipid interactions (Quest et al., 1992). It is also noteworthy that the C₃HC₄ domains are always at the carboxyl-termini of the proteins involved in organelle biogenesis. Therefore, a subfamily of RING-finger

proteins can be defined as those proteins which contain carboxyl-terminal C₃HC₄ domains and have roles in organelle biogenesis.

4.7.3 *Possible role of Pex2p in membrane biogenesis*

YIPex2p shows marginal homology to most C₃HC₄-containing proteins involved in organelle biogenesis outside of this domain, with the exception of other peroxins with the Pex2p designation (Fig. 4.6). Interestingly, *PaPex2p* was discovered by complementation of a karyogamy (nuclear fusion) mutant (Berteaux-Lecellier et al., 1995). Subsequently, *PaPex2p* was localized to peroxisomal membranes and found to be essential for fungal peroxisome development, as is the case for Pex2p in yeast and in mammals. We observed in our mutant strains the failure to form unilamellar peroxisomes. These morphological observations, combined with biochemical evidence of aberrant localization of ER and Golgi components, and results from studies of other defective RING-finger peroxins showing the accumulation of membrane sheets (Kalish et al., 1995; 1996) and membrane assembly defects (Berteaux-Lecellier et al., 1995; Waterham et al, 1996), we suggest Pex2p is a factor required for proper peroxisomal membrane assembly.

4.7.4 *Evolutionary conservation of peroxisomal membrane targeting signals*

The evolutionary conservation of the targeting mechanism of various peroxisomal matrix proteins is well established (Subramani, 1993). This study provides the first evidence that the mechanism of targeting integral membrane proteins to peroxisomes appears to be conserved in both yeast and mammals, since the yeast *YIPex2p* can be targeted to

peroxisomes of CHO cells *in vivo* (Fig. 4.8). However, our attempts to functionally complement a Pex2p-deficient CHO cell line, Z65 (Tsukamoto et al., 1991), with *Y*Pex2p have to date proven unsuccessful.

Recently, an internal targeting motif has been reported for the peroxisomal integral membrane protein, Pmp47p, of *C. boidinii* (Dyer et al., 1996). This signal consists of a cluster of basic amino acids in a hydrophilic loop between two hydrophobic domains (Table 4.1). A scan of the *Y*Pex2p amino acid sequence identified a highly similar region. Oddly, this *Y*Pex2p domain lies in a region of very low homology to other Pex2p family members. It is unknown if this region functions as a PTS for *Y*Pex2p.

Table 4.1 Amino acid alignment of putative Pmp47 internal PTS motifs and the corresponding Pex2p region.

Species		Block II ^a	Block III ^a
<i>C. boidinii</i>	Pmp47A	KIKKR	NITPVDA
<i>C. boidinii</i>	Pmp47B	KIKKR	NVTPVDA
<i>Y. lipolytica</i>	Pex2p	KLKRR	NVTRVGN
<i>S. cerevisiae</i>	47 ^b	RRKRE	IHLTNLET
<i>H. sapiens</i>	47 ^c	LLKKR	MKLSSLDV

^a Block II or Block III is sufficient for targeting chloramphenicol acetyl-transferase to peroxisomes (together they increase targeting efficiency)

^b possible homologue from Yeast Genome Sequencing project, accession number: YIL134W

^c possible homologue from human EST library, accession number: R54274

5. Over expression of the *Y. lipolytica* PEX16 gene encoding the peroxin Pex16p, an intraperoxisomal peripheral membrane protein, results in fewer but enlarged peroxisomes*

This chapter reports the characterization of the *Y. lipolytica pex16* mutant strains and the peroxin Pex16p. The *pex16* strains lack typical peroxisomes and mislocalize most peroxisomal matrix proteins. However, a subset of peroxisomal proteins is imported at, or near, wild-type levels into small vesicular structures that can be detected immuno-cytochemically. The *YIPEX16* gene was isolated by functional complementation of the *pex16-1* strain. It encodes a 391 amino acid residue peroxin, Pex16p (44,479 Da). Pex16p has no known homologues. It is a peripherally associated membrane protein located on the matrix face of the peroxisomal membrane. Removal or substitution of the carboxyl-terminal tripeptide Ser-Thr-Leu, which is similar to the PTS1 consensus sequence, does not affect targeting of Pex16p to peroxisomes. Pex16p is synthesized in wild-type cells grown in glucose-containing media, and its levels are only modestly increased by growth in oleic acid-containing medium. Overexpression of the *YIPEX16* gene leads to the appearance of a small number of enlarged, functional peroxisomes. These results suggest that Pex16p is a novel peroxin that can inhibit peroxisomal fission.

5.1 Isolation of the *YIPEX16* gene

The *pex16-1* mutant was isolated from randomly mutagenized *Y. lipolytica* cells by screening for the inability to utilize oleic acid as a sole carbon source (Fig. 5.1). Several biochemical and morphological criteria (data presented below) were used to determine that

*Portions of this chapter are reproduced from The Journal of Cell Biology (Eitzen et al., 1997 *In press*) with copyright permission of The Rockefeller University Press.

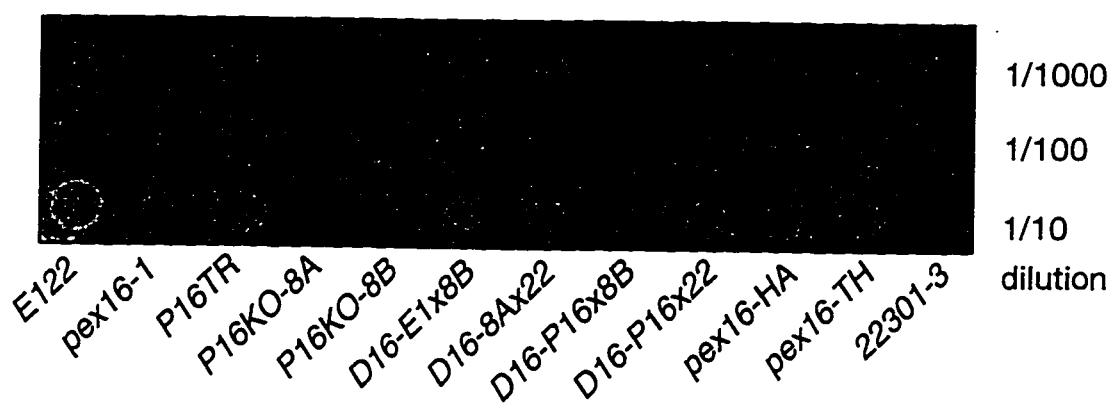


Figure 5.1 Growth of various *Y. lipolytica* *pex16* strains on oleic acid medium. Strains were grown for 3 d on YNO-agar. The appearance of the original *pex16-1* mutant is compared to that of the wild-type strain *E122*; the complemented strain *P16TR*; the gene disruption strains *P16KO-8A* and *P16KO-8B*; the diploid strains *D16-E1x8B*, *D16-8Ax22*, *D16-P16x8B* and *D16-P16x22*; the strain *pex16-HA* synthesizing Pex16p-HA; and the strain *pex16-TH* expressing the *YIPEX16* gene from the thiolase promoter. The wild-type strain *22301-3* was not supplemented for its auxotrophic requirements. Growth on YNO requires at least one copy of the intact *YIPEX16* gene.

this strain was affected in peroxisome assembly. The *YIPEX16* gene was isolated from a library of *Y. lipolytica* genomic DNA by functional complementation of the *pex16-1* strain. Approximately 10^6 Leu⁺ transformants were screened. Two strains recovered growth on oleic acid (ole⁻). Total DNA was isolated from these strains, and the complementing plasmids were recovered by transformation of *E. coli*. The recovered plasmids, p16N1 and p16C2, were mapped by restriction endonuclease digestion and were found to share a 5.5 kbp region (Fig. 5.2 A). Subfragments of this region were cloned, and the minimum complementing subfragment was localized to a 2.1 kbp *HindIII/ClaI* restriction fragment contained within plasmid p16HC2 (Fig. 5.2 A) in the transformed strain *P16TR* (Fig. 5.1).

Sequencing of the 2.1 kbp insert of p16HC2 revealed an open reading frame (ORF) encoding a protein of 391 amino acid residues, Pex16p, with a calculated molecular mass of 44,479 Da (Fig. 5.2 B). Hydropathy analysis predicted the presence of several hydrophobic segments capable of membrane interaction (Fig. 5.3). Pex16p was predicted to contain one membrane-spanning α -helix and three membrane-associated domains (Fig. 5.2 B). A search of protein data bases using the GENINFO(R) BLAST Network Service (Blaster) of the National Center for Biotechnology Information revealed no significant homology between Pex16p and any other known protein.

The putative *YIPEX16* gene was disrupted by targeted integration of the *Y. lipolytica* *LEU2* gene to make the strains *P16KO-8A* and *P16KO-8B* in the A and B mating types, respectively (Table 2.3). The *YIPEX16* gene was disrupted in such a manner as to lack its initiating methionine codon. Disruption strains *P16KO-8A* and *P16KO-8B* could not grow on oleic acid (Fig. 5.1) and acquired morphological and biochemical characteristics like those

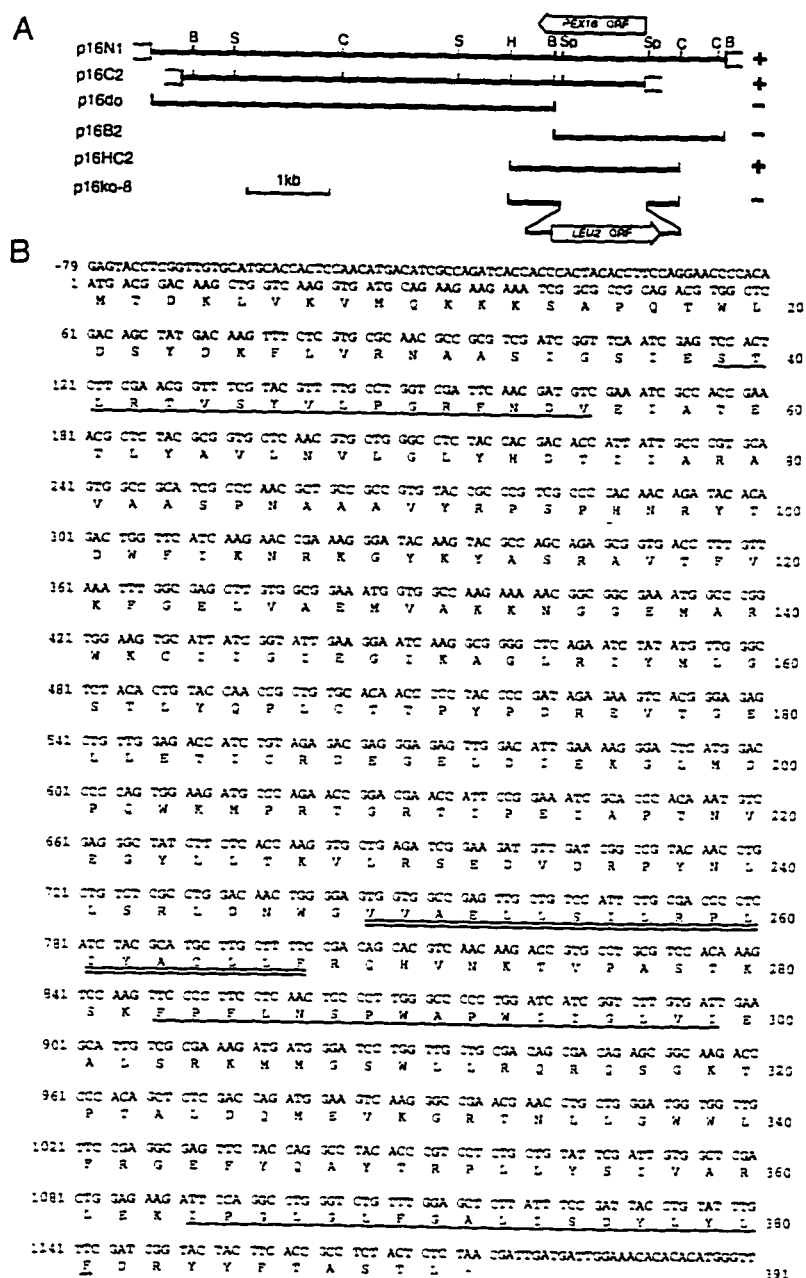


Figure 5.2 Cloning and analysis of the *YIPEX16* gene. (A) Complementation activity of inserts, restriction map analysis, and targeted gene disruption strategy for the *YIPEX16* gene. Solid lines, *Y. lipolytica* genomic DNA; open boxes, vector DNA. The ORFs of the *PEX16* and *LEU2* genes are indicated by the wide arrows. The (+) symbol denotes the ability and the (-) symbol the inability of an insert to confer growth on oleic acid to *pex16-1*. B, *Bam*HI; C, *Cla*I; H, *Hind*III; S, *Sal*I; Sp, *Sph*I. (B) Nucleotide sequence of the *YIPEX16* gene and deduced amino acid sequence of Pex16p. Underlined residues, predicted membrane-associated domains; doubly underlined residues, predicted transmembrane α -helix (see Section 3.5). The nucleotide sequence reported in this study has been submitted to GenBank with accession number U75433.

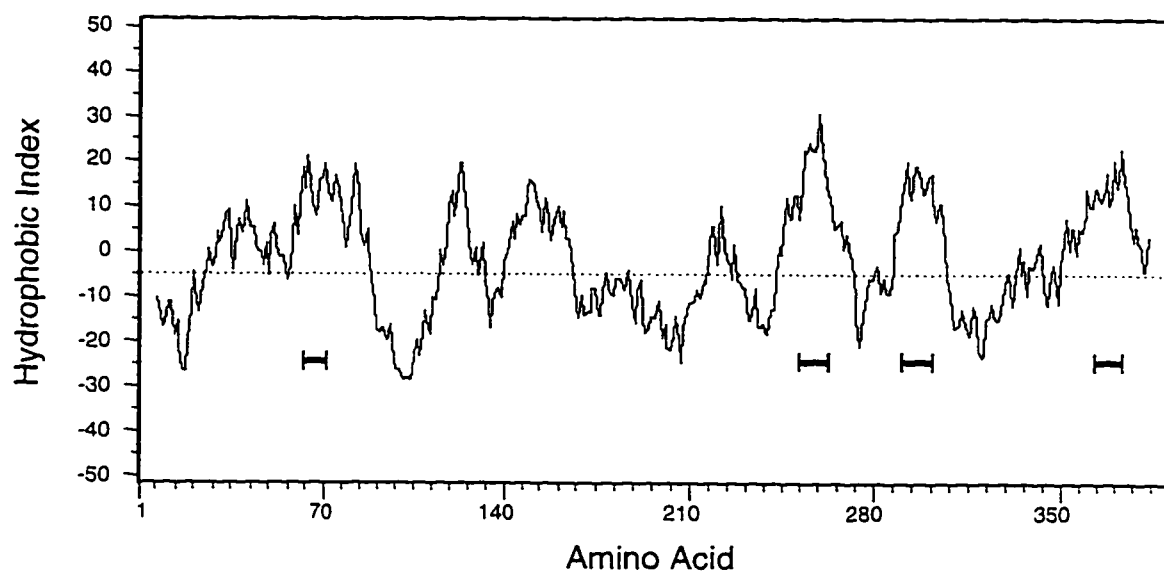


Figure 5.3 **Hydropathy profile of Pex16p.** Hydropathy analysis of Pex16p calculated according to Kyte and Doolittle (1982) with a window size of 15 amino acids. Four hydrophobic domains predicted to interact with membranes (see *Section 3.5*) are *underscored*.

of the original *pex16-1* strain (see below). The diploid strains *D16-8Ax22* and *D16-P16x22* from the mating of strains *P16KO-8A* and *pex16-1*, respectively, to wild-type strain 22301-3, and the diploid strain *D16-E1x8B* from the mating of wild-type strain *E122* to strain *P16KO-8B* (Table 2.3), could grow on oleic acid-containing medium (Fig. 5.1), showing the recessive nature of the *pex16-1* mutation. The diploid strain *D16-P16x8B* made by mating the original *pex16-1* mutant strain to strain *P16KO-8B* (Table 2.3) could not grow on oleic acid-containing medium (Fig. 5.1). Accordingly, the ability to utilize oleic acid as the sole carbon source required at least one intact copy of the *YIPEX16* gene, thereby confirming that the authentic gene had been cloned.

5.2 *pex16* mutant cells lack normal peroxisomes but do show evidence of vesicular structures containing peroxisomal proteins

Normal peroxisomes of *Y. lipolytica* appear as round vesicular structures, 0.3 - 0.5 μm in diameter, with a granular electron-dense core and a single unit membrane (Fig. 5.4 A). Typical peroxisomal structures were not seen in electron microscopic sections of the *pex16-1* mutant strain (Fig. 5.4 B) or the disruption strain *P16KO-8A* (Fig. 5.4 D) grown in oleic acid-containing medium. However, these mutant strains did show more prevalent clusters of small vesicles 40 - 50 nm in diameter (Fig. 5.4 B and D, *arrows* and Fig. 3 B, *inset*) and occasionally larger vesicles, 100 - 150 nm in diameter (Fig. 5.4 B and D, *arrowheads* and Fig. 3 D, *inset*). The transformed strain *P16TR* had the appearance of the wild-type strain and showed normal peroxisome morphology (Fig. 5.4 C).

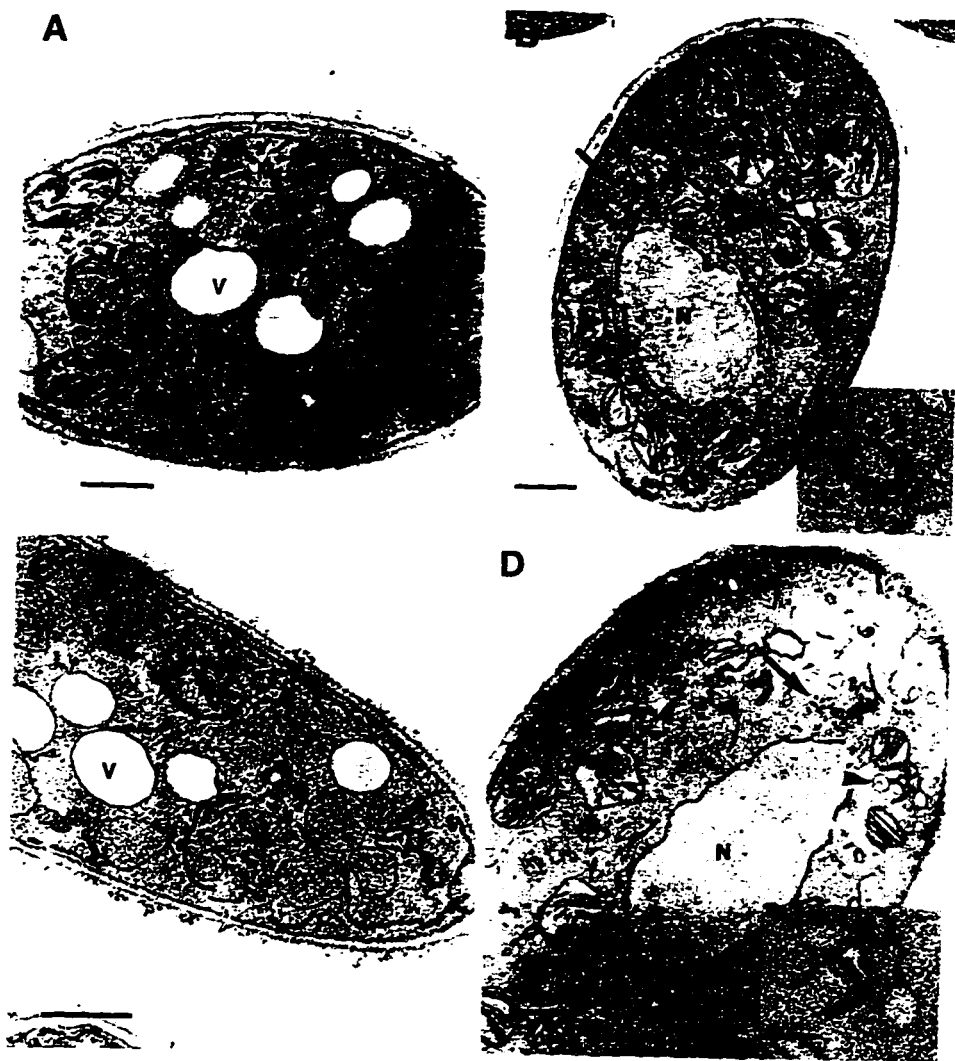


Figure 5.4 Ultrastructure of wild-type and *pex16* mutant strains. The *E122* (A), *pex16-1* (B), *P16TR* (C), and *P16KO-8A* (D) strains were grown for 16 h in YEPD medium to an OD_{600} of ~ 1.5 , transferred to YPBO medium at a 1:4 dilution, and grown for an additional 8 h in YPBO. Cells were fixed in $KMnO_4$ and processed for electron microscopy. *P*, peroxisome; *M*, mitochondrion; *N*, nucleus; *V*, vacuole. Arrows, vesicular structures 40 - 50 nm in diameter. Arrowheads, vesicular structures 100 - 150 nm in diameter. Bar = 0.5 μm . Inset in (B) shows a cluster of vesicles 40 - 50 nm in diameter. Inset in (D) shows vesicles ~ 100 nm in diameter. Inset bar = 0.1 μm .

Although *pex16* mutants did not show normal peroxisomes in electron microscopic sections, subcellular fractionation provided evidence of peroxisomal structures in these strains. Wild-type and mutant strains were grown in oleic acid-containing medium to proliferate peroxisomes and were then fractionated into a 20KgP fraction enriched for peroxisomes and mitochondria and a 20KgS fraction, as described in *Section 2.4.2*. In the wild-type strain *E122*, greater than 75% of each peroxisomal protein was localized to the 20KgP fraction (Fig. 5.5). In contrast, in the original mutant strain *pex16-1* and in the disruption strain *P16KO-8A*, several peroxisomal proteins were almost completely mislocalized to the 20KgS fraction, while others were only partially mislocalized (Fig. 5.5). Isocitrate lyase, thiolase and catalase were found almost exclusively (86% - 99%) in the 20KgS fraction of the mutant strains. Malate synthase and the peroxisomal membrane proteins Pex2p (Eitzen et al., 1996) and Pex5p (Szilard et al., 1995) were partially mislocalized (38% - 79%) to the 20KgS, while acyl-CoA oxidase and a 62 kDa anti-SKL reactive polypeptide were localized to the 20KgP fraction at levels comparable to those of the wild-type strain. The mitochondrial markers cytochrome *c* oxidase and fumarase were preferentially localized to the 20KgP (88 - 100%) in wild-type and mutant strains and therefore not affected by mutation of the *YIPEX16* gene (Fig. 5.5).

To determine if the portion of peroxisomal matrix proteins localized to the mutant 20KgS fraction were truly cytosolic or resided within light particles, the 20KgS fraction of the *pex16-1* mutant strain was subjected to centrifugation at $200,000 \times g_{\max}$. This yielded a cytosolic fraction (HS) and a high speed particulate fraction (HP) containing the remaining membrane-bound vesicles and their contents. Peroxisomal matrix proteins that were only

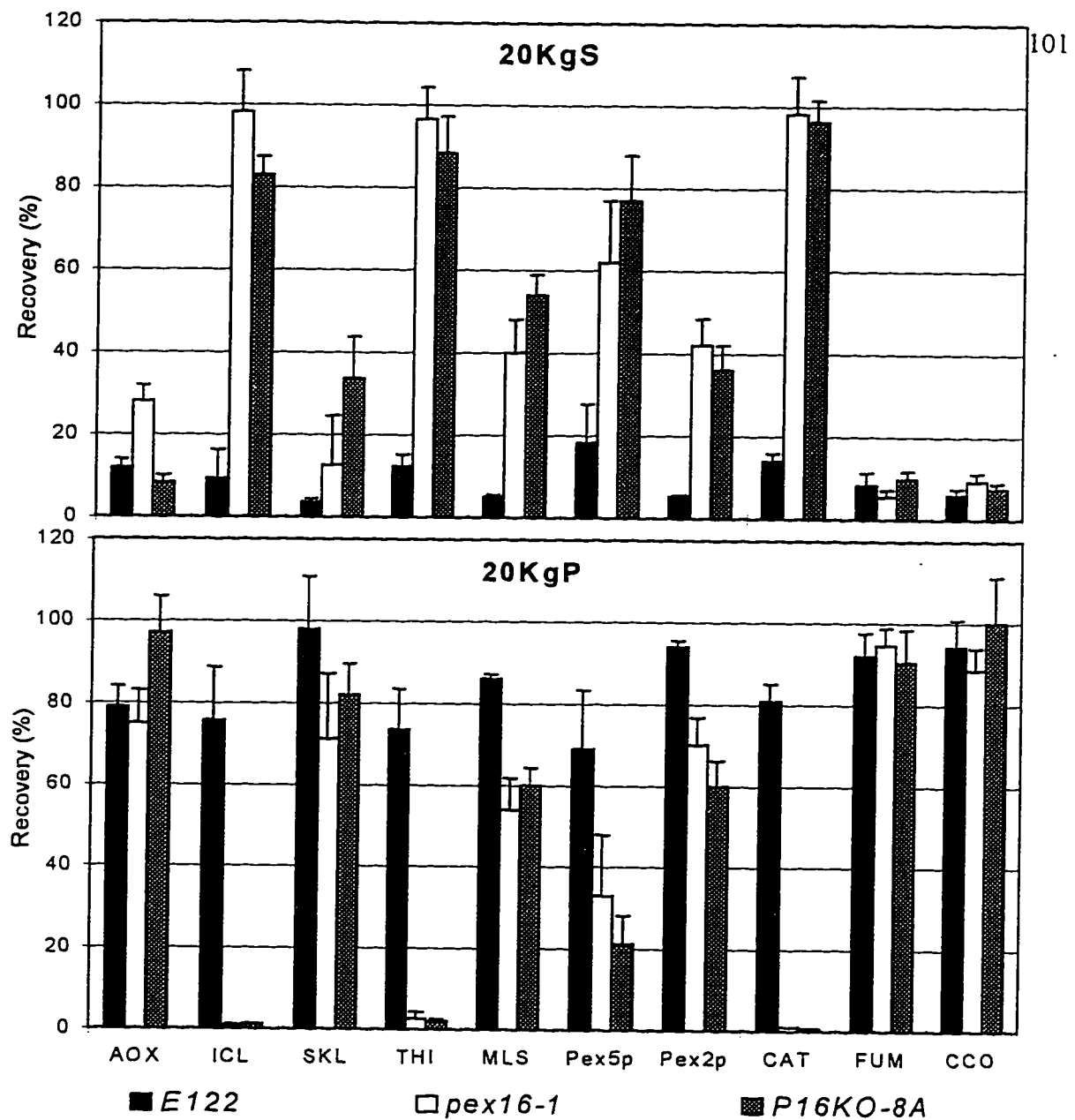


Figure 5.5 Peroxisomal proteins are mislocalized to the 20KgS to varying extents in *pex16* mutants. Wild-type strain *E122* (solid bar) and mutant strains *pex16-1* (open bar) and *P16KO-8A* (stippled bar) were grown as described in the legend to Figure 5.4. Cells were subjected to subcellular fractionation to yield 20KgS and 20KgP fractions. The distributions of the enzymatic activities of catalase (*CAT*), fumarase (*FUM*), and cytochrome *c* oxidase (*CCO*) and of the immunosignals of acyl-CoA oxidase (*AOX*), isocitrate lyase (*ICL*), a 62 kDa anti-SKL reactive polypeptide (*SKL*), thiolase (*THI*), malate synthase (*MLS*), Pex5p, and Pex2p to the 20KgS and 20KgP fractions are given as the percent recovery of the respective total enzymatic activity or immunosignal in the PNS fraction. Immunoblots were quantitated by densitometry. Values reported are the means \pm SD of four independent experiments, each analyzed in duplicate.

partially mislocalized to the mutant 20KgS, *i.e.* acyl-CoA oxidase and a 62 kDa anti-SKL reactive polypeptide, showed preferential localization to the HP fraction (Fig. 5.6 A, lanes S and HP). Matrix proteins significantly affected by the *pex16-1* mutation, *i.e.* thiolase and isocitrate lyase, were truly mislocalized to the cytosol (Fig 5.6 A, lanes S and HS).

Protease protection experiments were performed to determine if the peroxisomal matrix proteins localized to the 20KgP fraction of the *pex16-1* mutant cells were contained within vesicular structures. The peroxisomal matrix proteins tested were resistant to digestion by external proteases in the absence of detergent but not in the presence of detergent (added to disrupt membranes) (Fig. 5.6 B). These result demonstrate that most of the peroxisomal matrix proteins acyl-CoA oxidase and a 62 kDa anti-SKL immunoreactive polypeptide, and a small portion of thiolase (that which is localized to the 20KgP fraction) reside within vesicular structures in the *pex16-1* mutant strain.

Immunofluorescence microscopy showed the absence of typical peroxisomes in *pex16* mutant cells but did reveal the presence of small punctate structures when probed with anti-SKL antibodies (Fig. 5.7). Wild-type and *pex16-1* mutant cells were also prepared for electron microscopy and immunocytochemical analysis with anti-SKL antibodies. Several peroxisomes of typical size were decorated with gold particles in the wild-type cell (Fig. 5.8 A). In the *pex16-1* mutant, typical peroxisomal structures were not seen and periodic staining of the cytosol occurred. Some anti-SKL reactive proteins were detected in small vesicular structures 100 - 150 nm in diameter (Fig. 5.8 B), however, because of the limits of resolution, and poor membrane preservation and contrast using LR Gold resin (Berryman et al., 1990), it was difficult to assign gold particles to small vesicular structures within the cytoplasm.

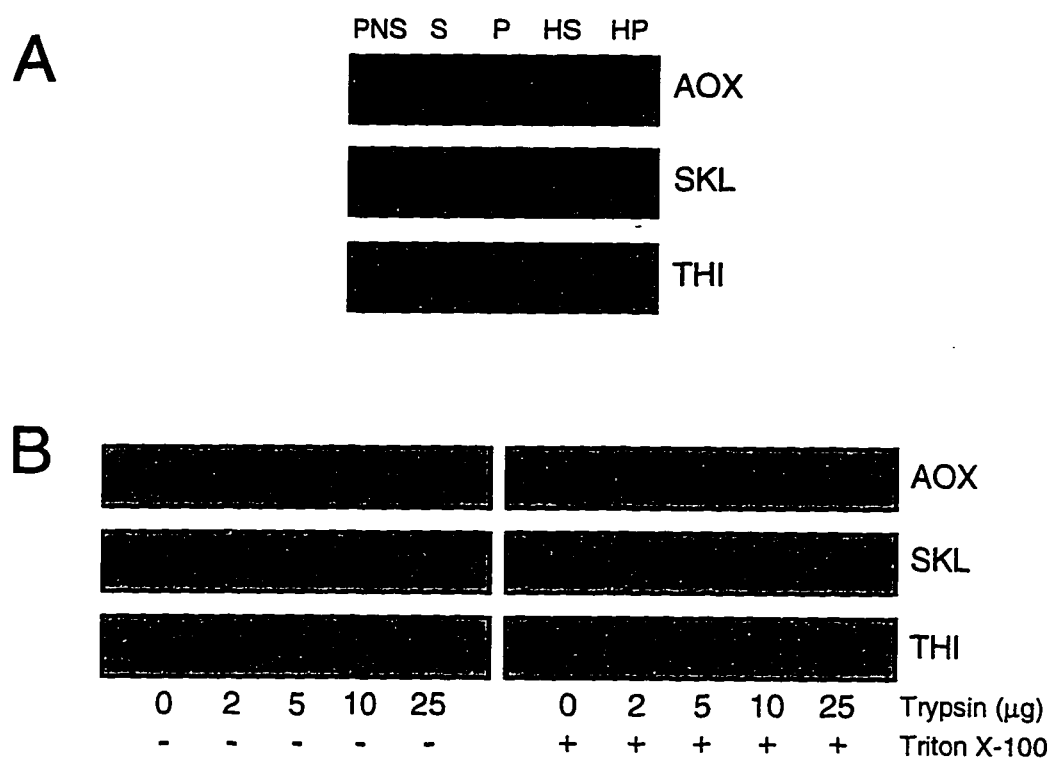


Figure 5.6 Peroxisomal matrix proteins localized to the 20KgP fraction of the *pex16-1* mutant reside within vesicles. (A) The 20KgP fraction of the *pex16-1* mutant strain was subjected to centrifugation at $200,000 \times g_{\max}$ to yield a particulate pellet fraction (HP) and cytosolic fraction (HS) as described in *Section 2.4.2*. Equivalent cellular fractions (0.1% of the total volume) of PNS, 20KgS (S), 20KgP (P) as in the legend to *Figure 5.5*, and 200KgS (HS) and 200KgP (HP) were subjected to immunoblot analysis with anti-acyl-CoA oxidase (AOX), anti-SKL (SKL) and anti-thiolase (THI) antibodies. The three anti-SKL immunoreactive polypeptides represent isocitrate lyase (*upper band*), an unknown 62 kDa protein (*middle band*) and a cytosolic degradation product (*lower band*) commonly seen in *pex* mutants. (B) The 20KgP fraction of the *pex16-1* mutant strain (isolated in the absence of protease inhibitors) was subjected to protease treatment. 100 µg of protein was incubated with 0, 2, 5, 10 and 25 µg of trypsin in the absence (-) or presence (+) of 0.5% (vol/vol) Triton X-100. Reactions were incubated at 4°C for 30 min and terminated by addition of hot SDS-PAGE sample buffer and immediate boiling. Samples were analyzed by immunoblotting with anti-acyl-CoA oxidase (AOX), anti-SKL (SKL) and anti-thiolase (THI) antibodies.

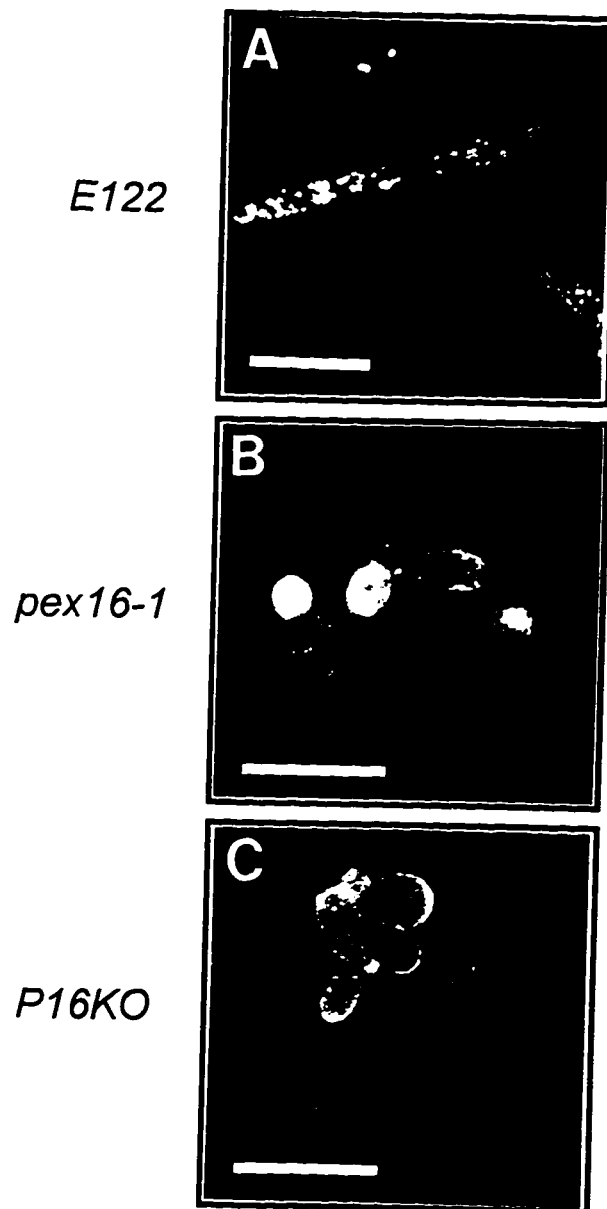


Figure 5.7 Immunofluorescence microscopy shows small vesicular structure in *pex16* mutant strains. The wild-type strain *E122* (A), and the mutant strains *pex16-1* (B) and *P16KO-8A* (C) were grown for 8 h in YPBO as described in the legend to *Figure 5.4*. Cells were processed for immunofluorescence (see *Section 2.6.1*) and probed with rabbit anti-SKL and FITC-conjugated goat anti-rabbit IgG antibodies. Typical peroxisomes are stained in *E122* cells, while the *pex16-1* and *P16KO* mutant strains showed staining of the cytosol and small vesicular structure. Bar = 5 μ m.

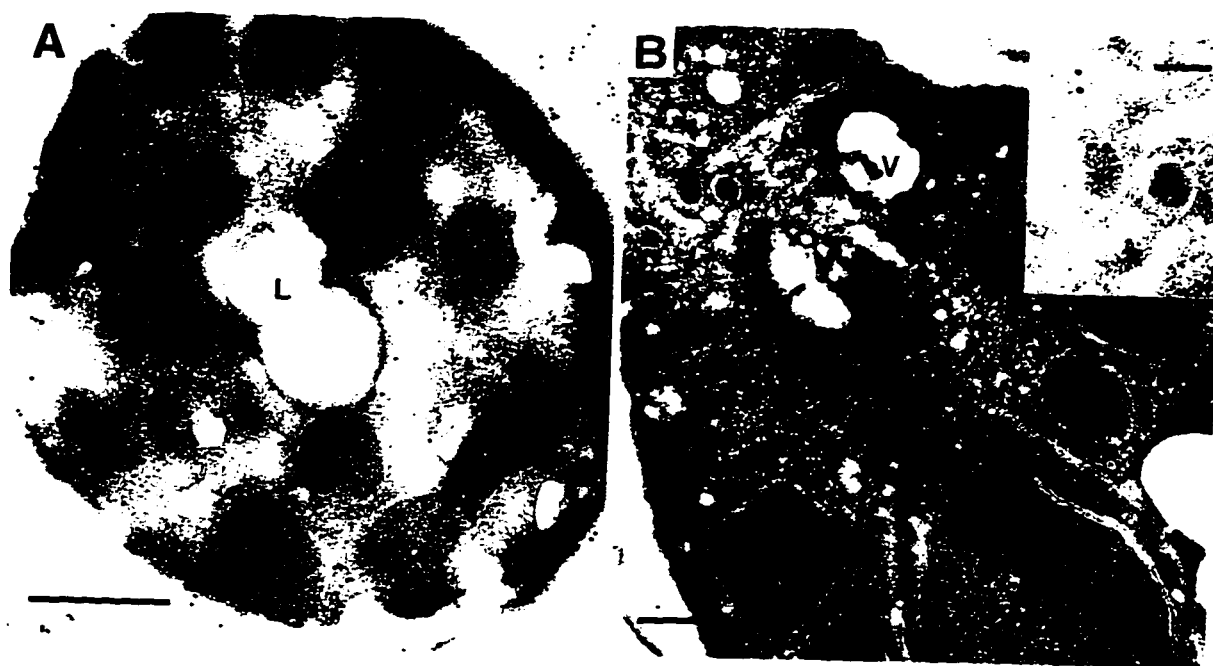


Figure 5.8 **Immunocytochemical analysis of *E122* and *pex16-1* cells with anti-SKL and gold conjugated antibodies.** The wild-type *E122* (A) and *pex16-1* mutant (B) strains were grown in YPBO as described in the legend to Figure 5.4 and fixed with 3% (wt/vol) paraformaldehyde/0.5% (wt/vol) glutaraldehyde, and processed for electron microscopy and immunocytochemical analysis with anti-SKL and 10 nm gold-conjugated antibodies. (A) *E122* cell section showing gold staining of typical peroxisomes. The inset in (B) shows a high magnification of gold stained vesicles (~100 nm in diameter) in a *pex16-1* mutant cell section. P, peroxisome; M, mitochondrion; V, vacuole; L, lipid droplet. Bar = 0.5 μ m; inset bar = 0.1 μ m.

To further examine the characteristics of the *YIPEX16* mutation, organelles from the 20KgP fractions of wild-type and mutant strains were further fractionated by isopycnic centrifugation on discontinuous sucrose gradients (see *Section 2.4.2*). Fractions were analyzed for density, protein content, catalase and fumarase activity (Fig. 5.9 A) and by immunoblotting with antibodies to peroxisomal matrix (anti-SKL reactive polypeptides, acyl-CoA oxidase, and thiolase) and membrane (Pex2p) proteins (Fig. 5.9 B). In the wild-type strain *E122*, peroxisomal proteins were localized primarily to fractions 3-5, peaking in fraction 4 at a density of 1.21 g/cm³, while mitochondria were well separated from peroxisomes in fractions 9-11, at a peak density of 1.18 g/cm³. In the *pex16-1* and *P16KO-8A* mutant strains, two peaks of peroxisomal proteins were observed, a lesser peak at a density of 1.21 g/cm³ and a greater peak at a density of 1.16 g/cm³ (fractions 9-12). Multiple peroxisomal subpopulations have been previously observed in *Y. lipolytica* (see *Chapter 4*; Titorenko et al., 1996), in other yeasts (Spong and Subramani, 1993; Heyman et al., 1994), and in mammalian cells (Heinemann and Just, 1992; Lüers et al., 1993). It has been proposed that these lighter fractions contain intermediates of the peroxisome assembly pathway.

It is noteworthy that the more slowly migrating anti-SKL reactive polypeptide of 64 kDa was not present in the immunoblots of the fractions of the *pex16* mutant strains (Fig. 5.9 B). This 64 kDa polypeptide corresponds to isocitrate lyase (see Fig 2.1), and as presented in Fig. 5.5, most isocitrate lyase was mislocalized to the 20KgS in the *pex16* strains.

To characterize the vesicular structures that contain these peroxisomal proteins, 20KgP and sucrose gradient fractions were prepared for electron microscopy and immunocytochemical analysis. The 20KgP fraction of the *E122* wild-type strain contained

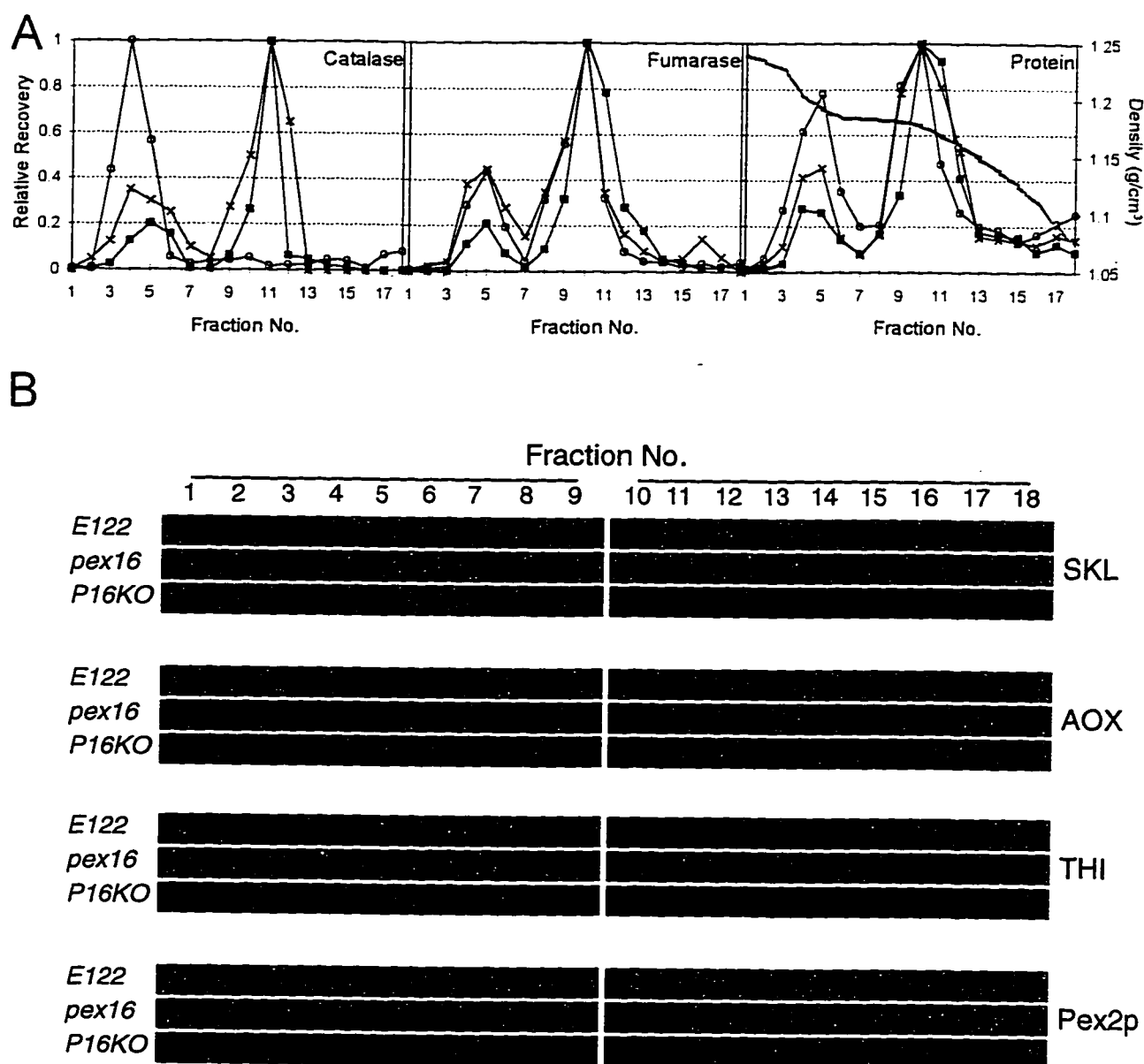


Figure 5.9 Isopycnic density gradient analysis of 20Kgp fractions of the wild-type and *pex16* strains. Strains were grown 8 h in YPBO, as described in the legend to *Figure 5.4*, and subjected to subcellular fractionation. The 20Kgp from each strain was subjected to centrifugation on a discontinuous sucrose gradient, as described in *Section 2.4.2*. Each gradient was collected in 18 equivolume fractions. (A) Distributions of catalase, fumarase and protein are shown for the strains *E122* (—○—), *pex16-1* (—x—), and *P16KO-8A* (—■—). The *stippled line* in the panel at right shows the density profile (g/cm^3) of the gradient. Results are the means of two independent experiments, each analyzed in duplicate. (B) Equal volumes of gradient fractions were analyzed by immunoblotting. Abbreviations are as in *Figure 5.5*.

typical peroxisomes, which were decorated with gold particles (Fig. 5.10 *A, P*), and predominantly unlabelled mitochondria (Fig. 5.10 *A, M*). The 20KgP *pex16-1* mutant fraction did not show typical peroxisomal structures; however, several small vesicular structures were periodically labelled (Fig. 5.10 *B*). Sucrose gradient fraction 4 (1.21 g/cm³, the normal density of peroxisomes) from the wild-type strain showed gold staining of large, round electron dense vesicles characteristic of peroxisomes and occasionally an unstained mitochondrion (Fig. 5.10 *C*). Fraction 4 of the *pex16-1* mutant showed gold staining of vesicles that were possibly smaller in diameter than wild-type peroxisomes (Fig. 5.10 *E*), and similar in appearance to the structures seen in whole cell sections (see Fig. 5.8 *B*). Wild-type fraction 11 (1.16 g/cm³) contained mainly unlabelled mitochondria (Fig. 5.10 *D*). Mutant fraction 11 contained mitochondria and, additionally, small electron-dense vesicular structures, heavily decorated with gold particles (Fig. 5.10 *E*).

5.3 Pex16p is an intraperoxisomal peripheral membrane protein

Antibodies raised against a maltose-binding protein-Pex16p fusion protein recognized a polypeptide of ~43 kDa in extracts of oleic acid-grown *E122* cells but not of *pex16-1* cells (Fig. 5.11 *A*). The molecular mass of this polypeptide is close to the predicted molecular mass of Pex16p, 44,479 Da. No immunoreactive 43 kDa polypeptide was seen in the lysate of the disruption strain *P16KO-8A*, but it was present in the lysate of the transformed strain *P16TR* (Fig. 5.11 *A*). Therefore, the antibodies specifically recognize Pex16p. The stronger signal in the transformant lysate is likely the result of increased *YIPEX16* expression from a multi-copy plasmid or differences in cellular proteins due to growth of *P16TR* in minimal media.

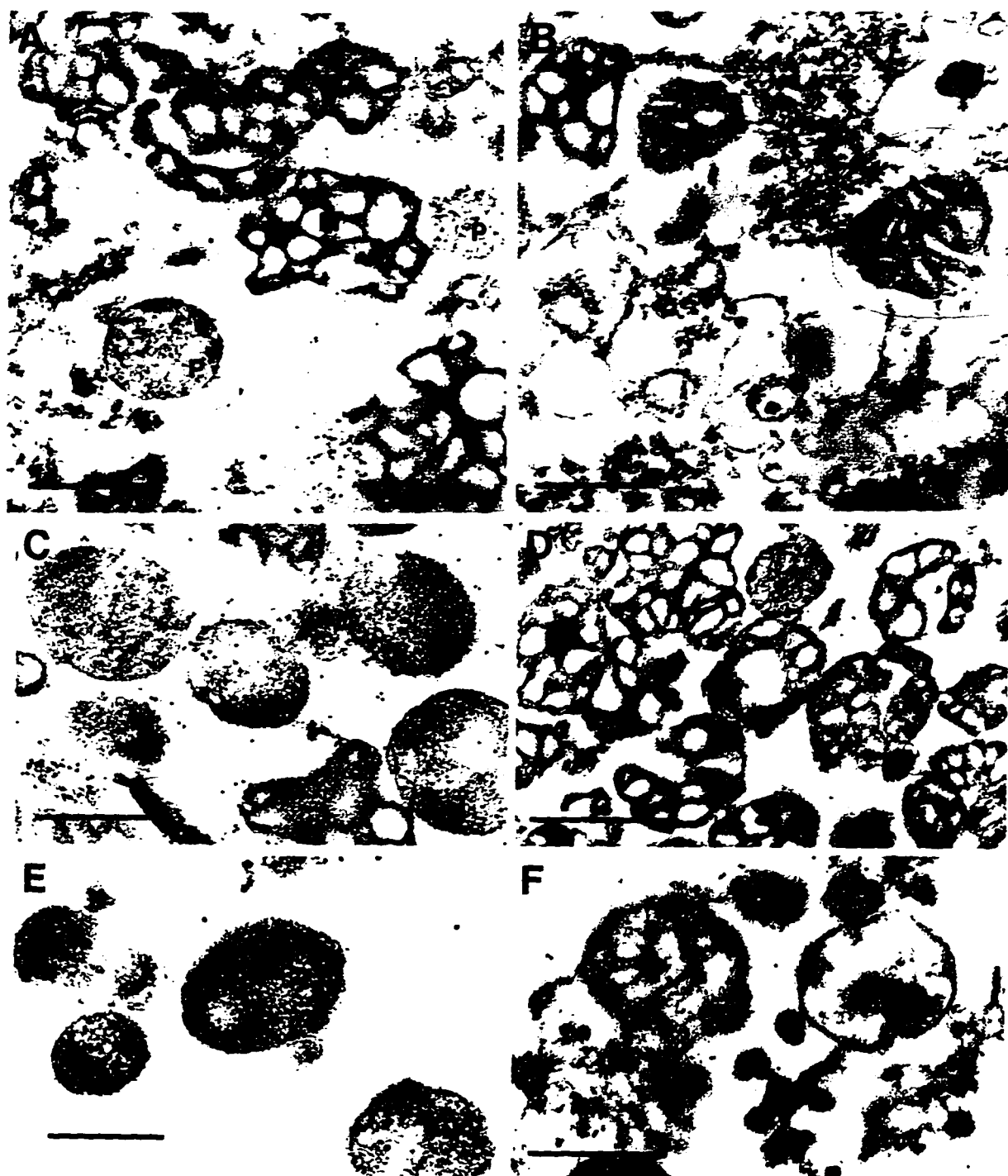


Figure 5.10 **Immunocytochemical analysis of wild-type and *pex16-1* subcellular fractions.** 20KgP fractions were prepared by differential centrifugation and sucrose gradient fractions were prepared by isopycnic centrifugation of 20KgP fractions isolated from wild-type *E122* and *pex16-1* mutant strains (cf. Figure 5.9). Fractions were fixed with 3% (wt/vol) paraformaldehyde/0.2% (wt/vol) glutaraldehyde and processed for electron microscopy and immunocytochemical analysis with anti-SKL and 10 nm gold-conjugated antibodies. Peroxisomes in fraction 4 of the wild-type strain (C) and vesicular structures in both fraction 4 (E) and fraction 11 (F) of the *pex16-1* mutant strain are decorated with gold particles. Mitochondria in the wild-type (D) and *pex16-1* mutant (F) fraction 11 are predominantly undecorated. P, peroxisome, M, mitochondrion. Bar = 0.5 μ m, except (E) bar = 0.25 μ m

Immunoblot analysis of subcellular fractions and peroxisomes purified from oleic acid-grown wild-type cells with anti-Pex16p antibodies showed Pex16p to be localized to peroxisomes (Fig. 5.11 *B*, *lane PX*). Pex16p was absent from the 20KgS fraction (Fig. 5.11 *B*, *lane S*). Lysis of peroxisomes with Ti8 buffer, followed by high-speed centrifugation, showed Pex16p to be localized exclusively to the pellet containing membrane proteins (Fig. 5.11 *C*, middle and bottom panels, *lane P_{Ti8}*) and not to the supernatant containing soluble matrix proteins (Fig. 5.11 *C*, top panel, *lane S_{Ti8}*). Increasing the stringency of the extraction buffer by the addition of 0.5 M KCl to the Ti8 buffer (TS buffer) led to partial extraction of Pex16p from the membrane pellet but not of Pex2p, a peroxisomal integral membrane protein (Fig. 5.11 *C*, middle and bottom panels, compare *lane P_{TS}* to *lane S_{TS}*). The more quickly migrating species in *lane S_{TS}* was probably due to nonspecific proteolysis. Treatment of peroxisomes with 0.1 M Na₂CO₃ (pH 11.5) led to the complete extraction of Pex16p but not of Pex2p from the membrane pellet (Fig. 5.11 *C*, middle and bottom panels, compare *lane P_{CO}* to *lane S_{CO}*). Therefore, Pex16p shows the characteristics of a protein that is peripherally associated with the peroxisomal membrane.

To examine the association of Pex16p with the peroxisomal membrane, a 20KgP fraction isolated from the *pex16-1* strain grown in oleic acid-containing medium was subjected to protease protection analysis (Fig. 5.11 *D*). Pex16p was mainly protected from the action of external protease in the absence, but not in the presence, of the detergent Triton X-100. Peroxisomal matrix proteins recognized by anti-SKL antibodies behaved similarly to Pex16p in this analysis (Fig. 5.11 *D*). These results suggest that Pex16p is associated with the matrix face of the peroxisomal membrane.

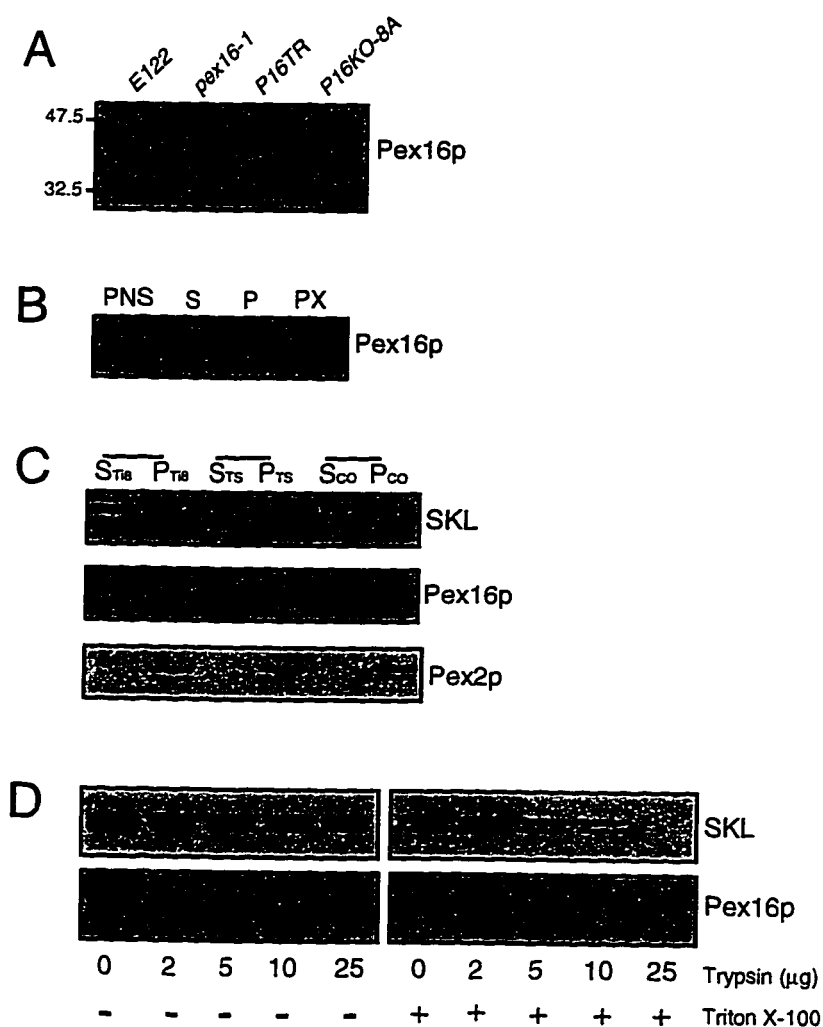


Figure 5.11 Pex16p is a peripheral protein preferentially associated with the matrix face of the peroxisomal membrane. (A) Immunoblot analysis of whole cell extracts (50 µg of protein) from strains grown for 8 h in YPBO medium, as described in the legend to *Figure 5.4*. Anti-Pex16p antibodies recognize a polypeptide of ~43 kDa in lysates of the wild-type strain *E122* and the transformed strain *P16TR* but not in lysates of the original mutant strain *pex16-1* or the disruption strain *P16KO-8A*. The *numbers* at left indicate the migrations of molecular mass standards (in kDa). (B) Immunoblot analysis of subcellular fractions PNS, 20KgS (*S*), and 20KgP (*P*) and of whole peroxisomes (*PX*, 30 µg of protein) of the wild-type strain grown as in (A) and probed with anti-Pex16p antibodies. Equal fractions (0.1% of the total volume) of the PNS, 20KgS, and 20KgP were loaded. (C) Immunoblot analysis of peroxisomes separated into pellet (*P*) and supernatant (*S*) fractions by treatment with Ti8, TS or sodium carbonate buffer (*CO*). The upper blot was probed with anti-SKL antibodies. The middle blot was probed with anti-Pex16p antibodies. The lower blot was probed with antibodies to the integral membrane protein Pex2p. (D) Protease protection analysis of anti-SKL reactive polypeptides and Pex16p. The 20KgP fraction (100 µg of protein) isolated in the absence of protease inhibitors from strain *E122* was incubated with the protease trypsin in the absence (-) or presence (+) of 0.5% (vol/vol) Triton X-100.

5.4 The carboxyl terminus of Pex16p is not essential for its function or targeting

Pex16p has at its carboxyl terminus, the tripeptide sequence, Ser-Thr-Leu (Fig. 5.2 B). Whether this tripeptide was a variant of the prototypical PTS1 sequence Ser-Lys-Leu and was necessary for targeting Pex16p to peroxisomes was investigated. The plasmid p16 Δ (see section 2.2.12) expresses a mRNA encoding a modified Pex16p that has at its carboxyl terminus the amino acids Ala-Asp-Leu, which is dissimilar to a PTS1 motif in that a negatively charged aspartate residue replaces an amino acid residue that is normally positively charged. The plasmid p16HA (see Section 2.2.12) encodes a modified Pex16p (Pex16p-HA) that has two copies of the HA epitope tag appended to its carboxyl terminus and ends in the tripeptide, Lys-Gly-Glu, which does not resemble the PTS1 consensus motif. The plasmid p16CN expresses an unmodified mRNA. Transformation of strains *pex16-1* and *P16KO-8A* with p16 Δ , p16HA or p16CN reestablished growth on oleic acid medium (data not shown). Therefore, these forms of Pex16p were capable of functional complementation of the *pex16* strains.

To ensure that functional complementation of the *pex16* strains by the plasmids p16 Δ and p16HA was not due to overexpression of the modified *YIPEX16* genes, the strain *pex16-HA* (Table 2.3) was constructed in the *pex16-1* background. This strain harbours a single integrated copy of the modified *YIPEX16* gene under the control of the *YIPEX16* promoter and coding for Pex16p-HA (see Section 2.3.5.5). This strain recovered growth on oleic acid medium (Fig. 5.1). Immunoblot analysis of subcellular fractions prepared from the *pex16-HA* strain grown in oleic acid-containing medium showed localization of Pex16p-HA to the 20K_gP fraction (Fig. 5.12 A, arrowhead, lane P) and to purified peroxisomes (Fig. 5.12 B).

A polypeptide with reduced electrophoretic mobility relative to Pex16p-HA was nonspecifically recognized by 12CA5 antibodies, as shown by its detection in wild-type *E122* cells not synthesizing Pex16p-HA (Fig. 5.12 *A*, *panel at right*). The portion of Pex16p-HA localized to the 20K_gS (Fig. 5.12 *A*, *lane S*) was contained within particles that could be pelleted at $200,000 \times g_{\max}$ (Fig. 5.12 *A*, compare *lane HP* to *lane HS*). Protease protection experiments showed that Pex16p-HA was resistant to digestion by externally added proteases in the absence but not in the presence of detergent and is therefore translocated into the peroxisome matrix (Fig. 12 *C*). These results verify the intraperoxisomal localization of Pex16p and demonstrate that the amino acids, Ser-Thr-Leu, at the carboxyl terminus of Pex16p are not essential for Pex16p function, or for targeting and import of Pex16p into peroxisomes.

5.5 Oversynthesis of Pex16p results in cells with a reduced number of enlarged peroxisomes

Immunofluorescence microscopic analysis of oleic acid-grown wild-type cells probed with antibodies directed against peroxisomal matrix proteins showed a punctate pattern of staining characteristic of normal peroxisomes (Fig. 5.14 *A*). In contrast, *pex16* strains showed a general cytosolic or a less intense punctate staining (*cf.* Fig 5.7). Expression of *YIPEX16* in the transformed strain *P16TR* restored the punctate pattern of staining (Fig. 5.14 *B*). To examine the effects of oversynthesis of Pex16p, the strain *pex16-TH* (Table 2.3, see Section 2.3.5.6) expressing the *YIPEX16* gene from the thiolase gene promoter was grown in oleic acid-containing medium. Immunoblot analysis showed that Pex16p synthesis was increased

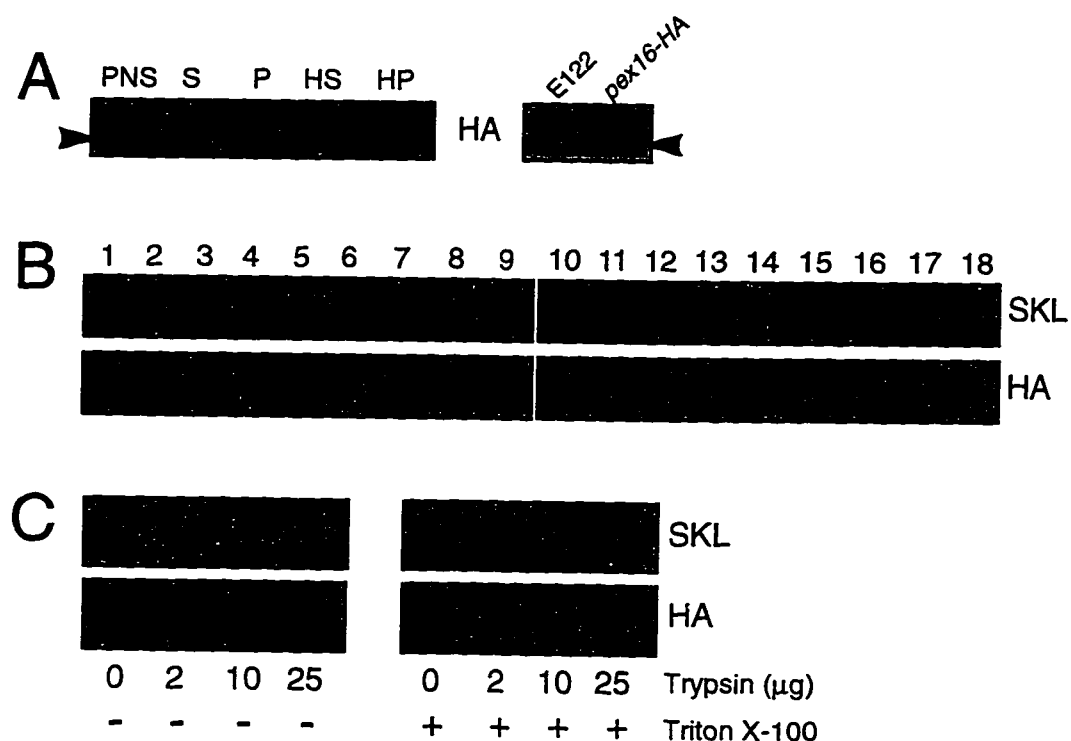


Figure 5.12 Pex16p-HA is targeted to peroxisomes and associates with the matrix face of the peroxisomal membrane. (A) Immunoblot analysis of strain *pex16-HA* grown 8 h in YPBO medium, as described in the legend to *Figure 5.4*, and then subjected to subcellular fractionation to yield PNS, 20KgS (*S*) and 20KgP (*P*) fractions. The 20KgS was further fractionated into high speed supernatant (*HS*) and pellet (*HP*) fractions by centrifugation at $200,000 \times g_{\max}$, as described in *Section 2.4.2*. Equal portions of the fractions (0.1% of the total volume) were probed with 12CA5 antibodies (*HA*) to localize Pex16p-HA (*arrowhead*). (B) Immunoblot analysis of the 20KgP of the *pex16-HA* strain fractionated by isopycnic density gradient centrifugation. Equal volumes of the fractions were probed with anti-SKL and 12CA5 (*HA*) antibodies. Anti-SKL reactive polypeptides and Pex16p-HA colocalize to fractions with the characteristic density of peroxisomes. (C) Protease protection analysis of anti-SKL reactive polypeptides and Pex16p-HA. The 20KgP fraction (100 μg of protein) isolated in the absence of protease inhibitors from strain *pex16-HA* was incubated with the protease trypsin in the absence (-) or presence (+) of 0.5% (vol/vol) Triton X-100.

10-fold after 8 h of growth in oleic acid-containing medium in the strain *pex16-TH* as compared to the wild-type strain *E122* (Fig. 5.13, *Pex16p*), while the levels of expression of peroxisomal matrix proteins in the two strains remained unchanged (Fig. 5.13, *SKL*). It is interesting to note that *Pex16p* was synthesized by wild-type cells grown in glucose-containing medium (time = 0 h) and that the level of *Pex16p* were only slightly increased during growth in oleic acid-containing medium (Fig. 5.13).

Immunofluorescence microscopy of the *pex16-TH* strain showed the effects of oversynthesis of *Pex16p*. After 8 h of growth in oleic acid-containing medium, cells of the *pex16-TH* strain contained 1-10 enlarged peroxisomes (Fig. 5.14, *C* and *D*) instead of 25-50 peroxisomes normally seen in wild-type cells grown under the same conditions (Fig. 5.14 *A*). These enlarged peroxisomes are functional, since the ability to grow in oleic acid-containing medium was restored in the strain *pex16-TH* (Fig. 5.1).

Analysis by electron microscopy showed that *pex16-TH* cells contained enlarged peroxisomes (average diameter of $0.87 \pm 0.14 \mu\text{m}$) compared to peroxisomes of wild-type cells (average diameter of $0.36 \pm 0.10 \mu\text{m}$). The increased size of peroxisomes in the *pex16-TH* strain apparently does not affect their inheritance, since cell sections routinely showed large peroxisomes in both halves of a dividing cell (Fig. 5.15).

Peroxisomal proteins were localized to the 20KgP isolated from the *pex16-TH* strain at levels approaching those of the wild-type strain (Fig 5.16 *A*). The slight reduction observed in the levels of some matrix proteins in the 20KgP of the *pex16-TH* strain could be due to enlarged peroxisomes being more susceptible to leakage and/or a reduction in the efficiency of protein import because of their increased size or their reduced number. The

giant peroxisomes of the *pex16-TH* strain could be isolated by isopycnic centrifugation of the 20K_gP on a discontinuous sucrose gradient (Fig. 5.16 *B*). These giant peroxisomes peaked at a density of 1.21 g/cm³, the same as wild-type peroxisomes (see Fig. 5.9 *A*) and contained catalase (Fig. 5.16 *B*) and all other peroxisomal matrix and membrane proteins tested (Fig. 5.16 *C*). Mitochondria from the *pex16-TH* strain peaked at a density of 1.18 g/cm³, like those of the wild-type strain (see Fig. 5.9 *A*). Therefore, oversynthesis of Pex16p appears to affect only peroxisome size and number.

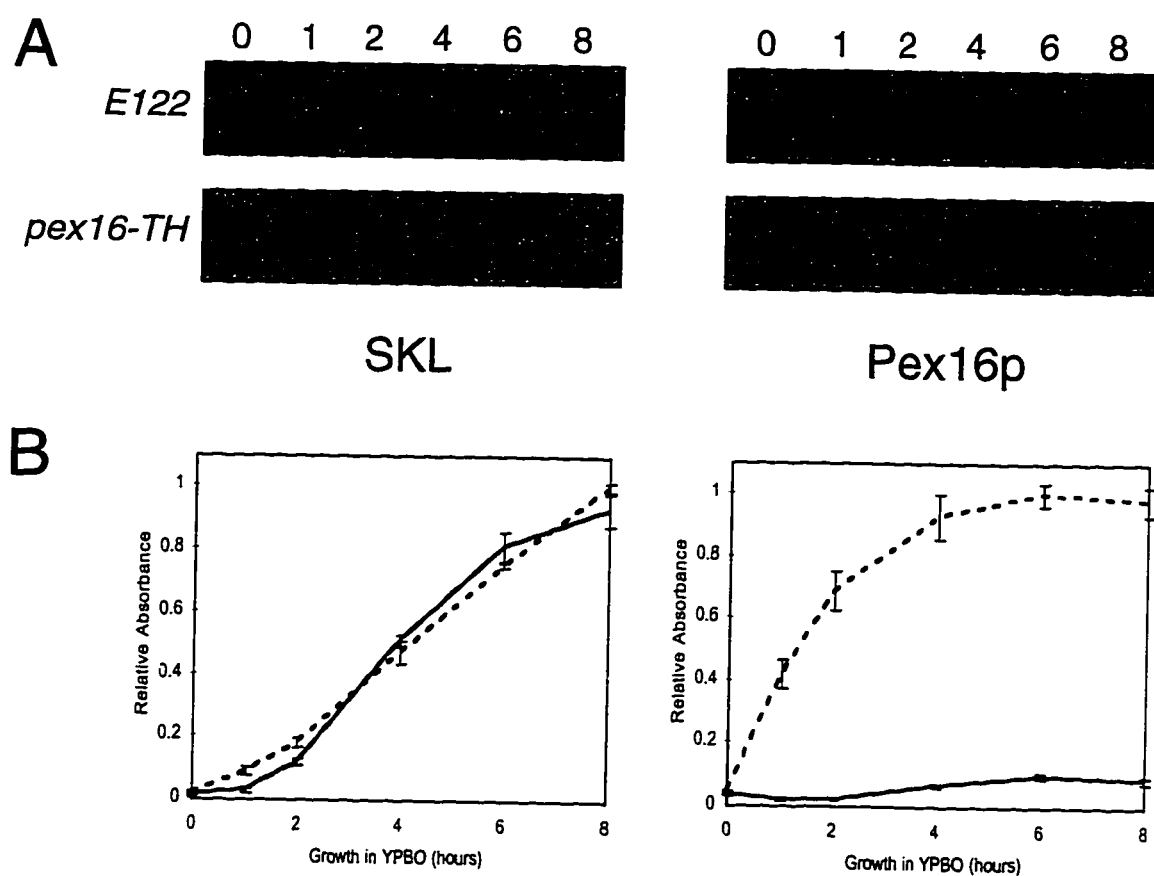


Figure 5.13 Pex16p is oversynthesized in the strain *pex16-TH*. (A) Immunoblot analysis of cell lysates of the wild-type strain *E122* and of the strain *pex16-TH*. Strains were grown to an OD_{600} of ~ 1.5 in YEPD medium (time = 0 h) and transferred to YPBO medium. Samples were removed at various times after transfer to YPBO medium. Lysates (50 μ g of protein) of cells sampled at times 0, 1, 2, 4, 6, and 8 h (*numbers* at top) after transfer to YPBO medium were analyzed by immunoblotting with anti-SKL and anti-Pex16p antibodies. (B) Quantitation of upper SKL-reactive polypeptide in immunoblots as in (A). Values reported are the means \pm SD for three independent experiments. *E122*, solid line; *pex16-TH*, dashed line.

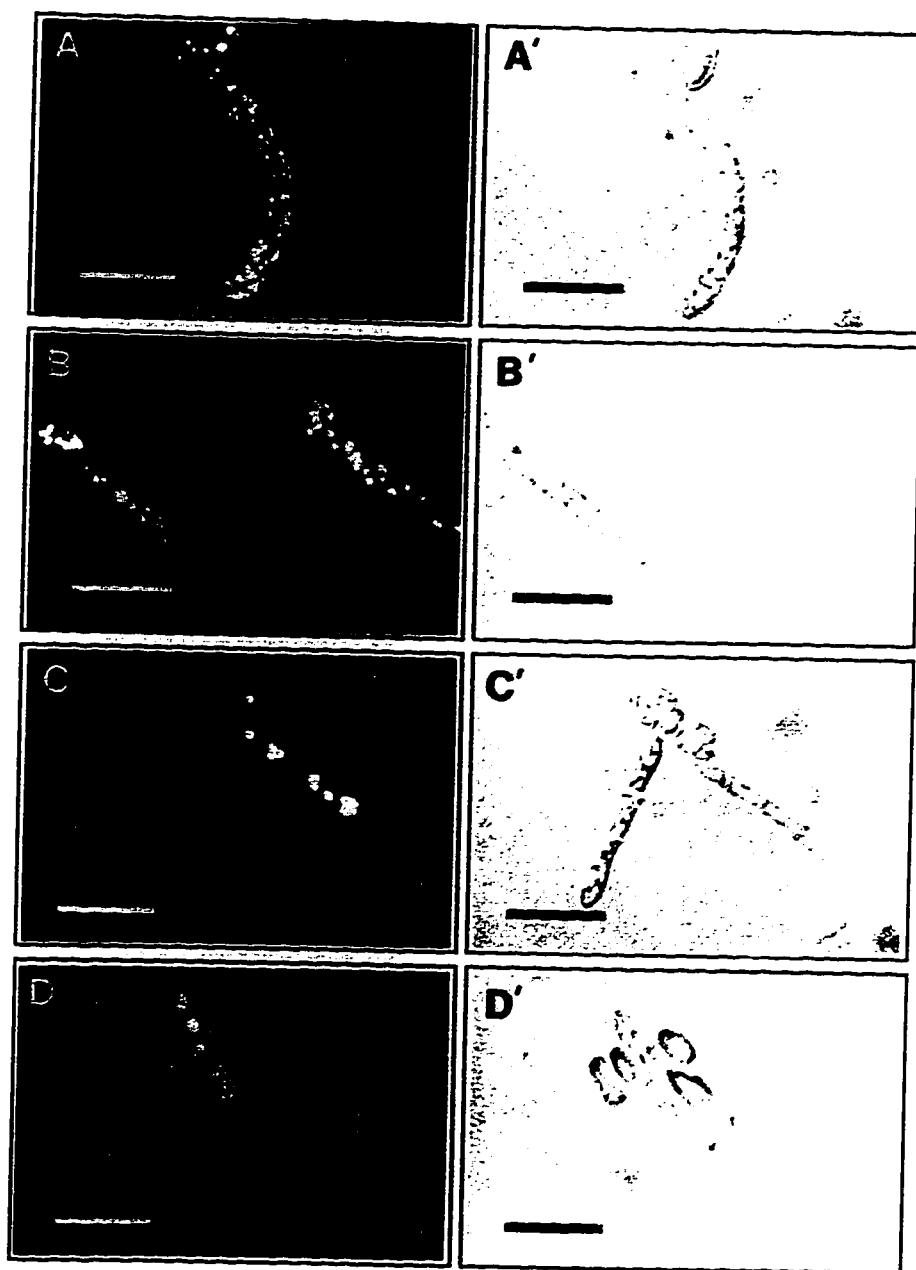


Figure 5.14 **Oversynthesis of Pex16p results in cells with a reduced number of enlarged peroxisomes.** The strains *E122* (A), *P16TR* (B), and *pex16-TH* (C and D) were grown for 8 h in YPBO medium, as described in the legend to Figure 5.4. Cells were processed for immunofluorescence microscopy with rabbit anti-thiolase and FITC-conjugated goat anti-rabbit IgG antibodies. (A' - D'), Nomarski images of (A - D). Unpermeabilized cells do not exhibit an immunofluorescence signal. Bar = 5 μ m.

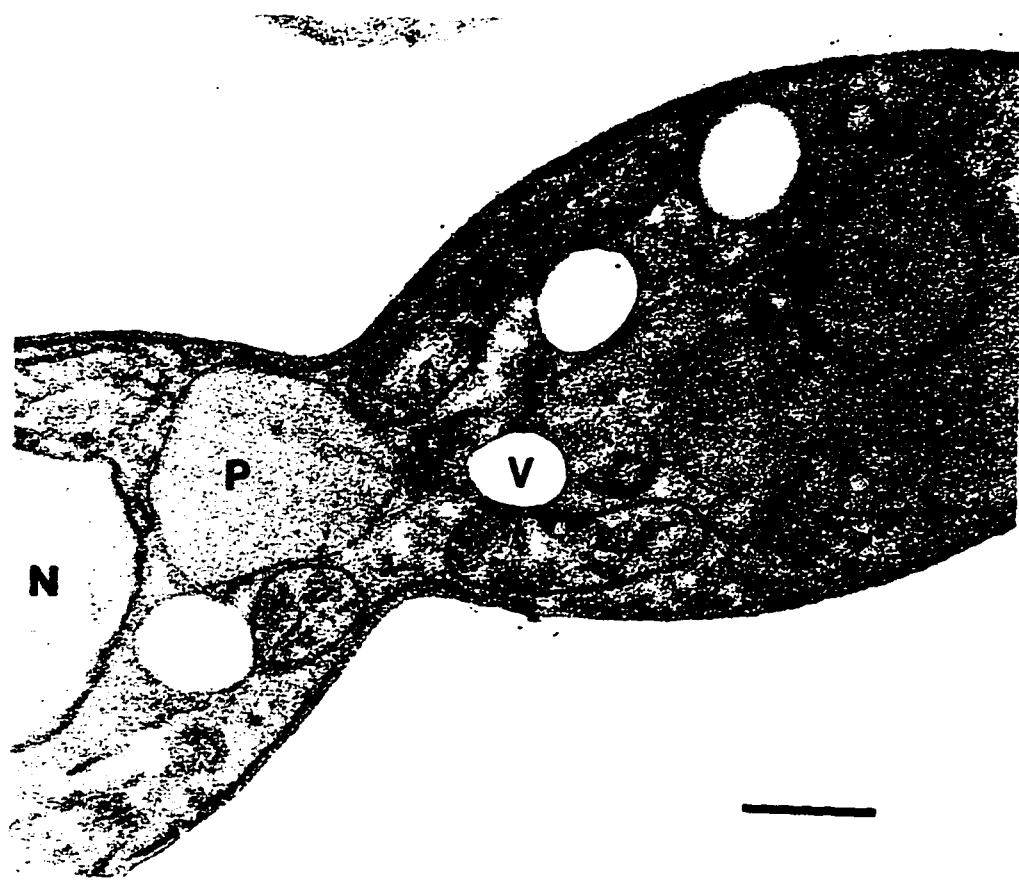


Figure 5.15 Ultrastructure of the *PEX16* overexpression strain *pex16-TH*. The *pex16-TH* strain was grown for 8 h in YPBO, as described in the legend to Figure 5.4. Electron microscopic section of a dividing cell is shown. The cell appears normal except for the presence of enlarged peroxisomes. Particularly noteworthy is that enlarged peroxisomes are present in both halves of the dividing cell, showing that segregation of these structures is not affected. *P*, peroxisome; *M*, mitochondrion, *N*, nucleus. Bar = 0.5 μm .

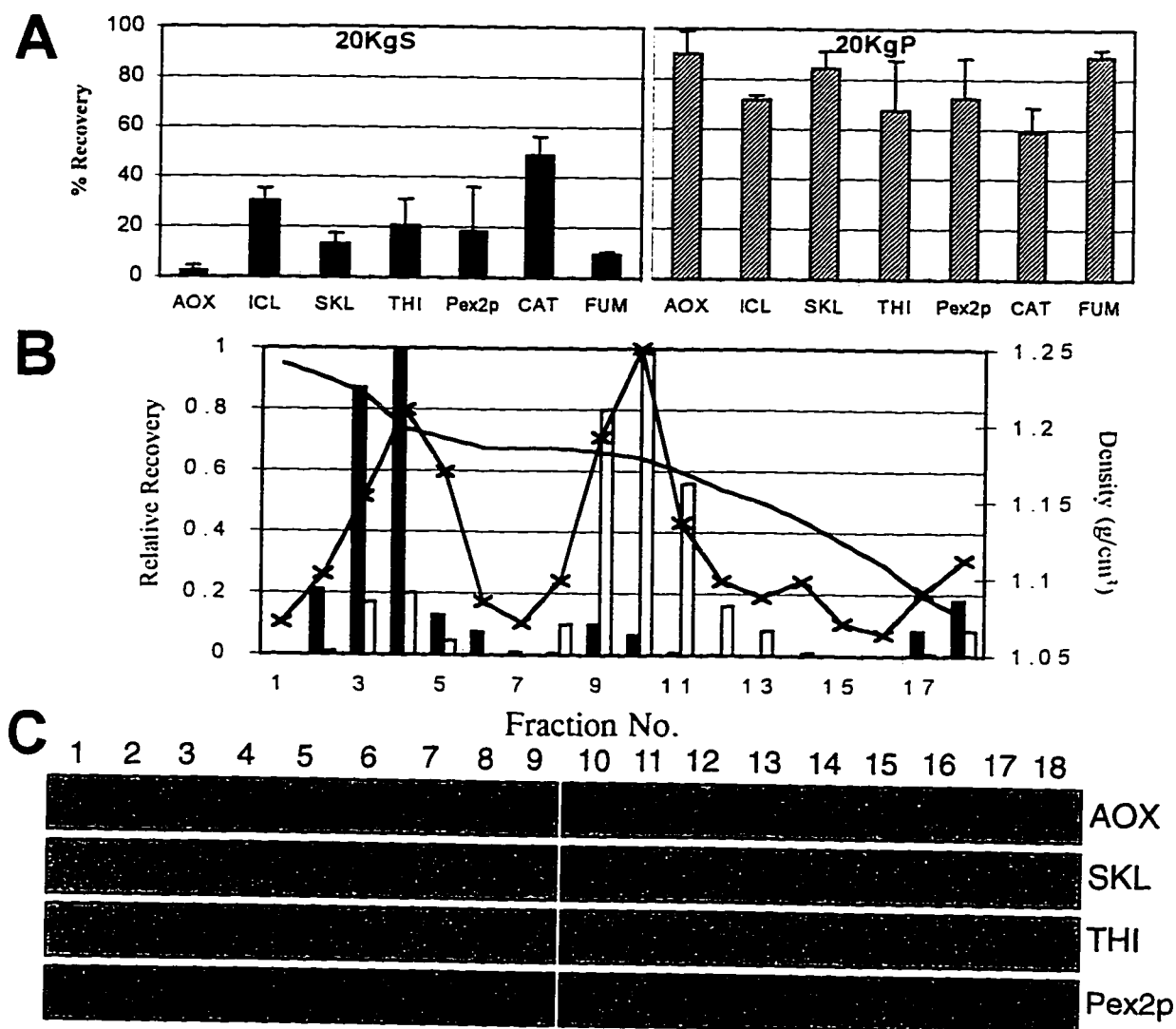


Figure 5.16 Characterization of the enlarged peroxisomes of the *pex16-TH* strain. The *PEX16* overexpression strain, *pex16-TH*, was grown for 8 h in YPBO medium, as described in the legend to *Figure 5.4*, and subjected to subcellular fractionation to yield 20KgS and 20KgP fractions. (A) The distribution of the enzymatic activities of catalase (*CAT*) and fumarase (*FUM*) and of the immunosignals of acyl-CoA oxidase (*AOX*), isocitrate lyase (*ICL*), a 62 kDa anti-SKL reactive polypeptide (*SKL*), thiolase (*THI*) and Pex2p to the 20KgS and 20KgP fractions is reported as the percent recovery of the respective total enzymatic activity or immunosignal in the PNS fraction. Immunoblots were quantitated by densitometry. Values reported are the means \pm SD of two independent experiments, each analyzed in duplicate. (B) Isopycnic density gradient analysis of the 20KgP from the strain *pex16-TH* grown for 8 h in YPBO medium. Distribution of protein (-x-), catalase (*solid bars*), fumarase (*open bars*) and density (*solid line*). Values reported are the means of two independent experiments, each analyzed in duplicate. (C) Equal volumes of gradient fractions were analyzed by immunoblot analysis. Abbreviations are as in (A).

5.6 Summary and discussion

Here we report the isolation of *Y. lipolytica pex16* mutant strains, their morphological and biochemical characterizations, the cloning and sequencing of the *YIPEX16* gene, and the identification and characterization of the peroxin, Pex16p.

5.6.1 *pex16* mutant strains contain abnormal peroxisomal structures

pex16 mutant strains cannot assemble functional peroxisomes. They are unable to grow using oleic acid as the sole carbon source, and under conditions of peroxisome induction, they fail to proliferate morphologically normal peroxisomes. However, subcellular fractionation showed that *pex16* strains import a subset of peroxisomal proteins at, or near, wild-type levels, suggesting that they are not generalized mutants of peroxisomal protein import. While isocitrate lyase, thiolase and catalase are completely mislocalized to the 20KgS in *pex16* mutants, other peroxisomal matrix (acyl-CoA oxidase, a 62 kDa anti-SKL reactive polypeptide, malate synthase) and membrane (Pex2p and Pex5p) proteins are localized to an organellar fraction pelletable at $20,000 \times g_{\max}$ (20KgP). Pelletable peroxisomal proteins are contained in vesicular elements that equilibrate at densities of 1.21 g/cm^3 and 1.16 g/cm^3 . Immunocytochemical analysis revealed that both of these fractions contained vesicular structures, 50 - 200 nm in diameter, that were labelled with anti-SKL and stained with gold particles (Fig 5.10 E and F). In contrast, analysis of similar subcellular fractions from the wild-type strain revealed peroxisomes, 300 - 500 nm in diameter, only at a density of 1.21 g/cm^3 (Fig. 5.10 C). Wild-type fractions equilibrating at a density of 1.16 g/cm^3 contained

primarily unlabelled mitochondria (Fig. 5.10 D).

The vesicular elements present in the *pex16-1* mutant strain may represent an intermediates along the peroxisome assembly pathway in *Y. lipolytica*. Import of peroxisomal proteins into peroxisomal intermediates seems to be temporally staggered, with some proteins being imported at an early stage and others only at a later stage of peroxisome development and maturation (Smith et al., 1997; Titorenko et al., 1996). It may be that *pex16* strains are blocked at a developmental stage that allows for the production of intermediates capable of importing only a subset of peroxisomal proteins. Progression from this intermediate stage to later stages and eventually to mature peroxisomes does not occur in *pex16* strains.

5.6.2 *The carboxyl-terminal tripeptide, Ser-Thr-Leu, of Pex16p is not essential for its targeting to peroxisomes*

Pex16p has at its carboxyl terminus the tripeptide, Ser-Thr-Leu. This sequence is very similar to the consensus sequence of PTS1 motifs, (Ser/Ala/Cys)(Lys/Arg/His)(Leu/Met). We therefore investigated whether this tripeptide motif is required for the targeting of Pex16p to peroxisomes. Elimination of the tripeptide by deletion or by replacement with the HA epitope does not prevent the import of Pex16p into peroxisomes (Fig. 5.12). Therefore, the carboxyl-terminal tripeptide of Pex16p is not required for its targeting or import into peroxisomes, however we cannot rule out the possibility that Ser-Thr-Leu-COOH may still function as a peroxisomal targeting signal.

Peroxisomes are able to import oligomeric and folded proteins (Glover et al., 1994; McNew and Goodman, 1994; 1996; Walton et al., 1995). The subunit composition of

Pex16p is unknown. However, the genes encoding Pex16-HA and Pex16p lacking its carboxyl-terminal tripeptide were expressed in the *P16KO-8A* background, in which the ORF of the nuclear *YIPEX16* gene is deleted. Accordingly, targeting of these carboxyl-terminal variants of Pex16p to peroxisomes cannot be the result of multimerization with a wild-type Pex16p having its carboxyl-terminal tripeptide intact. However, we cannot rule out the possibility that a carboxyl-terminal variant of Pex16p could gain access to the peroxisome by heterodimerizing with a different peroxisomal protein. Nevertheless, such a scenario would still be consistent with the carboxyl-terminal tripeptide of Pex16p being not necessary for its targeting or import into peroxisomes.

5.6.3 *A function for Pex16p in peroxisome growth and fission?*

What role might Pex16p play in peroxisome biogenesis? In glucose-grown cells, Pex16p is synthesized at low but measurable levels, which only modestly increase during growth of cells in oleic acid-containing medium. Pex16p may act to block proliferation of the small number of peroxisomal precursors that are normally present in glucose-grown yeast cells (Lazarow and Fujiki, 1985). Disruption of the *YIPEX16* gene and abolition of the synthesis of Pex16p relieves this block, and overproliferation of immature peroxisomes occurs. The resulting peroxisomal structures can be isolated by density gradient analysis of *pex16* cells and can be visualized by immunoelectronmicroscopy of these fractions (Figs. 5.9 and 5.10) as small vesicles containing some peroxisomal proteins. In contrast, overexpression of the *YIPEX16* gene, leading to an increased synthesis of Pex16p, maintains a block on proliferation of the peroxisomal templates normally found in glucose-grown cells. However,

the increased synthesis of peroxisomal matrix and membrane proteins during growth in oleic acid-containing medium is maintained in *YIPEX16* overexpressing cells. This leads to a situation in which the number of peroxisomes remains at or near that found in glucose-grown cells, although the peroxisomes are now greatly enlarged, since synthesis and import of peroxisomal proteins are largely unaffected (Figs. 5.13, 5.14). Therefore, Pex16p may act to inhibit peroxisome fission.

Pex16p may also have a secondary role in facilitating the import of some peroxisomal proteins, notably of catalase, thiolase, and isocitrate lyase. These enzymes are not localized to peroxisomal structures found in the 20KgP, but are mislocalized to the 20KgS in *pex16* cells. However, these enzymes are found in the enlarged peroxisomes of the *YIPEX16* overexpression strain (Figs. 5.14, 5.16). Whether facilitation of import of this subset of peroxisomal proteins can be attributed directly to the function of Pex16p cannot be answered at this time.

Other peroxins have been implicated in peroxisomal proliferation or fission, although their actions contrast with those of Pex16p. Overexpression of Pex3p and Pex10p in *H. polymorpha* (Baerends et al., 1996; Tan et al., 1995) and Pex11p in *S. cerevisiae* and *C. boidinii* (Marshall et al., 1995; Sakai et al., 1995) leads to a proliferation of normal peroxisomes, while elimination of Pex11p in these yeast species leads to a small number of enlarged peroxisomes (Erdmann and Blobel, 1995; Marshall et al., 1995; Sakai et al., 1995). Therefore, the mechanism of peroxisome proliferation is likely regulated by the coordination of positive and negative factors. Whether this coordination involves the molecular interaction of positive and negative regulatory proteins of peroxisome proliferation is currently unknown.

6. PERSPECTIVES

In the last few years, there have been many significant advances in uncovering the molecular mechanisms of peroxisome biogenesis. Much of this remarkable progress has been due to the isolation and analysis of peroxisome assembly (*pex*) mutants in a host of model organisms. Yeast systems have provided the greatest wealth of information, since genetic screens in these organisms are extremely simple and effective ways to clone important factors for peroxisome assembly (see *Section 2.3.2* and Erdmann et al., 1989; Cregg et al., 1990; Gould et al., 1992; Nuttley et al., 1993). Functional complementation of yeast *pex* mutants with DNA libraries has identified a number of *PEX* genes that encode proteins, called peroxins, required for peroxisome biogenesis (Table 6.1, adapted from Distel et al., 1996). Undoubtedly, within the next few years, many more *PEX* genes will be identified in this manner. Often times, having a number of homologues from different organisms has also contributed significantly to our understanding the functional roles of peroxins.

Based on a combination of morphological and biochemical properties, peroxins can be very broadly classified as i) those directly involved in protein targeting and import, and ii) those indirectly involved in targeting, but more likely involved in the assembly of peroxisomal structures (Table 6.1). However, these groupings are not mutually exclusive, since affecting membrane assembly likely affects protein import and *vice versa*. The ability to more stringently classify these factors is also hindered at this time by the limited attribution of functional characteristics to each and by the pleiotropic morphological effects of gene

disruption and overexpression experiments.

Using an approach combining phenotypic and morphological aspects of mutant strains and the implicated functions of peroxins, it is possible to develop a model of peroxisome assembly. The model presented in Fig. 6.1 makes use primarily of our own observations of peroxisome assembly in *Y. lipolytica*. Factors are assigned to specific stages of peroxisome assembly to define their roles. However, for those factors not yet identified in *Y. lipolytica*, peroxins from other yeast model systems are integrated. It is difficult to build a model that satisfies all experimental observations from all model organisms and therefore some personal judgements are made.

In a variety of *Y. lipolytica pex* mutants we have observed a heterogeneous population of peroxisomal structures which suggest that peroxisome assembly is a multistep process (Nuttley et al., 1994; Eitzen et al., 1995;1997; Titorenko et al., 1996; Smith et al., 1997). Three stages of peroxisome development can be defined: 1) the *proliferation stage*, where peroxisomal templates rapidly increase the number of small peroxisomal precursors; 2) the *assembly stage*, where intermediate peroxisomal vesicles assemble components needed for protein targeting and import; and 3) the *maturation stage*, where peroxisomes become competent for the import of all matrix proteins, increase their size and density, and are metabolically functional. A fourth peroxisome *disassembly stage* is not discussed here and is simply shown in this model as autophagic degradation by the vacuole (Tuttle et al., 1993).

Table 6.1 Description of yeast peroxins and *PEX* genes.

<i>PEX</i> gene	Peroxin description	Yeast homologues
<u>Genes affecting peroxisome membrane assembly:</u>		
<i>PEX1</i>	117 - 127 kDa, AAA-ATPase cytosolic(?) ^a NSF homology membrane addition/fusion (?)	<i>ScPAS1</i> (1) <i>PpPAS1</i> (2) <i>YIPAY1</i> (3)
<i>PEX2</i>	39 - 45 kDa, C ₃ HC ₄ -RING finger peroxisomal integral membrane protein group 10 of human PBD membrane assembly/sorting (?)	<i>ScCRT1</i> (7) <i>PpPER6</i> (7) <i>YIPAY5</i> (8)
<i>PEX3</i>	51 - 52 kDa peroxisomal integral membrane protein membrane maintenance	<i>ScPAS3</i> (12) <i>PpPAS2</i> (13) <i>HpPER9</i> (14)
<i>PEX4</i>	21 - 24 kDa. peroxisome-associated ubiquitin-conjugating enzyme important for peroxisome formation/proliferation	<i>ScPAS2</i> (29) <i>PpPAS4</i> (30)
<i>PEX6</i>	112 - 127 kDa, AAA-ATPase cytosolic and peroxisomal group 4 of human PBD ^b NSF/Cdc48 homology membrane addition/fusion (?)	<i>ScPAS8</i> (4) <i>PpPAS5</i> (5) <i>YIPAY4</i> (6)
<i>PEX10</i>	34 - 48 kDa, C ₃ HC ₄ -RING finger peroxisomal integral membrane protein peroxisome proliferation	<i>PpPAS7</i> (9) <i>HpPER8</i> (10)
<i>PEX11</i>	27 - 33 kDa peroxisomal integral membrane protein promotes peroxisome fission	<i>ScMP27</i> (15) <i>CbMP30</i> (16)
<i>PEX12</i>	48 kDa, C ₃ HC ₄ -RING finger peroxisomal integral membrane protein membrane translocation (?)	<i>PpPAS10</i> (11)
<i>PEX16</i>	42 - 45 kDa intraperoxisomal membrane-associated protein inhibits peroxisome fission	<i>YIPEX16</i> (20)

Genes affecting peroxisomal protein import:

<i>PEX5</i>	64 - 70 kDa, containing 7 - 8 tetratricopeptide repeats cytoplasmic and peroxisome-associated group 2 of human PBD PTS1 receptor	<i>ScPAS10</i> (21) <i>PpPAS8</i> (22) <i>HpPER3</i> (23) <i>YIPAY32</i> (24)
<i>PEX7</i>	42 kDa, containing 6 WD40 repeats cytoplasmic and peroxisome-associated PTS2 receptor	<i>ScPAS7</i> (25)
<i>PEX8</i>	71 - 81 kDa peroxisomal membrane-associated protein import of PTS1 (?)	<i>PpPER3</i> (17) <i>HpPER1</i> (18)
<i>PEX9</i>	42 - 45 kDa peroxisomal integral membrane protein general import factor	<i>YIPAY2</i> (26)
<i>PEX13</i>	40 - 43 kDa, SH3-containing peroxisomal integral membrane protein PTS1 docking factor	<i>ScPEX13</i> (27) <i>PpPEX13</i> (28)
<i>PEX14</i>	38 - 42 kDa, containing a coiled-coil region extraperoxisomal membrane-associated protein import factor interacting with both PTS receptors	<i>HpPEX14</i> (31) <i>ScPEX14</i> (32)
<i>PEX17</i>	70 kDa intraperoxisomal membrane-associated protein peroxisome maturation (?)	<i>YIPEX17</i> (19)

^a(?) putative function/location, with limited evidence according to author

^bmutations responsible for the human peroxisomal biogenesis disorder of group No.

(1) Erdmann et al., 1990; (2) Heyman et al., 1994; (3) unpublished, Rachubinski; (4) Voorn-Brouwer et al., 1993; (5) Spong et al., 1993; (6) Nuttley et al., 1994; (7) Waterham et al., 1996; (8) Eitzen et al., 1996; (9) Kalish et al., 1995; (10) Tan et al., 1995; (11) Kalish et al., 1996; (12) Höhfeld et al., 1991; (13) Baerends et al., 1996; (14) Wiemer et al., 1996; (15) Erdmann and Blobel, 1995; Marshall et al., 1995; (16) Sakai et al., 1995; (17) Liu et al., 1995; (18) Waterham et al., 1994; (19) Smith et al., 1997; (20) Eitzen et al., 1997; (21) van der Leij et al., 1993; (22) McCollum et al., 1993; (23) van der Klei et al., 1995; Nuttley et al., 1995; (24) Szilard et al., 1995; (25) Marzioch et al., 1994; Zhang and Lazarow, 1995; (26) Eitzen et al., 1995; (27) Elgersma et al., 1996; Erdmann and Blobel, 1996; (28) Gould et al., 1996; (29) Wiebel and Kunau, 1992; (30) Crane et al., 1994; (31) Komori et al., 1997; (32) Albertini et al., 1997.

STAGE 1

The temporal events of peroxisome biogenesis are initiated by the proliferation of many small peroxisomal precursor vesicles from the limited number of peroxisomal templates present during non-peroxisome inducing conditions. A factor blocking proliferation may first be targeted for degradation in this process, since mutants of Pex4p, a ubiquitin-conjugating enzyme, fail to assemble any morphologically identifiable peroxisomal structures (Wiebel and Kunau, 1992; Crane et al., 1994). Pex1p and Pex3p are also components required early in peroxisome development since mutants of these proteins fail to assemble peroxisomes (Heyman et al., 1994; Erdmann et al., 1991; Höhfeld et al., 1991). Pex1p is an *N*-ethylmaleimide sensitive factor (NSF) homologue and seems to associate from a cytosolic pool with peroxisome membranes, while Pex3p is an integral membrane component of peroxisomes. Interestingly, experiments in mammalian cell lines showed that the stability of Pex5p is reduced in *pex1* and *pex4* mutant cells and, therefore, stabilization of peroxins required for a later developmental stage may be another role of these factors (Yahraus et al., 1996; Dodt and Gould, 1996).

Peroxisomes elongate and then rapidly multiply in number by several fission events in a Pex11p-dependent manner (Marshall et al., 1995). Bulk delivery of membrane components necessitates peroxisomal elongation. The endoplasmic reticulum is likely the origin of these membranes, which could be delivered to peroxisome precursors via small transport vesicles or by a physical interconnection much like the membrane bridge mitochondrial-associated-membrane (MAM) structures postulated for the interchange of phosphatidylserine for phosphatidylethanolamine between the endoplasmic reticulum and

mitochondria (Shiao et al., 1995). Heterotypic membrane fusion is preeminent for the incorporation of lipids and likely requires the soluble NSF homologue, Pex1p, and peroxisomal membrane factors like Pex3p.

Several other peroxins also seem to act in the recruitment of lipids. A family of three unique proteins containing C₃HC₄ RING-finger motifs likely functions in the sorting and assembly of bulk membranes into peroxisomal vesicles. RING-finger motifs have been implicated to function in protein-lipid interactions (Quest et al., 1992). Disruption of the RING-finger proteins Pex2p and Pex10p results in the accumulation of membrane sheets and multiple peroxisomal subpopulations, while oversynthesis of Pex10p results in many enlarged peroxisomes (Titorenko et al., 1996; Kalish et al., 1995; Tan et al., 1995). The third family member, Pex12p, could also interact similarly, since multiple peroxisomal subpopulations are present in *pex12* mutant strains (Kalish et al., 1996). Another function of these proteins may be the facilitation of protein import, since the mutation of their genes results in the mislocalization of a subset of peroxisomal matrix proteins in a PTS-independent manner. However, this phenomenon may reflect a secondary effect of the developmental stage at which these peroxisomal remnants are blocked.

STAGE 2

As discussed in previous sections of the Results, many studies have shown that the events of peroxisomal membrane proliferation are independent of protein import. Thus, the second developmental stage of peroxisomes becomes predominant after membrane proliferation is complete, and fission is inhibited in a Pex16p-dependent manner, allowing

peroxisomes to increase in size and density (Eitzen et al., 1997). A second membrane fusion event likely occurs during this stage, catalyzed by a second NSF homologue, Pex6p, in order to support peroxisome enlargement (Spong et al., 1993; Nuttley et al., 1994). *pex6* mutant strains accumulate small peroxisomal remnants, unlike *pex1* mutant strains, and therefore the function of Pex6p is placed downstream of Pex1p (Heyman et al., 1994). As presented here, this second fusion event is deemed to be homotypic, involving the fusion of two peroxisomal intermediates, the contents of which contain either (a) identical or (b) unique subsets of peroxisomal matrix proteins. A homotypic fusion step at this stage would also support peroxisome enlargement by specific quanta and mature peroxisomes of a very homogenous size. The heterogenous subpopulation of peroxisomes seen in some mutants of peroxisome assembly may reflect import of matrix proteins at different stages rather than import into separate populations of peroxisomes. Therefore, regulation of import may be temporal or spatial (or both).

Assembly of the targeting and translocation machinery occurs during STAGE 2 of peroxisome development. Factors involved in the docking of the PTS1 receptor, Pex5p, and of the PTS2 receptor, Pex7p, are assembled into the peroxisome membrane. Pex13p is a docking factor for the PTS1 pathway (Elgersma et al., 1996; Erdmann and Blobel et al., 1996; Gould et al., 1996), and import of PTS1-containing proteins seems to be facilitated by Pex8p (Liu et al., 1995). Factors specific for the PTS2 pathway are not yet known, although Pex13p may also play a role in the import of proteins targeted by this pathway.

STAGE 3

This final stage of peroxisome maturation starts once all targeting and import machinery is in place and functioning efficiently. The bulk import of matrix proteins occurs, and peroxisomes become increasingly dense, eventually containing granular or paracrystalline cores. Peroxisomes blocked in import will be less dense than normal, and therefore mutations that do not allow progression to this final stage often accumulate less dense peroxisomal structures. Occasionally, these peroxisomal structures contain subsets of matrix proteins. Therefore, peroxisomal intermediates may be able to import and assemble some peroxisomal proteins (*e.g.* components needed for import) but not others. Factors required for import such as Pex9p, Pex14p and Pex17p, which apparently are not specific to any import pathway, must be active in this final stage. Mutant strains of *PEX9*, *PEX14* and *PEX17* form typical peroxisomal structures; however, they fail to mature dense, fully functional peroxisomes (Eitzen et al., 1995; Komori et al., 1997; Albertini et al., 1997; Smith et al., 1997). Pex14p is a peripheral peroxisomal membrane protein, tightly bound to the cytosolic face and could represent an initial point of convergence in the peroxisomal import pathways since it interacts with both PTS receptors and the PTS1 docking factor (Albertini et al., 1997). Interestingly, oversynthesis of Pex14p results in a peroxisome-deficient phenotype revealing the stoichiometric importance of this peroxin in the import mechanism (Komori et al., 1997). It has also been proposed that Pex5p and Pex7p act as internal chaperones that bind the PTS1 and PTS2 targeting signals from inside the peroxisome and act specifically in protein translocation (Szilard et al., 1995; Zhang and Lazarow, 1995). However, other studies propose that these factors shuttle in an on-off state between the peroxisomal outer membrane and the cytosol

and thus act as external chaperones (Gould et al., 1996; Marzioch et al., 1994). Accordingly, much of this model elucidated through genetic evidence still requires confirmation by biochemically explicit experimentation.

Finally, once peroxisomes have been fully assembled, they must become metabolically active. This involves the assembly of enzymes with cofactors (*e.g.* NADH, FADH₂) required for the multitude of metabolic processes which peroxisomes perform, as well as the transport of nutrients in (*e.g.* activated fatty acids) and metabolic end-products out (*e.g.* acetyl-CoA units) (van den Bosch et al., 1992). Two ABC transporters proteins, Pat1 and Pat2, involved in the import of long-chain fatty acids have recently been isolated from *S. cerevisiae* (Hettema et al., 1996). The underlying importance of these factors is manifested in the human peroxisomal disorder, X-linked adrenoleukodystrophy (X-ALD), which is characterized by the accumulation of long-chain fatty acids in the serum. The affected gene in X-ALD has been identified and shown to encode an ABC transporter involved in the transport of activated fatty acids into peroxisomes (Mosser et al., 1993).

If the metabolic demand on a cell is altered (*i.e.* a change in nutritional conditions), such that the function peroxisomes is not required for the assimilation of nutrients, then the number of peroxisomes is reduced in a degradative process (Tuttle et al., 1993).

Figure 6.1 A model of peroxisome biogenesis. Peroxisome biogenesis is broken down into four distinct developmental stages. *Black* and *white* peroxisomal structures identify a potential, early heterotypic population of peroxisomes that import defined subsets of proteins (shown in *inset*). Fusion of intermediates at a later stage (*grey vesicles*) results in peroxisomes that can import all required peroxisomal proteins. See the *text* for details of assembly stages and peroxin function.

Within the next few years, many additional peroxins will be identified using new positive genetic selection schemes (Elgersma et al., 1993) and by examining the kinetics of targeting PTS-green fluorescent protein chimeras in living cells (Kalish et al., 1996). Although genetic screens are becoming increasingly clever, the ability to attribute much functional information to peroxins cloned in this way will always be somewhat limited to speculation. Therefore, it will be of the utmost importance to place greater emphasis on the development of *in vitro* assays to confirm (or disprove) the speculated functions of peroxins. The ability to reconstitute the various stages of peroxisome assembly has been slow in coming due to technical difficulties of *in vitro* import assays. It seems that peroxisomes are either too fragile or too leaky for such assays, or the wrong developmental stage of peroxisomes is being employed. Possibly the use of permeabilized cell systems (Wendland and Subramani, 1993b) for the development of import assays will be more fruitful.

Finally I ask the question: Is the use of yeast model systems a valid experimental approach for the study of human peroxisome biogenesis disorders? In all cases of human peroxisome biogenesis disorders where the dysfunctional peroxin has been identified, several yeast orthologues exist and have already been characterized. It is likely that there will be yeast orthologues for all human peroxins. Human peroxins that have been identified include the C₃HC₄ RING-finger protein Pex2p (Shimozawa et al., 1992), the PTS1 receptor Pex5p (Dodt et al., 1995; Wiemer et al., 1995), and the late-acting NSF homologue Pex6p (Tsukamoto et al., 1995; Yahraus et al., 1996). Unfortunately, peroxin orthologues are not completely functional *interspecies*; for example, the human PTS1 receptor does not function in yeast and *vice versa*. Nor are there many data supporting interspecies complementation

of peroxins within yeast. With such a high degree of genetic diversity in peroxins, the use of several model organisms and a combination of results from them will produce a more meaningful understanding of peroxin function. Accordingly, the elucidation of the molecular basis of peroxisome biogenesis in amenable yeast model systems should lead to significant progress in our understanding of human peroxisomal biogenesis disorders, with the eventual goals of treatment and cure of these debilitating diseases.

7. BIBLIOGRAPHY

- Abeijon, C., P. Orlean, P.W. Robbins, C.B. Hirschberg. 1989. Topography of glycosylation in yeast: characterization of GDP mannose transport and lumenal guanosine diphosphatase activities in Golgi-like vesicles. *Proc. Natl. Acad. Sci. USA* 86:6935-6939.
- Aitchison, J.D., and R.A. Rachubinski. 1990. In vivo import of *Candida tropicalis* hydratase-dehydrogenase-epimerase into peroxisomes of *Candida albicans*. *Curr. Genet.* 17:481-486.
- Aitchison, J.D., W.W. Murray, and R.A. Rachubinski. 1991. The carboxyl-terminal tripeptide Ala-Lys-Ile is essential for targeting *Candida tropicalis* trifunctional enzyme to yeast peroxisomes. *J. Biol. Chem.* 266:23197-23203.
- Aitchison, J.D. 1992. Targeting of *Candida tropicalis* trifunctional enzyme to peroxisomes in yeast: identification of a carboxy-terminal tripeptide peroxisomal targeting signal. Ph.D. Thesis, McMaster University.
- Aitchison, J.D., R.K. Szilard, W.M. Nuttley, and R.A. Rachubinski. 1992. Antibodies directed against a yeast carboxyl-terminal peroxisomal targeting signal specifically recognize peroxisomal proteins from various yeasts. *Yeast* 8:721-734.
- Albertini M., P. Rehling, R. Erdmann, W. Girzalsky, J.A.K.W. Kiel, M. Veenhuis and W.-H. Kunau. 1997. Pex14p, a peroxisomal membrane protein binding both receptors of the two PTS-dependent import pathways. *Cell* 89:83-92.
- Ausubel, F.J., R. Brent, R.E. Kingston, D.D. Moore, J.G. Seidman, J.A. Smith, and K. Struhl. 1996. *In Current Protocols in Molecular Biology*. Green Publishing Associates, New York.
- Authier, F., J.J.M. Bergeron, W. Ou, R.A. Rachubinski, B.I. Posner, P.A. Walton. 1995. Degradation of the cleaved leader peptide of thiolase by a peroxisomal proteinase. *Proc. Natl. Acad. Sci. USA* 92:3859-3863.
- Avers, C.J., and M. Federman. 1968. The occurrence in yeast of cytoplasmic granules which resemble microbodies. *J. Cell Biol.* 37:555-559.
- Baerends, R.J.S., S.W. Rasmussen, R.E. Hilbrands, M. van der Heide, K.N. Faber, P.T.W. Reuvekamp, J.A.K.W. Kiel, J.M. Cregg, I.J. van der Klei, and M. Veenhuis. 1996. The *Hansenula polymorpha* PER9 gene encodes a peroxisomal membrane protein essential for peroxisome assembly and integrity. *J. Biol. Chem.* 271:8887-8894.
- Barth, G., and T. Scheuber. 1993. Cloning of the isocitrate lyase gene (ICL1) from *Yarrowia lipolytica* and characterization of the deduced protein. *Mol. Gen. Genet.* 241:422-430.

- Baudhuin, P., H. Beaufay, Y. Rahman-Li, O.Z. Sellinger, R. Wattiaux, P. Jacques, and C. deDuve. 1964. Intracellular distribution of monoamine oxidase, aspartate aminotransferase, alanine aminotransferase, D-amino acid oxidase and catalase in rat liver tissue. *Biochem. J.* 92:179-184.
- Berg, J.M. 1990. Zinc fingers and other metal-binding domains. *J. Biol. Chem.* 265:6513-6516.
- Berninger, G., R. Schmidtchen, G. Casel, A. Knorr, K. Rautenstrauss, W.-H. Kunau, and E. Schweizer. 1993. Structure and metabolic control of the *Yarrowia lipolytica* peroxisomal 3-oxoacyl-CoA thiolase gene. *Eur. J. Biochem.* 216:607-613.
- Berryman, M.A., and R.D. Rodewald. 1990. An enhanced method for post-embedding immunocytochemical staining which preserves cell membranes. *J. Histochem. Cytochem.* 38:159-170.
- Berteaux-Lecellier, V., M. Picard, C. Thompson-Coffe, D. Zickler, A. Panvier-Adoutte, and J.-M. Simonet. 1995. A nonmammalian homolog of the *PAF1* gene (Zellweger syndrome) discovered as a gene involved in caryogamy in the fungus *Podospora anserina*. *Cell* 81:1043-1051.
- Blobel, G. 1980. Intracellular protein topogenesis. *Proc. Natl. Acad. Sci. USA* 77:1596-1600.
- Brade, A.M. 1992. Peroxisome assembly in *Yarrowia lipolytica*. M.Sc. Thesis, McMaster University
- Bradford, M.M. 1976. A rapid and sensitive method for the quantification of microgram quantities of protein utilizing the principle of protein-dye binding. *Anal. Biochem.* 72:248-254.
- Burnette, W.M. 1981. "Western blotting" electrophoretic transfer of proteins from sodium dodecylsulphate polyacrylamide gels to unmodified nitrocellulose and radiographic detection with antibody and radioiodinated Protein A. *Anal. Biochem.* 112:195-203.
- Cigan, A.M., and T.F. Donahue. 1987. Sequence and structural features associated with translation initiator regions in yeast--a review. *Gene* 59:1-18.
- Cooperstein, S.J., and A. Lazarow. 1951. A microspectrophotometric method for determination for cytochrome oxidase. *J. Biol. Chem.* 189:665-670.
- Crane, D.I., J.E. Kalish, and S.J. Gould. 1994. The *Pichia pastoris* *PAS4* gene encodes a ubiquitin-conjugating enzyme required for peroxisome assembly. *J. Biol. Chem.* 269:21835-21844.

- Cregg, J.M., I.J. van der Klei, G.J. Sulter, M. Veenhuis, and W. Harder. 1990. Peroxisome-deficient mutants of *Hansenula polymorpha*. *Yeast* 6:87-97.
- de Boer, A.D., and P.J. Weisbeek. 1991. Chloroplast protein topogenesis: import, sorting and assembly. *Biochim. Biophys. Acta.* 1071:221-253.
- de Duve, C., and P. Baudhuin. 1966. Peroxisomes (microbodies and related particles). *Physiol. Rev.* 46:323-357.
- de Hoop, M.J., and G. AB. 1992. Import of proteins into peroxisomes and other microbodies. *Biochem. J.* 286:657-669.
- Distel, B., R. Erdmann, S.J. Gould, G. Blobel, D.I. Crane, J.M. Cregg, G. Dodt, Y. Fujiki, J.M. Goodman, W.W. Just, J.A.K.W. Kiel, W.-H. Kunau, P.B. Lazarow, G.P. Mannaerts, H. Moser, T. Osumi, R.A. Rachubinski, A. Roscher, S. Subramani, H.F. Tabak, D. Valle, I. van der Klei, P.P. van Veldhoven, and M. Veenhuis. 1996. A unified nomenclature for peroxisome biogenesis. *J. Cell Biol.* 135:1-3.
- Dmochowska, A., D. Dignard, P. Maleszka, and D.Y. Thomas. 1990. Structure and transcriptional control of the *Saccharomyces cerevisiae* *POX1* gene encoding acyl-coenzyme A oxidase. *Gene* 88:247-252.
- Donaldson, R.P., N.E. Tolbert, and C. Schnarrenberger. 1972. A comparison of microbody membranes with microsomes and mitochondria from plant and animal tissue. *Arch. Biochem. Biophys.* 152:199-215.
- Dodt, G., N. Braverman, C. Wong, A. Moser, H.W. Moser, P. Watkins, D. Valle, and S.J. Gould. 1995. Mutations in the PTS1 receptor gene, *PXR1*, define complementation group 2 of the peroxisome biogenesis disorders. *Nature Genet.* 9:115-124.
- Dodt., G, and S.J. Gould. 1995. Multiple PEX genes are required for proper subcellular distribution and stability of Pex5p, the PTS1 receptor: evidence that PTS1 protein import is mediated by a cycling receptor. *J. Cell Biol.* 135:1763-1774.
- Douma, A.C., M. Veenhuis, W. de Koning, M. Evers, and W. Harder. 1985. Dihydroxyacetone synthase is localized in the peroxisomal matrix of methanol-grown *Hansenula polymorpha*. *Arch. Microbiol.* 143:237-243.
- Dulic, V., and H. Riezman. 1989. Characterization of the *END1* gene required for vacuole biogenesis and gluconeogenic growth of budding yeast. *EMBO J.* 8:1349-1359.

- Dyer, J.M., J.A. McNew, and J.M. Goodman. 1996. The sorting sequence of the peroxisomal integral membrane protein PMP47 is contained within a short hydrophilic loop. *J. Cell Biol.* 133:269-280.
- Eitzen, G.A., J.D. Aitchison, R.K. Szilard, M. Veenhuis, W.M. Nuttley, and R.A. Rachubinski. 1995. The *Yarrowia lipolytica* gene *PAY2* encodes a 42-kDa peroxisomal integral membrane protein essential for matrix protein import and peroxisome enlargement but not for peroxisome membrane proliferation. *J. Biol. Chem.* 270:1429-1436.
- Eitzen, G.A., V.I. Titorenko, J.J. Smith, M. Veenhuis, R.K. Szilard, and R.A. Rachubinski. 1996. The *Yarrowia lipolytica* gene *PAY5* encodes a peroxisomal integral membrane protein homologous to the mammalian peroxisome assembly factor PAF-1. *J. Biol. Chem.* 271:20300-20306.
- Eitzen, G.A., R.K. Szilard, and R.A. Rachubinski. 1997. Enlarged peroxisomes are present in oleic acid-grown *Yarrowia lipolytica* overexpressing the *PEX16* gene encoding an intraperoxisomal peripheral membrane peroxin. *J. Cell Biol.* *In press*.
- Eisenberg, D., E. Schwarz, M. Komaromy, and R. Wall. 1984. Analysis of membrane and surface protein sequences with the hydrophobic moment plot. *J. Mol. Biol.* 179:125-142.
- Elgersma, Y., M. van den Berg, H.F. Tabak, and B. Distel. 1993. An efficient positive selection procedure for the isolation of peroxisomal assembly mutants of *Saccharomyces cerevisiae*. *Genetics* 135:731-740.
- Elgersma, Y., L. Kwast, A. Klein, T. Voorn-Brouwer, M. van den Berg, B. Metzger, T. America, H.F. Tabak, and B. Distel. 1996. The SH3 domain of the *Saccharomyces cerevisiae* peroxisomal membrane protein Pex13p functions as a docking site for Pex5p, a mobile receptor for the import of PTS1 containing proteins. *J. Cell Biol.* 135:97-109.
- Erdmann, R., M. Veenhuis, D. Mertens, and W.-H. Kunau. 1989. Isolation of peroxisome-deficient mutants in *Saccharomyces cerevisiae*. *Proc. Natl. Acad. Sci. USA* 86:2432-2436.
- Erdmann, R., F.F. Wiebel, A. Flessau, J. Rytka, A. Beyer, K.-U. Fröhlich, and W.-H. Kunau. 1991. *PAS1*, a yeast gene required for peroxisome biogenesis, encodes a member of a novel family of putative ATPases. *Cell* 64:499-510.
- Erdmann, R., and G. Blobel. 1995. Giant peroxisomes in oleic acid-induced *Saccharomyces cerevisiae* lacking the peroxisomal membrane protein Pmp27p. *J. Cell Biol.* 128:509-523.
- Erdmann, R., and G. Blobel. 1996. Identification of Pex13p, a peroxisomal membrane receptor for the PTS1 recognition factor. *J. Cell Biol.* 135:111-121.

- Fahimi, H.D., E. Baumgart, and A. Völkl. 1993. Ultrastructural aspects of the biogenesis of peroxisomes in rat liver. *Biochimie* 75:201-208.
- Flaspohler, J.A., W.L. Rickoll, S.M. Beverley, and M. Parsons. 1997. Functional identification of a *Leishmania* gene related to the peroxin 2 gene reveals common ancestry of glycosomes and peroxisomes. *Mol. Cell. Biol.* 17:1093-1101.
- Franzusoff, A., J. Rothblatt, and R. Schekman. 1991. Analysis of polypeptide transit through the yeast secretory pathway. *Methods Enzymol.* 194:662-682.
- Fujiki, Y., A.L. Hubbard, S. Fowler, and P.B. Lazarow. 1982. Isolation of intracellular membranes by means of sodium carbonate treatment: application to endoplasmic reticulum. *J. Cell Biol.* 93:97-102.
- Fujiki, Y., R.A. Rachubinski, and P.B. Lazarow. 1984. Synthesis of a major integral membrane polypeptide of rat liver peroxisomes on free polysomes. *Proc. Natl. Acad. Sci. USA* 81:7127-7131.
- Fujiki, Y., R.A. Rachubinski, A. Zentella-Dehesa, and P.B. Lazarow. 1986. Induction, identification, and cell-free translation of mRNAs coding for peroxisomal proteins in *Candida tropicalis*. *J. Biol. Chem.* 261:15787-15793.
- Gaillardin, C.M., V. Charoy, and H. Heslot. 1973. A study of copulation, sporulation and meiotic segregation in *Candida lipolytica*. *Arch. Mikrobiol.* 92:69-83.
- Gärtner, J., H.W. Moser, and D. Valle. 1992. Mutations in the 70K peroxisomal membrane protein gene in Zellweger syndrome. *Nature Genet.* 1:16-22.
- Giedroc, D.P., K.M. Keating, K.R. Williams, and J.E. Coleman. 1987. The function of zinc in gene 32 protein from T4. *Biochemistry* 26:5251-5259.
- Glover, J.R., D.W. Andrews, S. Subramani, and R.A. Rachubinski. 1994a. Mutagenesis of the amino terminal targeting signal of *Saccharomyces cerevisiae* 3-ketoacyl-CoA thiolase reveals conserved amino acids required for import into peroxisomes. *J. Biol. Chem.* 269:7558-7563.
- Glover, J.R., D.W. Andrews, and R.A. Rachubinski. 1994b. *Saccharomyces cerevisiae* peroxisomal thiolase is imported as a dimer. *Proc. Natl. Acad. Sci. USA* 91:10541-10545.
- Gödecke, A., M. Veenhuis, R. Roggenkamp, Z.A. Janowicz, and C.P. Hollenberg. 1989. Biosynthesis of the peroxisomal dihydroxyacetone synthase from *Hansenula polymorpha* in *Saccharomyces cerevisiae*. *Curr. Genet.* 16:13-20.

- Gleeson, M.A., and P.E. Sudbery. 1988. Genetic analysis in the methylotrophic yeast *Hansenula polymorpha*. *Yeast*. 4:293-303.
- Gorman, C.M., G.T. Merlino, M.C. Willingham, I. Pastan, and B.H. Howard. 1982. The Rous sarcoma virus long terminal repeat is a strong promoter when introduced into a variety of eukaryotic cells by DNA-mediated transfection. *Proc. Natl. Acad. Sci. USA* 79:6777-6781.
- Gould, S.J., G.-A. Keller, and S. Subramani. 1987. Identification of a peroxisomal targeting signal at the carboxy-terminus of firefly luciferase. *J. Cell Biol.* 105:2923-2931.
- Gould, S.J., G.-A. Keller, and S. Subramani. 1988. Identification of a peroxisomal targeting signal located at the carboxy-terminus of four peroxisomal proteins. *J. Cell Biol.* 107:897-905.
- Gould, S.J., G.-A. Keller, N. Hosken, J. Wilkinson, and S. Subramani. 1989. A conserved tripeptide sorts proteins to peroxisomes. *J. Cell Biol.* 108:1657-1664.
- Gould, S.J., G.-A. Keller, M. Schneider, S.H. Howell, L.J. Garrard, J.M. Goodman, B. Distel, H. Tabak, and S. Subramani. 1990. Peroxisomal protein import is conserved between yeast, plants, insects and mammals. *EMBO J.* 9:85-90.
- Gould, S.J., D. McCollum, A.P. Spong, J.A. Heyman, and S. Subramani. 1992. Development of the yeast *Pichia pastoris* as a model organism for a genetic and molecular analysis of peroxisome assembly. *Yeast* 8:613-628.
- Gould, S.J., J.E. Kalish, J.C. Morrell, J. Bjorkman, A.J. Urquhart, and D.I. Crane. 1996. An SH3 protein in the peroxisome membrane is a docking factor for the PTS1 receptor. *J. Cell Biol.* 135:85-95.
- Green, S., I. Issemann, and E. Sheer. 1988. A versatile in vivo and in vitro eukaryotic expression vector for protein engineering. *Nucleic Acids Res.* 16:369.
- Hajra, A.K., and J.E. Bishop. 1982. Glycerolipid biosynthesis in peroxisomes via acyl dihydroxyacetone pathway. *Ann. N.Y. Acad. Sci.* 386:170-182.
- Häusler, T., Y.-D. Stierhof, E. Wirtz, and C. Clayton. 1996. Import of a DHFR hybrid protein into glycosomes in vivo is not inhibited by the folate analogue aminopterin. *J. Cell Biol.* 132:311-324.
- Heikoop, J.C., R.J. Wanders, A. Strijland, R. Purvis, R.B. Schutgens, and J.M. Tager. 1992. Genetic and biochemical heterogeneity in patients with the rhizomelic form of chondrodysplasia punctata--a complementation study. *Hum. Genet.* 89:439-444.

Heinemann, P., and W.W. Just. 1992. Peroxisomal protein import. In vivo evidence for a novel translocation competent compartment. *FEBS Lett.* 300:179-182.

Hettema, E.H., C.W.T. van Roermund, B. Distel, M. van den Berg, C. Vilela, C. Rodrigues-Pousada, R.J.A. Wanders, and H.F. Tabak. 1996. The ABC transporter proteins Pat1 and Pat2 are required for import of long-chain fatty acids into peroxisomes of *Saccharomyces cerevisiae*. *EMBO J.* 15:3813-3822.

Heyman J.A., E. Monosov, and S. Subramani. 1994. Role of the *PAS1* gene of *Pichia pastoris* in peroxisome biogenesis. *J. Cell Biol.* 127:1259-1273.

Höhfeld, J., M. Veenhuis, and W.-H. Kunau. 1991. PAS3, a *Saccharomyces cerevisiae* gene encoding a peroxisomal integral membrane protein essential for peroxisome biogenesis. *J. Cell Biol.* 114:1167-1178.

Kalish, J.E., G.A. Keller, J.C. Morrell, S.J. Mihalik, B. Smith, J.M. Cregg, and S.J. Gould. 1996. Characterization of a novel component of the peroxisomal protein import apparatus using fluorescent peroxisomal proteins. *EMBO J.* 15:3275-3285.

Kalish, J.E., C. Theda, J.C. Morrell, J.M. Berg, and S.J. Gould. 1995. Formation of the peroxisome lumen is abolished by loss of *Pichia pastoris* Pas7p, a zinc-binding integral membrane protein of the peroxisome. *Mol. Cell. Biol.* 15:6406-6419.

Kamiryo, T., M. Abe, K. Okazaki, S. Kato, and N. Shimamoto. 1982. Absence of DNA in peroxisomes of *Candida tropicalis*. *J. Bacteriol.* 152:269-274.

Klein, P., M. Kanehisa, and C. DeLisi. 1985. The detection and classification of membrane-spanning proteins. *Biochim. Biophys. Acta* 815:468-476.

Komori, M., S.W. Rasmussen, J.A.K.W. Kiel, R.J.S. Baerends, J.M. Cregg, I.J. van der Klei, and M. Veenhuis. 1997. The *Hansenula polymorpha* *PEX14* gene encodes a novel peroxisomal membrane protein essential for peroxisome biogenesis. *EMBO J.* 16:44-53.

Kragler, F., A. Langeder, J. Raupachova, M. Binder, and A. Hartig. 1993. Two independent peroxisomal targeting signals in catalase A of *Saccharomyces cerevisiae*. *J. Cell Biol.* 120:665-673.

Krisans, S.K., S.L. Thompson, L.A. Pena, E. Kok, and N.B. Javitt. 1985. Bile acid synthesis in rat liver peroxisomes: metabolism of 26-hydroxycholesterol to 3 β -hydroxy-5-cholenoic acid. *J. Lipid Res.* 26:1324-1332.

Kunau, W.-H., A. Beyer, T. Franken, K. Gotte, M. Marzioch, J. Saidowsky, A. Skaletz-Rorowski, and F.F. Wiebel. 1993. Two complementary approaches to study peroxisome biogenesis in *Saccharomyces cerevisiae*: forward and reversed genetics. *Biochimie* 75:209-224.

Kyte, J., and R.F. Doolittle. 1982. A simple method for displaying the hydropathic character of a protein. *J. Mol. Biol.* 157:105-132.

Laemmli, U.K. 1970. Cleavage of structural proteins during the assembly of the head of bacteriophage T4. *Nature* 227:680-685.

Lazarow, P.B. and C. de Duve. 1976. A fatty acyl-CoA oxidizing system in rat liver peroxisomes: enhanced by clofibrate, a hypolipidemic drug. *Proc. Natl. Acad. Sci. USA* 73:2043-2046.

Lazarow, P.B., and Y. Fujiki. 1985. Biogenesis of peroxisomes. *Annu. Rev. Cell Biol.* 1:489-530.

Lazarow, P.B., and H.W. Moser. 1994. Disorders of peroxisome biogenesis. In *The Metabolic Basis of Inherited Disease*, 7th Ed. C.R. Scriver, A.L. Beaudet, W.S. Sly, and A.D. Valle, editors. McGraw-Hill, New York. 2287-2324.

Lill, R., F.E. Nargang, and W. Neupert. 1996. Biogenesis of mitochondrial proteins. *Curr. Opin. Cell Biol.* 8:505-512.

Lillie, J.W., P.M. Loewenstein, M.R. Green, and M.Green. 1987. Functional domains of adenovirus type 5 E1a proteins. *Cell* 50:1091-1100.

Lithgow, T., P.B. Hoj, and N.J. Hoogenraad. 1993. Do cytosolic factors prevent promiscuity at the membrane surface? *FEBS Lett.* 329:1-4.

Liu, H., X. Tan, M. Veenhuis, D. McCollum, and J.M. Cregg. 1992. An efficient screen for peroxisome-deficient mutants of *Pichia pastoris*. *J. Bacteriol.* 174:4943-4951.

Liu, H., X. Tan, K.A. Russel, M. Veenhuis, and J.M. Cregg. 1995. *PER3*, a gene required for peroxisome biogenesis in *Pichia pastoris*, encodes a peroxisomal membrane protein involved in protein import. *J. Biol. Chem.* 270:10940-10951.

Lovering, R., I.M. Hanson, K.L.B Borden, S. Martin, N.J. O'Reilly, G.I. Evan, D. Rahman, D.J.C. Pappin, J. Trowsdale, and P.S. Freemont. 1993. Identification and preliminary characterization of a protein motif related to the zinc finger. *Proc. Natl. Acad. Sci. USA* 90:2112-2116.

- Luck, H. 1963. Catalase. *In* Methods of Enzymatic Analysis. H-U. Bergmeyer, editor. Academic Press, New York. 885-888.
- Lüers, G., T. Hashimoto, H.D. Fahimi, and A. Völkl. 1993. Biogenesis of peroxisomes: isolation and characterization of two distinct populations from normal and regenerating rat liver. *J. Cell Biol.* 121:1271-1280.
- Maniatis T., E.F. Fritsch, and J. Sambrook. 1982. *In* Molecular Cloning, a Laboratory Manual. Cold Spring Harbor Laboratory, Cold Spring Harbor, New York.
- Marshall, P.A., Y.I. Krimkevich, R.H. Lark, J.M. Dyer, M. Veenhuis, and J.M. Goodman. 1995. Pmp27 promotes peroxisomal proliferation. *J. Cell Biol.* 129:345-355.
- Marzioch, M., R. Erdmann, M. Veenhuis, and W.-H. Kunau. 1994. PAS7 encodes a novel yeast member of the WD-40 protein family essential for import of 3-oxoacyl-CoA thiolase, a PTS2-containing protein, into peroxisomes. *EMBO J.* 13:4908-4918.
- McCammon, M.T., J.A. McNew, P.J. Willy, and J.M. Goodman. 1994. An internal region of the peroxisomal membrane protein PMP47 is essential for sorting to peroxisomes. *J. Cell Biol.* 124:915-925.
- McCollum, D., E. Monosov, and S. Subramani. 1993. The *pas8* mutant of *Pichia pastoris* exhibits the peroxisomal protein import deficiencies of Zellweger syndrome cells. The PAS8 protein binds to the COOH-terminal tripeptide peroxisomal targeting signal and is a member of the TPR protein family. *J. Cell Biol.* 121:761-774.
- McNew, J.A., and J.M. Goodman. 1994. An oligomeric protein is imported into peroxisomes *in vivo*. *J. Cell Biol.* 127:1245-1257.
- McNew, J.A., and J.M. Goodman. 1996. The targeting and assembly of peroxisomal proteins: some old rules do not apply. *Trends Biochem. Sci.* 21:54-58.
- Moser, H.W. 1993. Peroxisomal diseases. *Adv. Human Genet.* 21:1-106.
- Mosser, J., A.-M. Douar, C.-O. Sarde, P. Kioschis, R. Feil, H. Moser, A.-M. Poustka, J.-M. Mandel, and P. Aubourg. 1993. Putative X-linked adrenoleukodystrophy gene shares unexpected homology with ABC transporters. *Nature.* 361:726-730.
- Needleman, R.B., and A. Tzagoloff. 1975. Breakage of yeast: a simple method for processing multiple samples. *Anal. Biochem.* 64:545-549.
- Nunnari, J., and P. Walter. 1996. Regulation of organelle biogenesis. *Cell* 84:389-394.

Nuttley, W.M., A.M. Brade, C. Gaillardin, G.A. Eitzen, J.R. Glover, J.D. Aitchison, and R.A. Rachubinski. 1993. Rapid identification and characterization of peroxisomal assembly mutants in *Yarrowia lipolytica*. *Yeast* 9:507-517.

Nuttley, W.M., A.M. Brade, G.A. Eitzen, M. Veenhuis, J.D. Aitchison, R.K. Szilard, J.R. Glover, and R.A. Rachubinski. 1994. PAY4, a gene required for peroxisome assembly in the yeast *Yarrowia lipolytica*, encodes a novel member of a family of putative ATPases. *J. Biol. Chem.* 269:556-566.

Nuttley, W.M., R.K. Szilard, J.J. Smith, M. Veenhuis, and R.A. Rachubinski. 1995. The *PAH2* gene is required for peroxisome assembly in the methylotrophic yeast *Hansenula polymorpha* and encodes a member of the tetratricopeptide repeat family of proteins. *Gene* 160:33-39.

Osumi, M., N. Miwa, Y. Teranishi, A. Tanaka, and S. Fukui. 1974. Ultrastructure of *Candida* yeasts grown on *n*-alkanes. *Arch. Microbiol.* 99:181-201.

Osumi, M., F. Fukuzumi, Y. Teranishi, A. Tanaka, and S. Fukui. 1975. Development of microbodies in *Candida tropicalis* during incubation in a *n*-alkane medium. *Arch. Microbiol.* 103:1-11.

Osumi, T., and T. Hashimoto. 1979. Peroxisomal beta oxidation system of rat liver. Copurification of enoyl-CoA hydratase and 3-hydroxyacyl-CoA dehydrogenase. *Biochem. Biophys. Res. Commun.* 89:580-584.

Osumi, T., T. Tsukamoto, S. Hata, S. Yokota, S. Miura, Y. Fujiki, M. Hijikata, S. Miyazawa, and T. Hashimoto. 1991. Amino-terminal presequence of the precursor of peroxisomal 3-ketoacyl-CoA thiolase is a cleavable signal peptide for peroxisomal targeting. *Biochem. Biophys. Res. Commun.* 181:947-954.

Palade, G. 1975. Intracellular aspects of the process of protein synthesis. *Science* 189:347-358.

Pfanner, N., and W. Neupert. 1990. A mitochondrial machinery for membrane translocation of precursor proteins. *Biochem. Soc. Trans.* 18:513-515.

Preston, R.A., M.F. Manolson, K. Becherer, E. Weiderhammer, D. Kirkpatrick, R. Wright, and E.W. Jones. 1991. Isolation and characterization of *PEP3*, a gene required for vacuolar biogenesis in *Saccharomyces cerevisiae*. *Mol. Cell. Biol.* 11:5801-5812.

Quest, A.F.G., J. Bloomenthal, E.S.G. Bardes, and R.M. Bell. 1992. The regulatory domain of protein kinase C coordinates four atoms of zinc. *J. Biol. Chem.* 267:10193-10197.

- Rachubinski, R.A., and S. Subramani. 1995. How proteins penetrate peroxisomes. *Cell* 83:525-528.
- Rao, M.J.K., and P. Argos. 1986. A conformational preference parameter to predict helices in integral membrane proteins. *Biochim. Biophys. Acta* 869:197-214.
- Rehling, P., M. Marzioch, F. Niesen, E. Wittke, M. Veenhuis, and W.-H. Kunau. 1996. The import receptor for the peroxisomal targeting signal 2 (PTS2) in *Saccharomyces cerevisiae* is encoded by the *PAS7* gene. *EMBO J.* 15:2901-2913.
- Roberts, C.J., C.K. Raymond, C.T. Yamashiro, and T.H. Stevens. 1991. Methods for studying the yeast vacuole. *Methods Enzymol.* 194:644-661.
- Robinson, J.S., T.R. Graham, and S.D. Emr. 1991. A putative zinc finger protein, *Saccharomyces cerevisiae* Vps18p, affects late Golgi functions required for vacuolar protein sorting and efficient α -factor prohormone maturation. *Mol. Cell. Biol.* 12:5813-5824.
- Roscher A.A., and B. Rolinski. 1992. Peroxisomal disorders in man. *Cell Biochem. Funct.* 10:201-207.
- Rothstein, R. 1991. Targeting, disruption, replacement, and allele rescue: integrative DNA transformation in yeast. *Methods Enzymol.* 194:281-301.
- Sakai, Y., P.A. Marshall, A. Saiganji, K. Takabe, H. Saiki, N. Kato, and J.M. Goodman. 1995. The *Candida boidinii* peroxisomal membrane protein Pmp30 has a role in peroxisomal proliferation and is functionally homologous to Pmp27 from *Saccharomyces cerevisiae*. *J. Bacteriol.* 177:6773-6781.
- Sanger, F., S. Nicklen, and A.R. Coulson. 1977. DNA sequencing with chain terminating inhibitors. *Proc. Natl. Acad. Sci. USA* 83:6156-6158.
- Santos, M.J., T. Imanaka, H. Shio, and P.B. Lazarow. 1988a. Peroxisomal integral membrane proteins in control and Zellweger fibroblasts. *J. Biol. Chem.* 263:10502-10509.
- Santos, M.J., T. Imanaka, H. Shio, G.M. Small, and P.B. Lazarow. 1988b. Peroxisomal membrane ghosts in Zellweger syndrome--Aberrant organelle assembly. *Science* 239:1536-1538.
- Schnell, D.J. 1995. Shedding light on the chloroplast protein import machinery. *Cell* 83:521-524.

- Schram, A.W., A. Strijland, T. Hashimoto, R.J.A. Wanders, R.B.H. Schutgens, H. van der Bosch, and J.M. Tager. 1986. Biosynthesis and maturation of peroxisomal β -oxidation enzymes in fibroblasts in relation to Zellweger syndrome and infantile Refsum disease. *Proc. Natl. Acad. Sci. USA* 81:6156-6158.
- Shiao, Y.J., G. Lupo, and J.E. Vance. 1995. Evidence that phosphatidylserine is imported into mitochondrial-associated membrane and that the majority of mitochondrial phosphatidylethanolamine is derived from decarboxylation of phosphatidylserine. *J. Biol. Chem.* 270:11190-11198.
- Shimozawa, N., T. Tsukamoto, Y. Suzuki, T. Oori, Y. Shirayoshi, T. Mori, and Y. Fujiki. 1992. A human gene responsible for Zellweger syndrome that affects peroxisome assembly. *Science* 255:1132-1134.
- Small, G.M., J.J. Szabo, and P.B. Lazarow. 1988. Acyl-CoA oxidase contains two targeting sequences each of which can mediate protein import into peroxisomes. *EMBO J.* 7:1167-1173.
- Smith, J.J., R.K. Szilard, M. Marelli, and R.A. Rachubinski. 1997. The peroxin Pex17p of the yeast *Yarrowia lipolytica* is associated peripherally with the peroxisomal membrane and is required for the import of a subset of matrix proteins. *Mol. Cell. Biol.* 17:2511-2520.
- Spong, A.P., and S. Subramani. 1993. Cloning and characterization of *PAS5*: a gene required for peroxisome biogenesis in the methylotrophic yeast *Pichia pastoris*. *J. Cell Biol.* 123:535-548.
- Subramani, S. 1993. Protein import into peroxisomes and biogenesis of the organelle. *Annu. Rev. Cell Biol.* 9:445-478.
- Swinkels, B.W., S.J. Gould, A.G. Bodnar, R.A. Rachubinski, and S. Subramani. 1991. A novel, cleavable peroxisomal targeting signal at the amino-terminus of the rat 3-ketoacyl-CoA thiolase. *EMBO J.* 10:3255-3262.
- Szilard, R.K., V.I. Titorenko, M. Veenhuis, and R.A. Rachubinski. 1995. Pay32p of the yeast *Yarrowia lipolytica* is an intraperoxisomal component of the matrix protein translocation machinery. *J. Cell Biol.* 131:1453-1469.
- Tan, X., H.R. Waterham, M. Veenhuis, and J.M. Cregg. 1995. The *Hansenula polymorpha* *PER8* gene encodes a novel peroxisomal integral membrane protein involved in proliferation. *J. Cell Biol.* 128:307-319.
- Tanaka, A., M. Osumi, and S. Fukui. 1982. Peroxisomes of alkane-grown yeast: fundamental and practical aspects. *Ann. N.Y. Acad. Sci.* 386:183-199.

Terlecky, S.R., W.M. Nuttley, D. McCollum, E. Sock, and S. Subramani. 1995. The *Pichia pastoris* peroxisomal protein PAS8p is the receptor for the C-terminal tripeptide peroxisomal targeting signal. *EMBO J.* 14:3627-3634.

Thieringer, R., H. Shio, Y. Han, G. Cohen, and P.B. Lazarow. 1991. Peroxisomes in *Saccharomyces cerevisiae*: immunofluorescence analysis and import of catalase A into isolated peroxisomes. *Mol. Cell. Biol.* 11:510-522.

Thompson, S.L., R. Burrows, R.J. Laub, and S.K. Krisans. 1987. Cholesterol synthesis in rat liver peroxisomes. Conversion of mevalonic acid to cholesterol. *J. Biol. Chem.* 262:17420-17425.

Titorenko, V.I., G.A. Eitzen, and R.A. Rachubinski. 1996. Mutations in the *PAY5* gene of the yeast *Yarrowia lipolytica* cause the accumulation of multiple subpopulations of peroxisomes. *J. Biol. Chem.* 271:20307-20314.

Tolbert, N.E. 1974. Isolation of subcellular organelles of metabolism on isopycnic sucrose gradients. *Methods Enzymol.* 31:734-746.

Tolbert, N.E. 1981. Metabolic pathways in peroxisomes and glyoxysomes. *Annu. Rev. Biochem.* 50:133-157.

Tsukamoto, T., S. Yokota, and Y. Fujiki. 1990. Isolation and characterization of Chinese hamster ovary cell mutants defective in assembly of peroxisomes. *J. Cell Biol.* 110:651-660.

Tsukamoto, T., S. Miura, and Y. Fujiki. 1991. Restoration by a 35K membrane protein of peroxisome assembly in a peroxisome-deficient mammalian cell mutant. *Nature* 350:77-81.

Tsukamoto, T., N. Shimozawa, and Y. Fujiki. 1994. Peroxisome assembly factor 1: nonsense mutation in a peroxisome-deficient Chinese hamster cell mutant and deletion analysis. *Mol. Cell. Biol.* 14:5458-5465.

Tsukamoto, T., S. Miura, T. Nakai, S. Yokota, N. Shimozawa, U. Suzuki, T. Orii, Y. Fujiki, F. Sakai, A. Bogaki, H. Yasumo and T. Osumi. 1995. Peroxisome assembly factor-2, a putative ATPase cloned by functional complementation on a peroxisome-deficient mammalian cell mutant. *Nature Genet.* 11:395-401.

Tuttle, D.L., A.S. Lewin, and W.A. Dunn, Jr. 1993. Selective autophagy of peroxisomes in methylotrophic yeasts. *Eur. J. Cell Biol.* 60:283-290.

Van den Bosch, H., R.B.H. Schutgens, R.J.A. Wanders, and J.M. Tager. 1992. Biochemistry of peroxisomes. *Annu. Rev. Biochem.* 61:157-197.

- Van der Klei, I.J., W. Harder, and M. Veenhuis. 1991. Biosynthesis and assembly of alcohol oxidase, a peroxisomal matrix protein in methylotrophic yeasts: a review. *Yeast* 7:195-209.
- Van der Klei, I.J., R.E. Hibrands, G.J. Swaving, H.R. Waterham, E.G. Vrieling, V.I. Titorenko, C.J.M.W. Harder, and M. Veenhuis. 1995. The *Hansenula polymorpha* *PER3* gene is essential for the import of PTS1 proteins into the peroxisome matrix. *J. Biol. Chem.* 270:17229-17236.
- Van der Leij, I., M. van den Berg, R. Boot, M. Franse, B. Distel, and H.F. Tabak. 1992. Isolation of peroxisome assembly mutants from *Saccharomyces cerevisiae* with different morphologies using a novel positive selection procedure. *J. Cell Biol.* 119:153-162.
- Van der Leij, I., M.M. Franse, Y. Elgersma, B. Distel, and H.F. Tabak. 1993. PAS10 is a tetratricopeptide-repeat protein that is essential for the import of most matrix proteins into peroxisomes of *Saccharomyces cerevisiae*. *Proc. Natl. Acad. Sci. USA* 90:11782-11786.
- Veenhuis, M., I. Keizer, and W. Harder. 1979. Characterization of peroxisomes in glucose-grown *Hansenula polymorpha* and their development after the transfer of cells into methanol-containing media. *Arch. Microbiol.* 120:167-175.
- Veenhuis, M., M. Mateblowski, W.-H. Kunau, and W. Harder. 1987. Proliferation of microbodies in *Saccharomyces cerevisiae*. *Yeast* 3:77-84.
- Veenhuis, M., and J.M. Goodman. 1990. Peroxisome assembly: membrane proliferation precedes the induction of the abundant matrix proteins in the methylotrophic yeast *Candida boidinii*. *J. Cell Sci.* 96:583-590.
- Voorn-Brouwer, T., I. van der Leij, W. Hemika, B. Distel, and H.F. Tabak. 1993. Sequence of the PAS8 gene, the product of which is essential for biogenesis of peroxisomes in *Saccharomyces cerevisiae*. *Biochim. Biophys. Acta* 1216:325-328.
- Walter, P., and A.E. Johnson. 1994. Signal sequence recognition and protein targeting to the endoplasmic reticulum membrane. *Annu. Rev. Cell Biol.* 10:87-119.
- Walton, P.A., S.J. Gould, J.R. Feramisco, and S. Subramani. 1992. Transport of microinjected proteins into peroxisomes of mammalian cells: inability of Zellweger cell lines to import proteins with the SKL tripeptide peroxisomal targeting signal. *Mol. Cell. Biol.* 12:531-541.
- Walton, P.A., P.E. Hill, and S. Subramani. 1995. Import of stably folded proteins into peroxisomes. *Mol. Biol. Cell* 6:675-683.
- Warren, G., and W. Wickner. 1996. Organelle inheritance. *Cell* 84:395-400.

Waterham, H.R., V.I. Titorenko, I.J. van der Klei, W. Harder, and M. Veenhuis. 1992. Isolation and characterization of peroxisomal protein import (Pim⁻) mutants of *Hansenula polymorpha*. *Yeast* 8:961-972.

Waterham, H.R., V.I. Titorenko, G.J. Swaving, W. Harder, and M. Veenhuis. 1993. Peroxisomes in the methylotrophic yeast *Hansenula polymorpha* do not necessarily derive from pre-existing organelles. *EMBO J.* 12:4785-4794.

Waterham, H.R., V.I. Titorenko, P. Haima, J.M. Cregg, W. Harder, and M. Veenhuis. 1994. The *Hansenula polymorpha* *PER1* gene is essential for peroxisome biogenesis and encodes a peroxisomal matrix protein with both carboxy- and amino-terminal targeting signals. *J. Cell Biol.* 127:737-749.

Waterham, H.R., Y. de Vries, K.A. Russel, W. Xie, M. Veenhuis, and J.M. Cregg. 1996. The *Pichia pastoris* *PER6* gene product is a peroxisomal integral membrane protein essential for peroxisome biogenesis and has sequence similarity to the Zellweger syndrome protein PAF-1. *Mol. Cell. Biol.* 16:2527-2536.

Wilcke, M., K. Hultenby, and S.E. Alexson. 1995. Novel peroxisomal populations in subcellular fractions from rat liver. Implications for peroxisome structure and biogenesis. *J. Biol. Chem.* 270:6949-6958.

Wilson, G.N., R.D. Holmes, and A.K. Hajra. 1988. Peroxisomal disorders: clinical commentary and future prospects. *Am. J. Med. Genet.* 30:771-792.

Wilson, I.A., H.L. Niman, R.A. Houghten, A.R. Cherenon, M.L. Connolly, and R.A. Lerner. 1984. The structure of an antigenic determinant in a protein. *Cell* 37:767-778.

Wendland, M., and S. Subramani. 1993a. Presence of cytoplasmic factors functional in peroxisomal protein import implicates organelle-associated defects in several human peroxisomal disorders. *J. Clin. Invest.* 92:2462-2468.

Wendland, M., and S. Subramani. 1993b. Cytosol-dependent peroxisomal protein import in a permeabilized cell system. *J. Cell Biol.* 120:675-685.

Wiebel, F.F., and W.-H. Kunau. 1992. The Pas2 protein essential for peroxisome biogenesis is related to ubiquitin-conjugating enzymes. *Nature* 359:73-76.

Wiemer, E.A.C., W.M. Nuttley, B.L. Bertolaet, X. Li, U. Franke, M.J. Wheelock, W.K. Anne, K.R. Johnson, and S. Subramani. 1995. Human peroxisomal targeting signal-1 receptor restores peroxisomal protein import in cells from patients with fatal peroxisomal disorders. *J. Cell Biol.* 130:51-65.

- Wiemer, E.A.C., G.H. Luers, K.N. Faber, T. Wenzel, M. Veenhuis, and S. Subramani. 1996. Isolation and characterization of Pas2p, a peroxisomal membrane protein essential for peroxisome biogenesis in the methylotrophic yeast *Pichia pastoris*. *J. Biol. Chem.* 271:18973-18980.
- Yahraus, T., N. Braverman, G. Dodt, J.E. Kalish, J.C. Morrell, H.W. Moser, D. Valle, and S.J. Gould. 1996. The peroxisome biogenesis disorder group 4 gene, *PXAAA1*, encodes a cytoplasmic ATPase required for stability of the PTS1 receptor. *EMBO J.* 15:2914-2923.
- Yajima, S., Y. Suzuki, N. Shimozawa, S. Yamaguchi, T. Orii, Y. Fujiki, T. Osumi, T. Hashimoto, and H.W. Moser. 1992. Complementation study of peroxisome-deficient disorders by immunofluorescence staining and characterization of fused cells. *Hum. Genet.* 88:491-499.
- Zhang, H., R. Scholl, J. Browse, and C. Somerville. 1988. Double stranded DNA sequencing as a choice for DNA sequencing. *Nucleic Acids Res.* 16:1220
- Zhang, J.W., Y. Han, and P.B. Lazarow. 1993. Novel peroxisome clustering mutants and peroxisome biogenesis mutants of *Saccharomyces cerevisiae*. *J. Cell Biol.* 123:1133-1147.
- Zhang, J.W., and P.B. Lazarow. 1995. *PEB1 (PAST)* in *Saccharomyces cerevisiae* encodes a hydrophilic, intra-peroxisomal protein that is a member of the WD repeat family and is essential for the import of thiolase into peroxisomes. *J. Cell Biol.* 129:65-80.
- Zoeller, R.A., and C.R.H. Raetz. 1986. Isolation of animal cell mutants deficient in plasmalogen biosynthesis and peroxisome assembly. *Proc. Natl. Acad. Sci. USA* 83:5170-5174.